NAVAL POSTGRADUATE SCHOOL

MONTEREY, CALIFORNIA

THESIS

AN OPERATIONAL MODEL OF CRITICAL SUPPLY CHAIN FOR THE U.S. VIRGIN ISLANDS

by

Jeffrey E. Good

September 2019

Co-Advisors:	David L. Alderson Jr. Daniel Eisenberg
Second Reader:	Jefferson Huang

Approved for public release. Distribution is unlimited.

THIS PAGE INTENTIONALLY LEFT BLANK

REPORT DOCUMENTATION PAGE			*Form Approved OMB No. 0704-0188*
Public reporting burden for this collection of information is estimated to average 1 hour per response, including the time for reviewing instruction, searching existing data sources, gathering and maintaining the data needed, and completing and reviewing the collection of information. Send comments regarding this burden estimate or any other aspect of this collection of information, including suggestions for reducing this burden, to Washington headquarters Services, Directorate for Information Operations and Reports, 1215 Jefferson Davis Highway, Suite 1204, Arlington, VA 22202-4302, and to the Office of Management and Budget, Paperwork Reduction Project (0704-0188) Washington, DC 20503.			
1. AGENCY USE ONLY ***(Leave blank)***	**2. REPORT DATE** September 2019	**3. REPORT TYPE AND DATES COVERED** Master's thesis	
4. TITLE AND SUBTITLE AN OPERATIONAL MODEL OF CRITICAL SUPPLY CHAIN FOR THE U.S. VIRGIN ISLANDS			**5. FUNDING NUMBERS** RNMQA
6. AUTHOR(S) Jeffrey E. Good			
7. PERFORMING ORGANIZATION NAME(S) AND ADDRESS(ES) Naval Postgraduate School Monterey, CA 93943-5000			**8. PERFORMING ORGANIZATION REPORT NUMBER**
9. SPONSORING / MONITORING AGENCY NAME(S) AND ADDRESS(ES) N/A			**10. SPONSORING / MONITORING AGENCY REPORT NUMBER**
11. SUPPLEMENTARY NOTES The views expressed in this thesis are those of the author and do not reflect the official policy or position of the Department of Defense or the U.S. Government.			
12a. DISTRIBUTION / AVAILABILITY STATEMENT Approved for public release. Distribution is unlimited.			**12b. DISTRIBUTION CODE** A

13. ABSTRACT (maximum 200 words)

In September 2017, two Category-5 hurricanes struck the U.S. Virgin Islands (USVI) within a period of two weeks, causing massive devastation to homes, businesses, and infrastructure. These storms deposited over 660,000 tons of debris on roads and also created mudslides, rock slides, sinkholes, and washouts that blocked surface transportation for months. The damage to surface roads caused significant last-mile distribution problems that affected the ability to distribute disaster relief supplies within the islands and limited community access to these supplies during post-disaster curfews. Working directly in support of the Virgin Islands Department of Public Works and the Federal Emergency Management Agency, this thesis (1) develops computer models and supporting data of surface road transportation and supply chain infrastructure in the USVI and (2) uses the models to conduct a series of analyses that inform efficacy and prioritization of proposed infrastructure modifications and/or investment on community mobility and disaster relief. Specifically, we consider the island of St. Croix and model its transportation system and supply chain for food, fuel, and emergency supplies as a multi-commodity network flow problem. We assess system performance and potential vulnerabilities of the existing road network in order to inform investment decisions to strengthen the resilience of transportation and other interdependent lifeline infrastructure systems.

14. SUBJECT TERMS supply chain, transportation, network flow, optimization, U.S. Virgin Islands, hurricane, hazard mitigation plan			**15. NUMBER OF PAGES** 109
			16. PRICE CODE
17. SECURITY CLASSIFICATION OF REPORT Unclassified	**18. SECURITY CLASSIFICATION OF THIS PAGE** Unclassified	**19. SECURITY CLASSIFICATION OF ABSTRACT** Unclassified	**20. LIMITATION OF ABSTRACT** UU

NSN 7540-01-280-5500 Standard Form 298 (Rev. 2-89) Prescribed by ANSI Std. 239-18

THIS PAGE INTENTIONALLY LEFT BLANK

Approved for public release. Distribution is unlimited.

AN OPERATIONAL MODEL OF CRITICAL SUPPLY CHAIN FOR THE U.S. VIRGIN ISLANDS

Jeffrey E. Good
Lieutenant Commander, United States Navy
BBA, National University, 2007

Submitted in partial fulfillment of the
requirements for the degree of

MASTER OF SCIENCE IN OPERATIONS RESEARCH

from the

NAVAL POSTGRADUATE SCHOOL
September 2019

Approved by: David L. Alderson Jr.
Co-Advisor

Daniel Eisenberg
Co-Advisor

Jefferson Huang
Second Reader

W. Matthew Carlyle
Chair, Department of Operations Research

THIS PAGE INTENTIONALLY LEFT BLANK

ABSTRACT

In September 2017, two Category-5 hurricanes struck the U.S. Virgin Islands (USVI) within a period of two weeks, causing massive devastation to homes, businesses, and infrastructure. These storms deposited over 660,000 tons of debris on roads and also created mudslides, rock slides, sinkholes, and washouts that blocked surface transportation for months. The damage to surface roads caused significant last-mile distribution problems that affected the ability to distribute disaster relief supplies within the islands and limited community access to these supplies during post-disaster curfews. Working directly in support of the Virgin Islands Department of Public Works and the Federal Emergency Management Agency, this thesis (1) develops computer models and supporting data of surface road transportation and supply chain infrastructure in the USVI and (2) uses the models to conduct a series of analyses that inform efficacy and prioritization of proposed infrastructure modifications and/or investment on community mobility and disaster relief. Specifically, we consider the island of St. Croix and model its transportation system and supply chain for food, fuel, and emergency supplies as a multi-commodity network flow problem. We assess system performance and potential vulnerabilities of the existing road network in order to inform investment decisions to strengthen the resilience of transportation and other interdependent lifeline infrastructure systems.

THIS PAGE INTENTIONALLY LEFT BLANK

Table of Contents

List of Figures

THIS PAGE INTENTIONALLY LEFT BLANK

List of Tables

THIS PAGE INTENTIONALLY LEFT BLANK

List of Acronyms and Abbreviations

BIR Virgin Islands Bureau of Internal Revenue

BPR Bureau of Public Roads

BVI British Virgin Islands

CBP U.S. Customs and Border Protection

CRS Coordinate Reference System

DHS U.S. Department of Homeland Security

DPW Virgin Islands Department of Public Works

DoD Department of Defense

DOE Department of Energy

DOT U.S. Department of Transportation

DPNR Department of Planning and Natural Resources

EPA Environmental Protection Agency

EPSG European Petroleum Search Group

FAA Federal Aviation Administration

FEMA Federal Emergency Management Agency

FHWA Federal Highway Administration

FTA Federal Transit Authority

MPH miles per hour

NPS Naval Postgraduate School

USCG U.S. Coast Guard

USG United States Government

USVI U.S. Virgin Islands

UVI University of the Virgin Islands

VIPA Virgin Islands Port Authority

VIPD Virgin Islands Police Department

VIPFA Virgin Island Public Finance Authority

VITEMA Virgin Island Territory Emergency Management Agency

VIWMA Virgin Islands Waste Management Authority

VPH vehicles per hour

WAPA Virgin Islands Water and Power Authority

WICO West Indian Company Limited

Executive Summary

In September 2017, the U.S. Virgin Islands (USVI) territory was struck by two Category-5 hurricanes within a two-week period (Hurricane Irma on September 6-7 and Hurricane Maria on September 20). The resulting devastation from these storms prompted the United States Government, the USVI Territorial government, local infrastructure providers, universities, community groups, philanthropy organizations, and numerous other stakeholders to work together to recover failed infrastructure systems and bring the territory back to a normal state of life.

The remote geographic location of the islands makes a robust and highly reliable transportation network crucial to support economic and personal requirements due to the heavy reliance on the port and surface road infrastructures. Of the many lifeline systems impacted by hurricanes Irma and Maria, critical supply chain systems were some of the most damaged and important for territory recovery.

This thesis focuses on the capacity of the USVI critical supply chain system to deliver food and materials via ports and surface roads. We define the basic components of critical supply chain systems in the USVI as roads for local mobility, ports of entry onto the islands (e.g., piers, shipyards, airports, etc.), and locations of supply access (e.g., supermarkets). These components comprise the last-mile of the Territorial supply chain and enable the movement of goods and services from ports of entry to the communities that need them. Our goal is to assess how USVI food supply chains and transportation systems perform during normal and post-hurricane conditions, and to identify emergency relief stations across the islands that minimize household travel time, maximize supply chain access, and support faster recovery.

This thesis performs three modeling and analysis tasks:

1. *Data Curation and Network Construction:* We construct a dataset useful for the analysis of traffic congestion and shipping supplies on surface roads within the island of St. Croix.
2. *Model Formulation and Implementation:* We develop a four-stage traffic model that measures the round-trip travel times for supplies and civilians to reach locations of distribution during normal and degraded traffic conditions. Specifically, we model the

St. Croix network as a minimum cost, multi-commodity flow problem with 887 nodes, 2353 directed arcs, and 1474 commodities representing unique origin-destination pairings.

3. *Last-Mile Supply Chain Analysis:* Using data and models to determine the capability of surface roads in St. Croix to enable access to disaster relief supplies, we identify which St. Croix communities may have the greatest difficulty accessing locations of distribution during normal and worst-case situations.

We consider several questions in turn.

For populations, what are the resulting round trip times and congestion when travelers pick their destinations "selfishly" in contrast to when when traveler destinations are "coordinated"? The "coordinated" traffic assignment protocol is an equilibrium model by nature, and as such it tends to seek flows that "balance" the objective function cost across all of the various routes. This results in lower average round trip times as compared to allowing travelers to pick their destinations "selfishly."

For the port, what are the resulting travel times under "selfish" and "coordinated" traffic patterns? The movement of goods from the port to stores is modeled as specific origin-destination pairs for both the "selfish" and "coordinated" traffic assignment protocols. There is no choice in location of delivery, and each store must receive a delivery. As a result, we note similar average round trip delivery times for each traffic assignment protocol.

Which road segments, if blocked, have the potential to create the most congestion and hardship on travelers? The Christiansted Bypass near VI 703 is the road segment that, when blocked, causes the most congestion for each traffic assignment protocol. However, the system is "flexible" enough to reroute traffic in such a way as to avoid dropped demands. This indicates that service times at stores play a larger role in the population's inability to complete tasks within an intended maximum travel period of six hours than does the operation of the surface road network.

What other analyses are possible with the current model? The model formulation presented in this work proves to be "flexible" enough to allow analytical excursions of many types, to include; the impact of losing supply access points, disruptions to multiple road segments, or the impact of additional roads in the system, to name a few.

Acknowledgments

To my thesis co-advisors, Dr. David Alderson and Dr. Daniel Eisenberg, thank you for your mentorship and patience as we worked through this project. I appreciate the trust you had in me to truly take ownership of what is but a small piece of a very large project. This experience has served as a great capstone in my journey into the world of analytics. I can never fully express what your support has meant to me and I look forward to our future work together.

To our colleagues at the University of the Virgin Islands, Dr. Kim Waddell, Dr. Greg Guannel, and Dr. David Morris, thank you for allowing me to contribute to and be a part of your community. It is not lost on me that the work we have completed involves very real people living through very real situations and goes well beyond a simple postgraduate school requirement. I am very appreciative of your support and understanding. Furthermore, to Dr. Greg Guannel, always remember to "Don't get got!!"

To the people of the United States Virgin Islands, thank you for sharing in your culture and your community. Thank you for allowing us to experience the USVI, and for allowing us to assist in making the islands everything they should be.

Finally, to my wife, Elaina, thank you for all of your support and patience as I struggled through the final months of this thesis. I could not have gotten through it without your support and understanding. It is but another of our many adventures and I look forward to many, many more.

THIS PAGE INTENTIONALLY LEFT BLANK

CHAPTER 1:
Introduction

In September 2017, the U.S. Virgin Islands (USVI) territory was struck by two Category-5 hurricanes within a two-week period. The resulting devastation from these storms prompted the United States Government (USG), the USVI Territorial government, local infrastructure providers, universities, community groups, philanthropy organizations, and numerous other stakeholders to work together to recover failed infrastructure systems and bring the territory back to a normal state of life.

This thesis is in support of Federal Emergency Management Agency (FEMA) response and recovery activities to these storms as part of a broader FEMA-funded effort by the Naval Postgraduate School (NPS) and Department of Energy (DOE) to assess and improve the resilience of interdependent USVI lifeline infrastructure systems: energy, water, transportation, and telecommunications (Alderson et al. 2018). This thesis additionally supports several other complementary efforts with the University of the Virgin Islands (UVI) to develop a next-generation Hazard Mitigation and Resilience Plan for the territory.

1.1 Overview of the U.S. Virgin Islands

The USVI covers a land area of about 135 square miles and is comprised of the three main islands of St. Thomas, St. Croix, and St. John, and the two smaller islands of Water Island and Hassel Island. The USVI is located in the Caribbean Sea approximately 1,100 miles to the southeast of Florida and roughly 40 miles to the east of Puerto Rico. The USVI boasts a population of about 105,000 people with approximately 51,000 residing on St. Thomas, 50,000 on St. Croix, and 4,000 on St. John (U.S. Virgin Islands Bureau of Economic Research 2014). Each of the three primary islands within the USVI has its own distinct topography and "personality." Figure 1.1 shows the geographical relationship of the three islands.

St. Thomas, to the northwest, is a hilly island covering approximately 31 square miles of land (Figure 1.2). As the home of the territory's capital, Charlotte Amalie, St. Thomas serves as the USVI's center of government. Furthermore, the island serves as the territory's

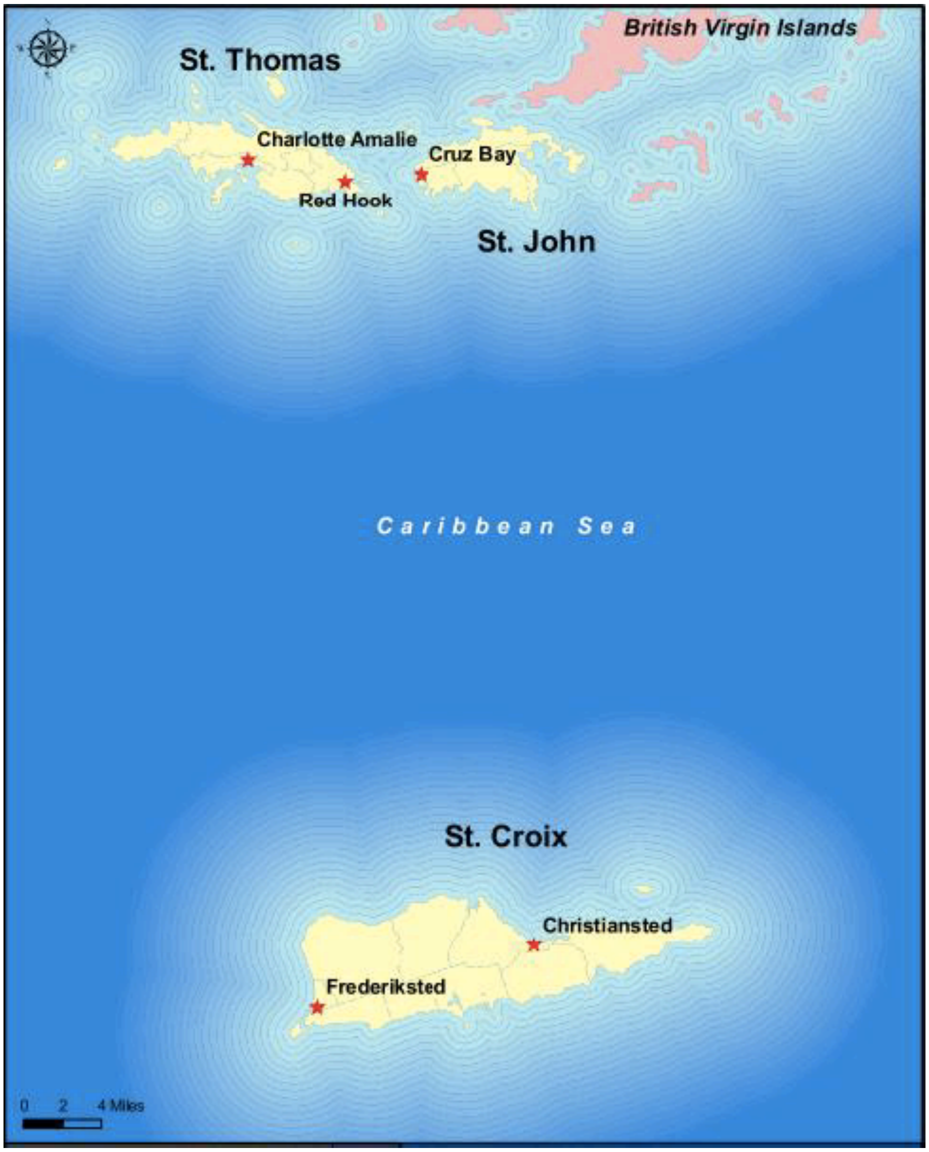

Figure 1.1. The three main islands in the USVI are St. Thomas and St. John to the north and St. Croix approximately 40 miles to the south. Source: USVI Department of Public Works (2014)

base of tourism, trade, commerce, and finance. The Crown Bay Cargo Port serves as a primary transshipment port for items being shipped throughout the Caribbean and further serves as a point of interest along a key shipping lane for vessels bound for the Panama Canal (U.S. Virgin Islands Bureau of Economic Research 2014).

The island of St. John lies just three miles east of St. Thomas and has an area of approximately

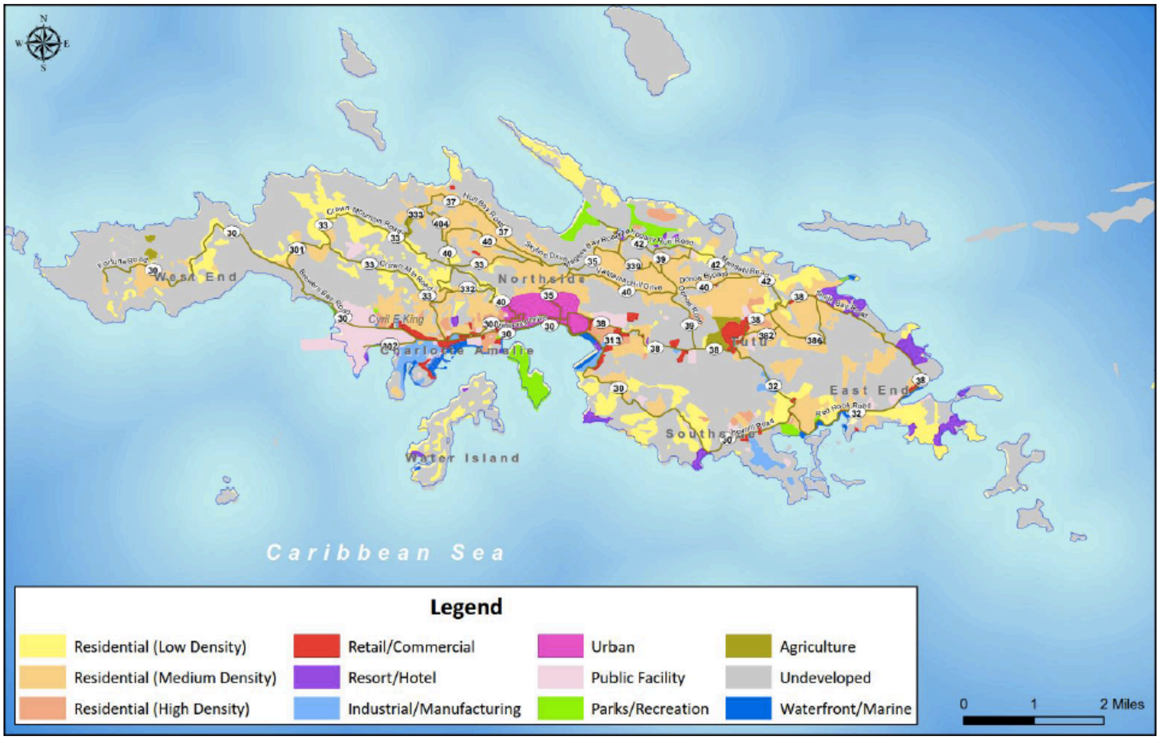

Figure 1.2. Land use map of St. Thomas. St. Thomas has a large volume of high and medium density residential, commercial, resort, and urban areas on the island, with limited agriculture and industrial/manufacturing facilities. Source: USVI Department of Public Works (2014)

20 square miles that is dominated by the Virgin Islands National Park land (Figure 1.3). The presence of the national park land has led St. John to remain relatively undeveloped; however, the land that has been developed contains high-end residences and lodging for the "rich and famous" vacationers (U.S. Virgin Islands Bureau of Economic Research 2014).

Finally, St. Croix, located approximately 40 miles to the south of St. Thomas and St. John, is the largest of the three primary islands with an area of approximately 84 square miles (Figure 1.4). The island's topography varies more than either St. Thomas or St. John, with mountainous terrain to the northwest, cliffs to the east, and predominately flat, rural terrain on the remainder of the island. Historically, St. Croix has derived its economy from oil, rum production, and light manufacturing; however, the closure of the HOVENSA oil refinery in 2012 had a clear impact to the island and its economy causing job losses, business closures, and the loss of government tax revenues (U.S. Virgin Islands Bureau of Economic Research

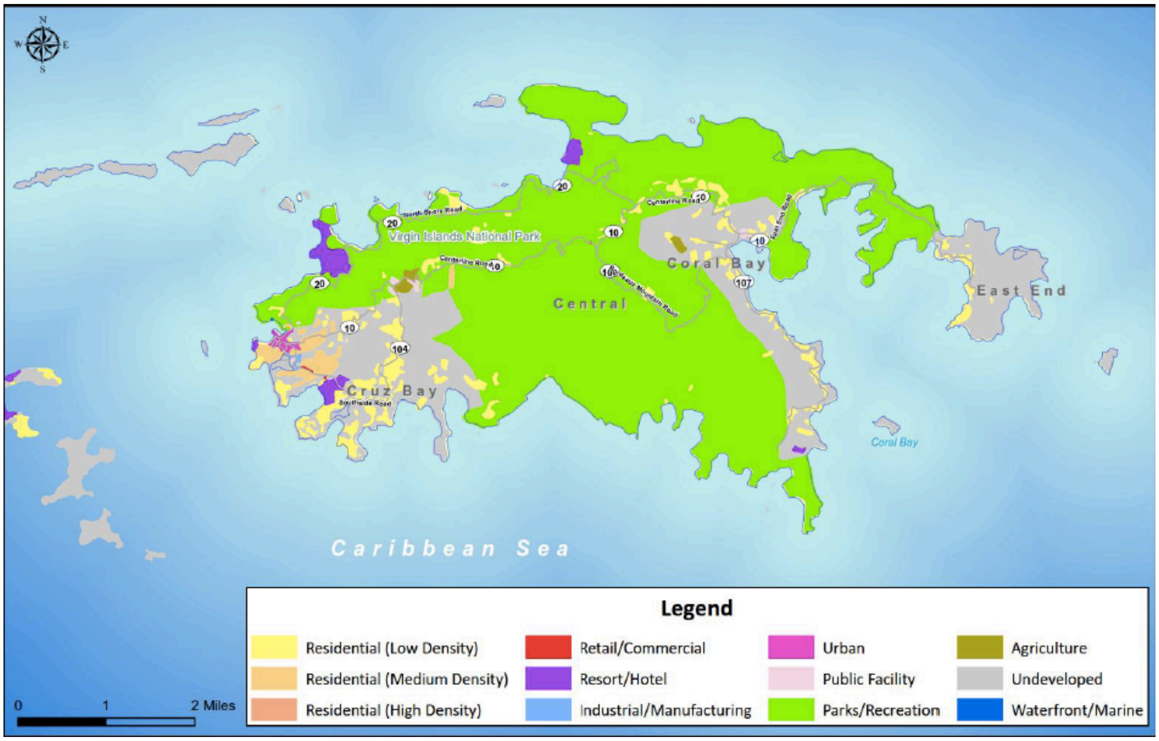

Figure 1.3. Land use map of St. John. Approximately two-thirds of St. John's land area is National Parks land leaving little room for commercial or residential development on the island. Source: USVI Department of Public Works (2014)

2014).

The USVI's economy relies heavily on tourism, rum production, and light manufacturing to remain successful. The USVI's transportation infrastructure, specifically its ports and surface roads, play a key role in maintaining the territory's economy. The Virgin Islands Department of Public Works (DPW) and Virgin Islands Water and Power Authority (WAPA) are two agencies that play a key role in maintaining and supporting the critical transportation infrastructure. DPW is responsible to "plan, construct and maintain the territory's public roads, highways, storm drainage systems, public transportation systems, public parking facilities, public buildings and public cemeteries," while WAPA is responsible for producing and distributing electricity throughout the island (U.S. Virgin Islands Department of Public Works 2018; U.S. Virgin Islands Water and Power Authority 2018). As for the economy that infrastructure supports, the U.S. Virgin Islands Bureau of Economic Research (2014)

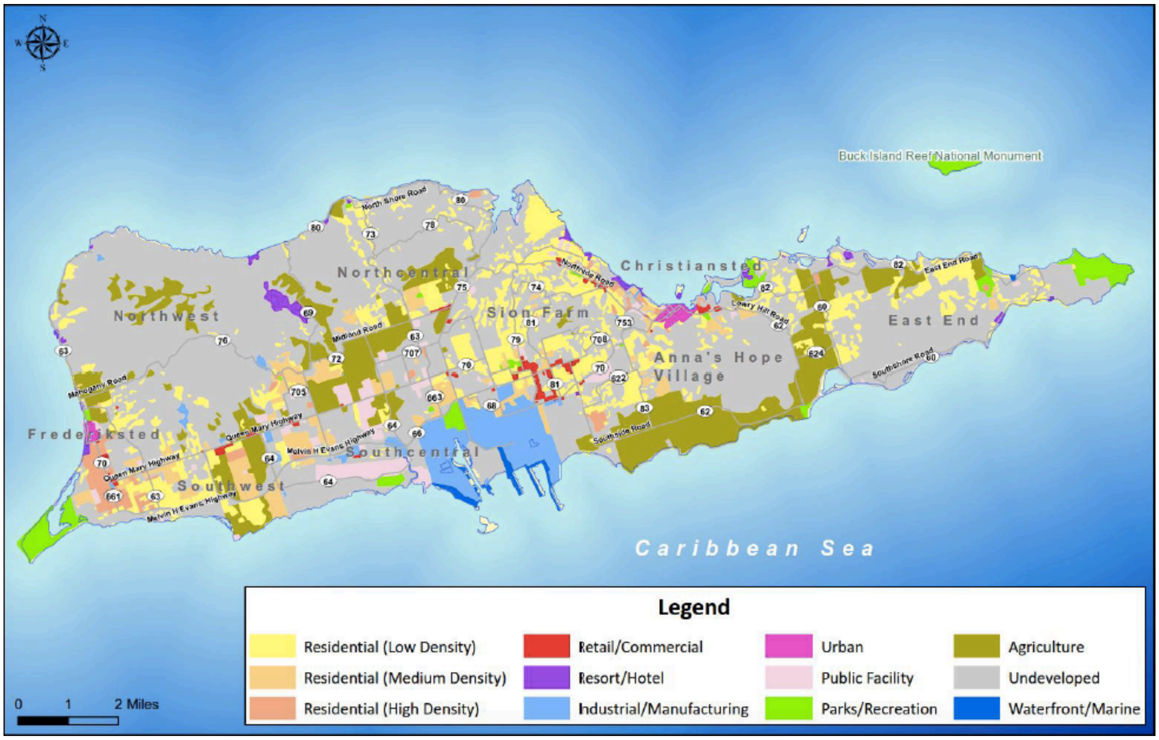

Figure 1.4. Land use map of St. Croix. The flatter topography on St. Croix allows for greater agriculture and industrial/manufacturing development on the island. This results in a lower volume of tourism compared to St. Thomas or St. John. Source: USVI Department of Public Works (2014)

identifies several of the territory's strengths and weakness with regards to its economy. Specifically, the report recognizes the territory's "strategic location and ease of access and ties to the U.S. mainland economy" as well as its good tourism product among the USVI's strengths. However, the report recognizes the islands' "insufficient investment in public infrastructure" among its many weaknesses (U.S. Virgin Islands Bureau of Economic Research 2014).

1.2 Hurricanes Irma and Maria

On the evening of September 6 into the morning of September 7, 2017, Hurricane Irma struck the USVI as a Category 5 hurricane on the Saffir-Simpson wind scale (Schott et al. 2012) with maximum sustained winds of 180 miles per hour. The storm caused massive damage to critical infrastructure on St. Thomas and St. John prior to turning north towards

Florida and the Continental United States. At the time, Hurricane Irma was the fifth costliest Atlantic hurricane to be recorded with an estimated 50 billion dollars in damages (National Hurricane Center 2018). Following Hurricane Irma, emergency supplies were sent from Puerto Rico and St. Croix to aid in the recovery operations.

Exactly two weeks later, on the evening of September 20, 2017, Hurricane Maria hit St. Croix and then Puerto Rico. The storm was designated as a Category 5 hurricane with sustained winds of 175 miles per hour; however, first person accounts report wind gusts as high as 240 miles per hour at the Limetree Bay facility on St. Croix. The timing was unfortunate—in response to Hurricane Irma, St. Croix had already sent much of their relief supplies to St. Thomas and St. John two weeks prior.

All told, the storms deposited over 660,000 tons of debris on roads and surfaces, blocking access to neighborhoods and critical supplies required by the population. Hurricanes Irma and Maria were responsible for a cumulative ten to 20 inches of rainfall creating mudslides, rock slides, potholes, sinkholes, and washouts causing massive devastation to roadways within the USVI (Figure 1.5). Storm-water runoff exceeded the capacity of the territory's existing storm-water systems. Signage, streetlights, and traffic signals were all but destroyed throughout the territory (USVI Hurricane Recovery and Resilience Task Force 2018). In her testimony before the House Transportation and Infrastructure Committee, Congresswoman Plaskett (2017) states "The islands were completely cut off from the world until the air and sea ports could at least resume basic operations." The territory remained in the vulnerable and degraded state for a significant amount of time, as many of these systems took weeks or months to recover back to normal operation. Overall, it was estimated that the storms caused approximately 10.7 billion dollars of damage with 6.9 billion dollars being attributed to infrastructure.

1.3 Critical Supply Chain Infrastructure in the USVI Before and After the Hurricanes

Of the many lifeline systems impacted by hurricanes Irma and Maria, critical supply chain systems were some of the most damaged and important for territory recovery. For the purposes of this thesis, we define the basic components of critical supply chain systems in the USVI as roads for local mobility, ports of entry onto the islands (e.g., piers, shipyards,

Figure 1.5. Examples of Damage to Critical Infrastructures in the USVI following Hurricanes Irma and Maria. Source: USVI Hurricane Recovery and Resilience Task Force (2018).

airports, etc.), and locations of supply access (e.g., supermarkets). These components comprise the last-mile of the Territorial supply chain and enable the movement of goods and services from ports of entry to the communities that need them. Post hurricanes, each of these systems must be repaired and functioning to recover the territory back to normal life.

1.3.1 Roads in the USVI

The remote geographic location of the islands makes a robust and highly reliable transportation network crucial to support economic and personal requirements due to the heavy reliance on the port and surface road infrastructures. The USVI Hurricane Recovery and Resilience Task Force (2018) notes that "much of the transportation infrastructure is aging and fragile due to lack of funds, deferred maintenance, and challenging environmental conditions." Further exacerbating critical infrastructure issues, much of the transportation infrastructure was not built to withstand Category 4 and 5 hurricanes (USVI Hurricane Recovery and Resilience Task Force 2018). From her November 2, 2017 testimony before the House Transportation and Infrastructure committee, Congresswoman Plaskett (2017) states

> Territorial roads continued to be under stress from inadequate capacity, and in the Virgin Islands most of the federal highways did not meet current standards. Again, this was before two category 5 storms. Because the territories are islands, much of the road construction is more expensive than on the mainland to accommodate supply costs. As a result of inadequate funds, crucial projects have been shelved, leaving only stop-gap repairs to resolve maintenance issues, even on primary highways (Plaskett 2017).

Overall, the USVI's transportation system includes a road network, two airports, numerous maritime ports, nearly non-existent public transportation, and limited walking and cycling paths. The territory's road network consists of approximately 1,230 miles of road. With the USVI, approximately 340 miles of road are designated as federal routes, 410 miles are classified as local roads, and 480 miles are considered private roads. Private roads are often unpaved or only semi-paved. They are often poorly built and delinquent on maintenance (USVI Hurricane Recovery and Resilience Task Force 2018).

The USVI, and more specifically DPW, does not have a current inventory of roads or bridges and their condition for the territory (Gajewski 2019). According to informal surveys conducted for the 2040 Comprehensive Transportation Master Plan Report, the condition of the roads on St. Thomas and St. John is considered to be fair to poor, while St. Croix roads are considered to be good. The road conditions among the islands differ due to their geographic diversity. The topography on St. Thomas and St. John results in narrow, two-lane roads with narrow or non-existent shoulders and numerous blind corners. Pavement markings throughout the territory are mostly faded and many locations have damaged or missing guardrails (USVI Department of Public Works 2014).

The USVI continues to experience decreased household sizes, increased availability of vehicles, and an increased suburbanization of the population and jobs resulting in increased usage of the territory's roadways. According to USVI Department of Public Works (2014), the number of households with vehicles in the USVI has increased significantly from 2000 to 2010 with St. Thomas experiencing a 24 percent increase in households with two or fewer vehicles and St. Croix reporting a nearly 50 percent increase in households with three or greater vehicles. Furthermore, an average of 66 percent of all workers in the territory commute to work alone.

1.3.2 Ports and Supply Access Points in the USVI

As the center for tourism and commerce, St. Thomas is home to five primary seaports. Cruise ships arriving in the area will dock at one of two places on St. Thomas: The Virgin Islands Port Authority (VIPA)-operated Austin "Babe" Monsanto Marine Facility or the West Indian Company Limited (WICO) dock located across the harbor in Havensight. WICO is a public corporation owned by the Virgin Island Public Finance Authority (VIPFA) to support tourism within the USVI. Furthermore, the WICO dock is the only public dock in the territory and is not operated by VIPA. The WICO dock is the primary cruise ship berth in the territory (USVI Hurricane Recovery and Resilience Task Force 2018). WICO has the ability to dock container ships, but the pier facilities do not have a crane to support the offloading of vessels. This requires any cargo ships docking at WICO to have the ability to self-load and unload (USVI Hurricane Recovery and Resilience Task Force 2018).

Also located on St. Thomas, the Edward Wilmoth Blyden IV Marine Terminal on Charlotte Amalie's waterfront is the ferry boat dock that supports passenger vessels transiting between numerous islands in the area. The Edward Wilmoth Blyden IV Marine Terminal also houses the U.S. Customs clearance point on St. Thomas for vessels entering U.S. waters. The Charlotte Amalie waterfront also offers berths for public and private vessels (U.S. Virgin Islands Port Authority 2018). Nearby, the Crown Bay Cargo Port serves as the primary transshipment center for the island and houses St. Thomas' three primary shipping companies: Crowley Shipping, Tropical Shipping, and Priority RoRo. The Crown Bay Cargo Port is undersized with only 10 acres of lay-down area causing it to get bogged down during high traffic times (Raimondi 2019). The cargo port serves as the initial step in the supply chain to feed the various supply access points, such as Pueblo Supermarkets, Pricemart, K-Mart, and Home Depot, throughout the island (Frazier 2019). On the East End of St. Thomas, the Urman Victor Fredericks Marine Terminal in Red Hook supports passenger travel between St. Thomas and St. John, as well as to and from the British Virgin Islands (BVI) (U.S. Virgin Islands Port Authority 2018). Figure 1.6 shows the numerous transportation facilities located on St. Thomas.

Figure 1.6. Map of transportation facilities on St. Thomas. As the center of tourism, St. Thomas relies heavily on its numerous ports and surface roads. The island also serves as a transportation hub in the USVI with ferry access to the remaining islands in the territory. Source: USVI Department of Public Works (2014)

On St. Croix, Gallows Bay dock on the northern edge of the island can accommodate a variety of watercraft types and sizes. However, no cargo handling gear, such as cranes, exists at Gallows Bay, which requires vessels berthing there to have the ability to self-load and unload. The single cruise ship dock is the Ann E. Abramson Marine Facility located adjacent to historic Frederiksted on the west end of the island. The Wilfred "Bomba" Allick Port is the primary location for offloading and loading commercial shipping vessels on the island of St. Croix (U.S. Virgin Islands Port Authority 2018). Also known as the "Transshipment Port," its lay-down area is approximately 15 acres in size and is much less congested than the Crown Bay Cargo Port on St. Thomas (Raimondi 2019). Similarly, the Transshipment Port serves to supply the various supply access points located predominately along Centerline Road on St. Croix. The Gordon A. Finch Molasses Pier, just east of the Transshipment Port, has historically been used to import molasses for the distillery plants on the island. The Molasses Pier has also been used to import vital construction materials such as "liquid asphalt, bulk cargo such as gravel, cement blocks, and other construction materials critical to St. Croix's construction industry" (USVI Hurricane Recovery and Resilience Task Force 2018). Figure 1.7 shows the geographical locations of St. Croix's transportation facilities.

St. John typically does not receive large cruise vessels or container ships into port. Much of the marine traffic to St. John arrives via barge or car ferry from one of the nearby islands. The Loredon L. Boynes Sr. Dock in Cruz Bay on St. John serves as the main passenger port to the island. The Theovald Eric Moorehead Dock and Terminal at Enighed Pond is the main cargo and car barge facility on St. John. The Victor William Sewer Marine Facility is the Customs dock for St. John and is used to berth commercial passenger ferries and privately-owned vessels on their way to the BVI, as well as U.S.-registered privately-owned vessels waiting to clear customs in order to return to U.S. waters (USVI Hurricane Recovery and Resilience Task Force 2018). Figure 1.8 shows the relatively small amount of transportation infrastructure on St. John.

The USVI is home to only two major airports, Cyril E. King on St. Thomas and Henry E. Rohlsen on St. Croix. Both airports are owned by VIPA; however, the air traffic control towers are owned and operated by the Federal Aviation Administration (FAA) (U.S. Virgin Islands Port Authority 2018).

Figure 1.7. Map of transportation facilities on St. Croix. The Wilfred "Bomba" Allick Port serves as the centerpiece of St. Croix's supply chain supporting the island's manufacturing and industrial base. St. Croix's road network is laid out in a grid-like pattern, unlike the numerous roads on St. Thomas. Source: USVI Department of Public Works (2014)

Figure 1.8. Map of transportation facilities on St. John. The smallest of the three islands in the territory, St. John has a much smaller transportation infrastructure footprint than the other two islands. Source: USVI Department of Public Works (2014)

1.3.3 Hurricane Impacts and Recovery of Critical Supply Chain Infrastructure Systems

It is difficult to comprehend the damage done by two Category 5 storms within a two week period. Clearing the territory's ports became a priority in order to begin receiving much needed critical supplies support the recovery efforts. Furthermore, clearing the roadways allowed households access to relief supplies and allowed utility workers access to other damaged critical infrastructure systems, such as power and water systems. Congresswoman Plaskett (2017) had this to say about funding in her testimony to the House Transportation and Infrastructure Committee,

> The islands are also in need of other important recovery funding left out of the most recent disaster bill. For example, it did not include economic development programs, nor additional support for repair of our water infrastructure, seaports, airports, and roadways, all of which has been included in previous disaster relief legislation. With an economy that primarily relies on tourism, the Virgin Islands depends heavily on this infrastructure (Plaskett 2017).

Due to the severity of the storms, Federal and Territorial government agencies, local utilities, and communities required significant coordination to recover critical supply chain systems. Clearing roadways of debris is primarily the responsibility of the DPW; however, residents were the ones to actually clear their neighborhoods and their access to the primary roadways (USVI Hurricane Recovery and Resilience Task Force 2018). The WAPA took several months to clear all downed power-lines from roadways within the territory. This caused some delay in DPW's ability to complete clearance operations. Once DPW removed debris from the roadways, it became the Virgin Islands Waste Management Authority (VIWMA)'s responsibility to clear the debris from the islands (Gajewski 2019). Immediately following the storms, a mandatory curfew was established due to safety concerns and to support repairs to damaged roadways. The curfew was in place from 6 p.m. to 12 p.m. at its most restrictive point causing rush hour like conditions that limited the population's ability to access critical supplies (USVI Hurricane Recovery and Resilience Task Force 2018). In an interview with Megan Frazier (2019), she stated that people made a daily choice to either get gas for their vehicles or generators, food for their families, or ice, but they could not do more than one per day due to traffic restraints and lines at the stores.

Roadway repairs are expected to be ongoing for several years and costs are expected to exceed 100 million dollars. Seaports within the USVI experienced varying levels of damage. The WICO dock was inundated with silt and sand runoff rendering it too shallow for larger vessels to make port (USVI Hurricane Recovery and Resilience Task Force 2018). Over 400 vessels were sunk in the territory's harbors forcing the U.S. Coast Guard (USCG) and VIPA to impose draft restrictions for inbound maritime traffic. It took several months to get the necessary side-scan sonar to properly clear the harbors in order to lift the draft restrictions; however, cargo vessels with shallower drafts were able to return to port within a couple of days following the storms (Brewer and Hatfield 2019).

Shipping companies wished to clear their lay-down yards quickly following the storm in order to receive much needed supplies; however, extensive road damage and increased inbound cargo made the task difficult. Further exacerbating the issue was the loss of electrical power to the area resulting in the shipping companies being unable to verify actual inventory in many of the containers in their lay-down yard. Many of the companies resorted to scheduling shipments via personal cellphone until their company's systems were restored (Frazier 2019).

1.4 Thesis Goals

This thesis focuses on the capacity of the USVI critical supply chain system to deliver food and materials via ports and surface roads. The goal is to assess how USVI food supply chains and transportation systems perform during normal and post-hurricane conditions, and to identify emergency relief stations across the islands that minimize household travel time, maximize supply chain access, and support faster recovery. Ultimately, we seek to explore the interdependent nature of critical infrastructure systems by integrating road, port, and supply access models with power and water distribution models being developed in parallel.

THIS PAGE INTENTIONALLY LEFT BLANK

CHAPTER 2:
Literature Review

The needs of USVI stakeholders to build back better and protect their critical supply chain infrastructure from future disaster requires the integration of several distinct areas of research to develop new models and analysis methods. The USVI Territorial Government lacks data that can inform traffic and supply chain modeling and provide decision-support for worst-case disaster situations. Even with appropriate data, there are idiosyncrasies of the USVI critical supply chain system that are not normally considered in normal traffic and congestion models. Finally, methods developed in the literature for understanding the impacts of crises on mobility tend to not fit the island's remote context, requiring further advancement in this area.

Here, we present a review of relevant literature that informs the creation of appropriate data sets for modeling critical supply chain infrastructure, facilitates development of a roadway congestion model that suits the USVI context and supply chain needs, and incorporates appropriate methods of disaster modeling. We organize this literature into three broad categories: infrastructure functions and interdependencies, traffic and supply models, and disaster impact assessments. We further frame our integrated and USVI-focused research contributions in this context.

2.1 Critical Supply Chain Infrastructure Functions and Interdependencies

Critical supply chains embed multiple, separate infrastructure systems together to provide services. In practice, this means a basic understanding of supply chains relies on various other systems to supply commodities, services, or information in order to operate. The research on interdependent critical infrastructure systems is still nascent, yet informative to the different ways supply chains should be represented in congestion models. Rinaldi et al. (2001) defines four primary classes of interdependencies: physical, cyber, geographic, and logical. In a similar vein, Derrible (2017) discusses the notion that modern infrastructure should not be viewed as a network tree structure, but is better represented by a semi-lattice structure due to its interdependent nature. Lee II et al. (2007) utilizes a network flow model of lower Manhattan in New York city to introduce a scenario that causes major disruptions in the power, telecommunications, and subway systems as a means to demonstrate the use of modeling to inform decisions in support of system restorations. Dixon (2011) uses an adversarial attacker-defender model to investigate the effects of disruptions on notional interdependent infrastructure models. Dickenson (2014) formulates an operational model of interdependent fuel and electric power systems in order to solve the minimum cost for operating both systems. Bunn (2018) investigates an interdependent potable water and electric power distribution model in order to define the key attributes and critical interdependencies of both systems. This thesis focuses on the interdependence of ports and surface road transportation within the USVI.

2.2 Traffic and Supply Chain Models

There are a number of relevant studies that develop models for both roadway systems and port operations.

2.2.1 Roadway Models

Maerivoet and De Moor (2005) provides a thorough review of transportation planning and traffic flow propagation models. They introduce a four-step traffic model with a comparison of static and dynamic traffic assignment methodologies. The four-step model is broken down into trip generation, trip distribution, mode choice or modal split, and traffic assignment. The first step, trip generation, consists of designating trip start locations, known as origins, and trip end locations, known as destinations. Step two, trip distribution, connects trip origins with destinations resulting in a full origin-destination table. If people routinely move by mixed modes of transportation (e.g., bus, private auto, walking), that decision is assigned in step three, mode choice or modal split. Finally, the fourth step determines which routes the travelers are likely to follow from their origins to their destinations. This is referred to as the traffic assignment step.

The Transportation Research Board (2000) Highway Capacity Manual provides a collection of techniques for producing roadway capacity estimates and levels of service for transportation facilities. Sharma et al. (2012) develops a model to present speed-flow analysis under heterogeneous traffic constraints, driving behavior, vehicle characteristics, and traffic controls. Moses and Mtoi (2012) quantitatively compare multiple methods for predicting free flow speed using root mean square error and coefficient of determination calculations.

2.2.2 Port Operations Models

With an economy and workforce depending heavily on imports, it is easy to recognize the vital role that port operations play within the USVI and island territories as a whole. Many studies have been conducted on operations at ports of entry for both island territories and land based facilities. Delacruz (2011) conducted research on the Hawaiian Maritime Transportation System and its ability to recover from unexpected disruptions. Alderson et al. (2012) produced an optimization-based decision support model for evaluating the resilience of the Maritime Transport System responsible for the movement of coal in the Port of Pittsburgh. Mintzer (2014) modeled containerized cargo throughput at the Port of Los Angeles with particular interest in identifying the types of disruptions that would reduce throughput to less than 25 percent of normal capacity. Finally, Wenke (2015) considered vulnerabilities to movement of containerized cargo and fuel through the Port of Anchorage. The focus of this thesis will be confined to the movement of critical supplies on the territory's surface roads from the ports of entry to various supply access points.

2.3 Methods for Assessing the Impacts of Disasters on Critical Supply Chain Infrastructure Systems

The two primary ways to consider the impact of disaster on critical supply chains are either with disaster response models that focus on evacuation and relief prepositioning and with infrastructure vulnerability assessments that focus on traffic and supply response to worst-case roadway disruptions.

2.3.1 Disaster Response Models

Evacuation Models

Lahmar et al. (2006) uses a macroscopic approach to model hurricane evacuation, and Yusoff et al. (2008) provides a survey of various macroscopic evacuation models. Yuhas (2011) utilizes these models to examine multiple evacuation scenarios near Sacramento, California due to flooding, while Malveo (2013) investigates the role congestion plays on a population's ability to successfully evacuate an area prior to a natural disaster. While of interest, evacuation models have little bearing on island nations, such as the USVI, where evacuation may not be feasible.

Prepositioning Models

Much work has been done in the area of prepositioning. Of particular interest, McCall (2006) utilizes an optimization model to recommend prepositioning of humanitarian assistance pack-up kits to support the U.S.'s Pacific theater of operations. Heidtke (2007) utilizes the Pre-positioning Optimization Model to investigate the resource gap that exists between exhaustion of state or local resources and the receipt of federal support in the aftermath of a natural disaster. Farlow (2011) utilizes the same model to recommend relief locations in the Sacramento, California area to support emergency response immediately following a flooding disaster. Apte (2011) provides a survey of operational and strategic considerations for prepositioning humanitarian assistance in the event of natural disasters, while Sabbaghtorkan et al. (2019) provides a broad overview of the research conducted in the area from 2000 to 2018.

2.3.2 Critical Supply Chain Vulnerability Assessments

Network Interdiction for Critical Infrastructure

Alderson et al. (2013) uses specific examples to show that our initial reaction is often incorrect when it comes to identifying vital components or arcs in a system. They conclude by stating that the criticality of components is dependent on which combination of individual components are affected and not the individual components themselves. Alderson et al. (2014) demonstrates a defender-attacker-defender framework for building and solving optimization models as a method of analyzing and improving critical infrastructure systems. Alderson et al. (2015) defines infrastructure resilience in a manner that views the operation of the infrastructure as a system of interacting components that can be quantitatively analyzed. By modeling critical infrastructure as a system, they are able to conduct "what-if" analysis to evaluate the results on the system operation from changes in the system components. Alderson et al. (2017b) demonstrates this technique on the bridges and roadways in the San Francisco Bay region of California.

2.4 Our Contribution

We model the transportation infrastructure of the USVI using a multi-commodity equilibrium model of congestion based on the territory's road conditions and designated origin-destination pairings of interest. We seek to calculate round trip times between households and supply access points with special interest on the impact of mandated curfews. Furthermore, we estimate round trip times to supply access points from shipping ports to calculate expected delivery volumes for the supply access points.

The primary contributions of this thesis are (i) development of surface road network, port, and supply access data useful for supply chain capacity analysis, (ii) formulating an operational model of the USVI critical supply chain system that measures flows of supplies and local communities to and from local access points, and (iii) facilitating decision-making to support local needs and expedited recovery following future large-scale disasters.

THIS PAGE INTENTIONALLY LEFT BLANK

CHAPTER 3:
Model

Based on literature review and stakeholder needs, this thesis performs three modeling and analysis tasks:

1. **Data Curation and Network Construction:** We construct a dataset useful for the analysis of traffic congestion and shipping supplies on surface roads within the island of St. Croix.
2. **Model Formulation and Implementation:** We develop a four-stage traffic model that measures the round-trip travel times for supplies and civilians to reach locations of distribution during normal and degraded traffic conditions.
3. **Last-Mile Supply Chain Analysis:** Using data and models to determine the capability of surface roads in St. Croix to enable access to disaster relief supplies, we identify which St. Croix communities may have the greatest difficulty accessing locations of distribution during normal and worst-case situations.

Figure 3.1 depicts the workflow, software tools, and file types used throughout the thesis process. The workflow is an iterative process and is repeated throughout the execution of the thesis.

3.1 Data Curation and Network Construction

Currently, the USVI does not have an up-to-date inventory of road assets or building and repair assets located within the territory. The USVI Hurricane Recovery and Resilience Task Force (2018) noted the need to "develop and implement asset and resource management system for all territorial roadways" and documented as much under Transportation Initiative 19. Therefore, our starting point was to collect and curate a dataset in order to support our research and any future research on the roadways within the USVI.

3.1.1 Ports and Supply Access Points

Our starting point in manipulating data made use of QGIS (QGIS Development Team 2019), Google Maps (Google, Inc. 2019), and Python GeoPandas (GeoPandas Development Team

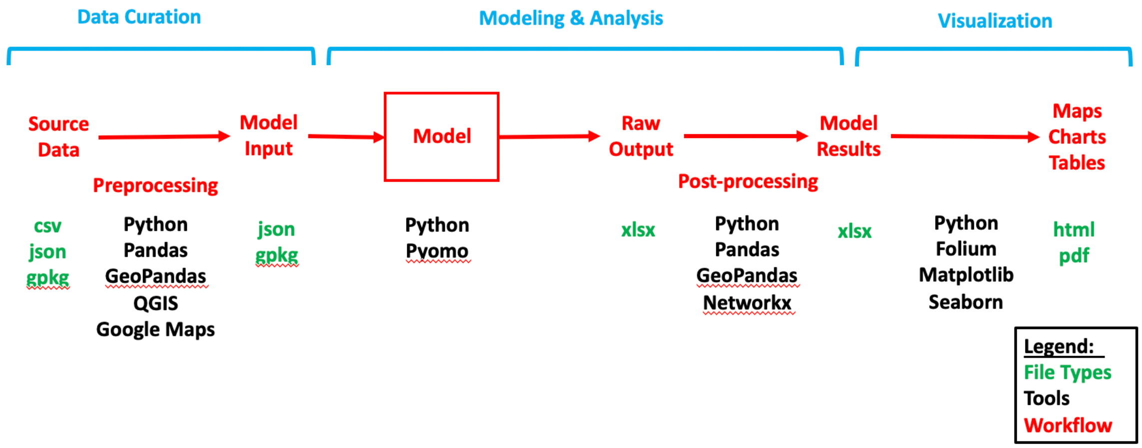

Figure 3.1. Diagram of project workflow. Light blue indicates the three modeling and analysis tasks. Red represents the project workflow. Green identifies the file types used throughout the workflow. Finally, black indicates the software tools used during the project.

2019) software tools. We plotted initial points of interest (e.g., ports, stores, and gas stations) using Google Maps and exported them as .kml files, which were then read into GeoPandas for further manipulation. The files were exported as .gpkg (geopackage) files for use in QGIS, where they were plotted on an OpenStreetMap base layer (OpenStreetMap contributors 2019) using Coordinate Reference System (CRS) 4326 as defined by the European Petroleum Search Group (EPSG), commonly referred to as EPSG:4326. Figure 3.2 shows resulting port and supply access points.

3.1.2 Estates and Population Centers

The USVI uses legally defined *estates* that serve as, but are smaller than, traditional Census Subdistricts for the purpose of census tracking. These estate boundaries are provided to the U.S. Census Bureau prior to the Dicennial Census by the USVI Office of the Lieutenant Governor. The U.S. Census Bureau (2018) maintains a database of defined estate shapefiles with associated population counts. To establish initial population nodes, we plot the estate shapefiles in QGIS utilizing CRS EPSG:4326 and create centroids for each shape utilizing the geometry tools included in QGIS. We then added a "Google Sat Hybrid" base layer to the QGIS plot in order to visually inspect and place the population nodes over known neighborhoods. If multiple neighborhoods, with separate surface road access, existed within

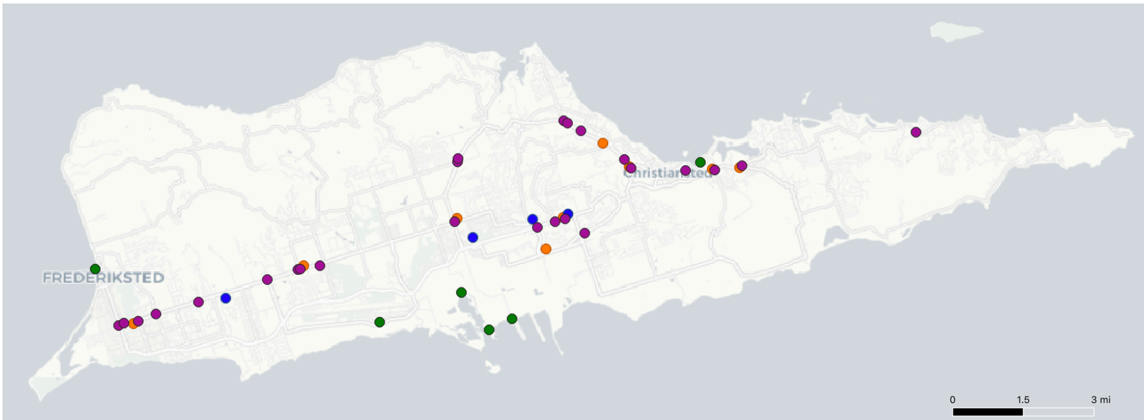

Figure 3.2. Ports and supply access points plotted in QGIS utilizing CRS EPSG:4326. Ports are represented by green points, gas stations purple, grocery stores orange, and hardware/miscellaneous stores blue. Created using QGIS Development Team (2019) on 12 August 2019.

a given estate, we created additional population nodes within the estate and the total estate population count was uniformly distributed across all population nodes within the estate. Figure 3.3 shows the final population centers and estate boundaries for St. Croix.

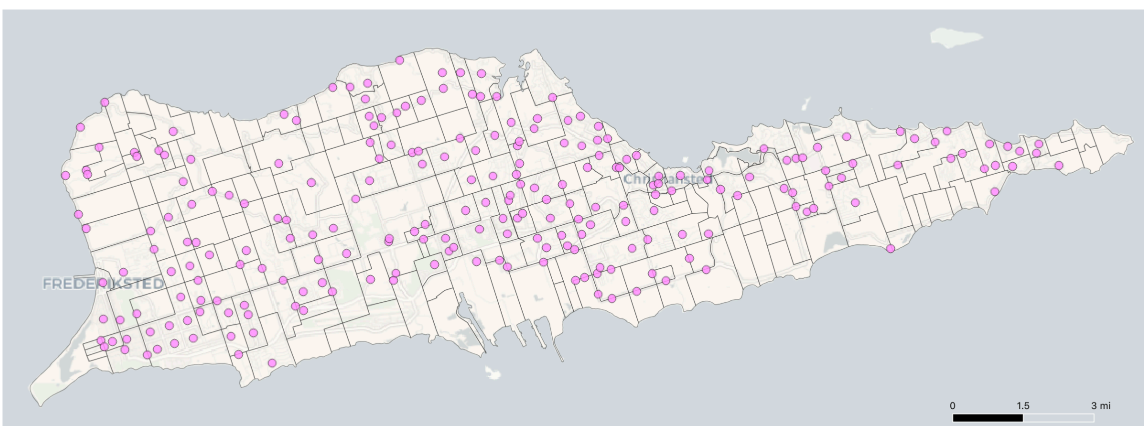

Figure 3.3. U.S. Census Bureau estate boundaries are represented by gray boxes. The pink dots represent the final population centers following visual confirmation utilizing QGIS with "Google Sat Hybrid" base layer. Created using QGIS Development Team (2019) on 12 August 2019.

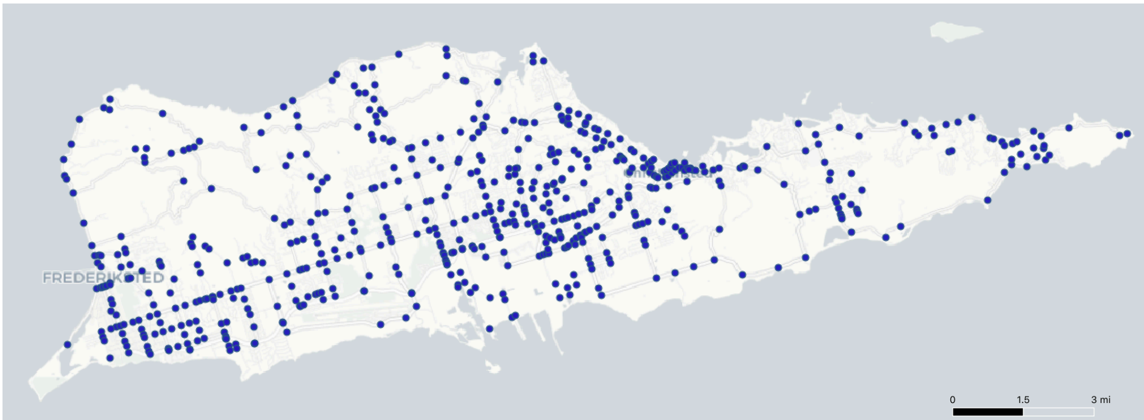

Figure 3.4. Dots indicate location of transshipment nodes established to build the surface road network on St. Croix. Created using QGIS Development Team (2019) on 12 August 2019.

3.1.3 Transshipment Nodes

Initial transshipment nodes were created by placing markers on major intersections of an OpenStreetMap base layer in QGIS utilizing CRS EPSG:4326. Intermediate transshipment nodes were added along major roadways to increase fidelity of the network. Finally, nodes were added in locations in order to facilitate access to the network from the previously established ports, supply access points, and population centers. Figure 3.4 shows the locations of the transshipment nodes for St. Croix.

3.1.4 Network Construction

We begin network construction by creating a distance matrix consisting of calculated distances from each node to every other node. We use a haversine function to calculate the great-circle distances between any given two points based on their longitudes and latitudes. The haversine distance gives us a rough estimate to use in finding adjacent nodes with the recognition that actual distances between nodes will differ due to curvatures in the actual roads. The distances within the matrix will be utilized to assign "cost" values to each of the network arcs. We then create a dictionary with each node as the key and its 20-nearest neighbors as the value. This dictionary is then manually compared to nodes plotted in QGIS in order to visually determine node adjacency to build an adjacency list. With the verified adjacency list, we are able to construct the network depicted in Figure 3.5.

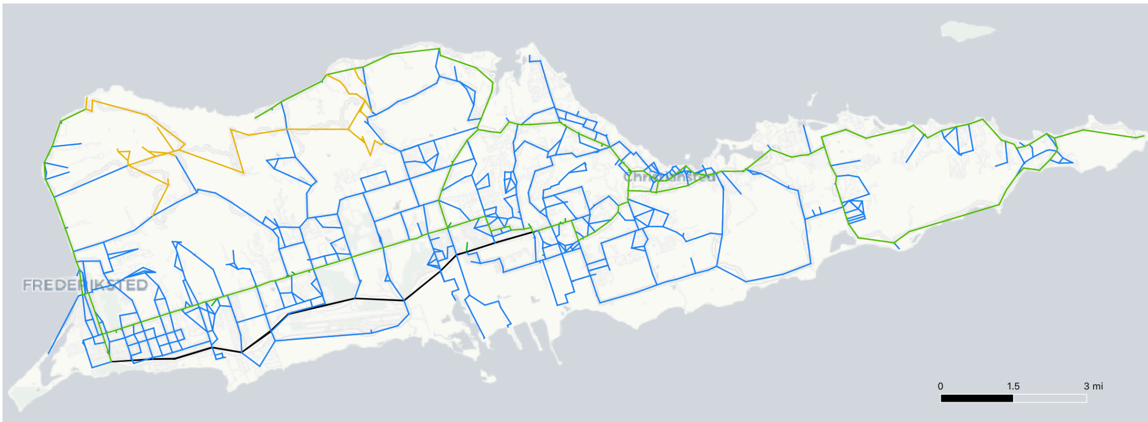

Figure 3.5. Arcs representing surface road network on St. Croix. Yellow lines represent dirt roads. Green lines represent rural roads. Blue lines represent urban roads. Black lines represent highways. Created using QGIS Development Team (2019) on 12 August 2019.

To test the network and gauge the amount of error introduced by using haversine distances, we compared a shortest-path distance calculated using Dijkstra's algorithm with results from Google Maps. We use the western most port node as the origin and the eastern most supply access point as the destination in an attempt to induce the most amount of error within the network. The Dijkstra's shortest-path returned a calculated distance of 31.345 kilometers and Google Maps returned a calculated distance of 31.5 kilometers giving us an estimated error of approximately 1.1 percent.

3.2 Four Step Traffic Assignment

We follow the four-step modeling process discussed by Maerivoet and De Moor (2005).

3.2.1 Step 1: Trip Generation

Trip generation begins with the assignment of origins and destinations. For the purposes of our model, the ports and population centers serve as our origins and the supply access points serve as our destinations. Furthermore, we are specifically concerned with the number of vehicles we expect to complete a round-trip trip from origin to destination. This requires the calculation the expected number of vehicles for each origin node.

Table 3.1. Calculated vehicle distribution per household based on 2010 Census Date for the island of St. Croix. Source: USVI Department of Public Works (2014).

Vehicles Per Household	Vehicle Count	Percent of Total
None	3530	18%
1	8690	44%
2	5420	27%
3 or more	2130	11%

Population Center Vehicle Count

Based on 2010 Census Data, the average household size for St. Croix is 2.5 people and the distribution for the number of vehicles per household can be seen in Table 3.1 (USVI Department of Public Works 2014).

From this, we calculate the number of households for each population node by dividing the population count for the node by 2.5 and rounding up to the nearest integer value. We then calculate the expected number of vehicles per household within the population node by utilizing the vehicle distribution in Table 3.1 and rounding down to the nearest integer value. We treat the "3 or more" vehicles category as simply three vehicles for the purpose of this study.

Port Vehicle Count

For the purpose of this thesis, we simplify to two types of vehicles originating at the port nodes: containerized cargo from the Transshipment Port and fuel trucks from the Limetree Bay Terminal adjacent to the Transshipment Port.

Crowley Shipping on St. Croix receives approximately 100 containers of goods every Monday and an additional 60 containers on Wednesday (Frazier 2019). We assume similar numbers for Tropical Shipping and Priority RO-RO (Calderon 2019). Given a six-day work week, we calculate approximately 80 containerized deliveries per day with each company operating roughly eight trucks per day.

According to Hendrickson (2019), all fuels for the island of St. Croix are delivered by three private haulers; St. Croix Fuel, Petrol Max, or Bunkers of St. Croix, Inc. Under normal operations, each gas station receives fuel no more than twice per week. Bunkers of St. Croix has two stations that receive fuel once per week and six stations that receive fuel twice per week. Each private hauler handles approximately the same volume of deliveries per week. We assume normal delivery operations five days a week resulting in 24 fuel deliveries per day. We assume each truck takes approximately one hour to either load or unload fuel. Assuming an eight hour work day, we calculate that each hauler operates three vehicles per day.

3.2.2 Step 2: Trip Distribution

Once trips have been generated, we connect the origins to destinations by distributing the trips resulting in an origin-destination table. The full table consists of 38 rows representing the possible destinations (supply access nodes), 234 columns representing the possible origins (population centers and transshipment port node), and values reflecting the vehicle count for each origin node.

3.2.3 Step 3: Mode Choice or Modal Split

Only 5.8 percent of the population utilize public transportation for work on the island of St. Croix, while 69.8 percent choose to drive alone (USVI Department of Public Works 2014). Based on this information, we assume all trips take place by car utilizing the maximum number of available vehicles per origin node.

3.2.4 Step 4: Traffic Assignment

The final step of the model is to establish which routes travelers follow from their origin to their destination. Initially, we restrict the population centers to their nearest supply access points by type. We assume that traffic from each population center is distributed with 40% traveling to gas stations, 40% to grocery stores, and the remaining 20% to hardware or miscellaneous stores. We further assign only a single trip per vehicle originating from any given population center based on firsthand accounts of population behavior following Hurricanes Irma and Maria (Frazier 2019). Furthermore, we assume a single delivery to each supply access point.

Finally, and most importantly, we assume that there are two ways that individuals make the decision on which supply access points they travel to: 1) there is no cooperation between individuals and decisions are only being made with self-interest in mind, and 2) there is perfect knowledge among individuals and decisions are made with information sharing. In the first situation, all individuals will travel to the nearest supply access point that serves their supply need (gas, food, or hardware/misc.). In the second situation, individuals travel to the supply access point that has the shortest travel time given roadway congestion.

3.3 Model Formulation

We build a network flow optimization model to study congestion on surface roads in St. Croix. We model the St. Croix network as a minimum cost, multi-commodity flow problem with 887 nodes, 2353 directed arcs, and 1474 commodities representing unique origin-destination pairings.

Indices and Sets

$i \in N$	nodes (alias j, s, t)
$(i, j) \in A \subseteq N \times N$	arcs
$(s, t) \in D \subseteq N \times N$	set of all origin and destination pairs
$r \in R$	sections for piece-wise linear approximation
	($\bar{r}$ = total number of sections)
$Out_i \subset A$	set of all outbound arcs from node i
$In_i \subset A$	set of all inbound arcs to node i

Data [units]

b_{st}	supply rate at node s destined for node t
	($b_{st} < 0$ represents demand) [vehicles per hour (VPH)]
u_{ij}	nominal capacity of arc (i, j) [VPH]
s_{ij}	unrestricted speed of arc (i, j) [miles per hour (MPH)]
d_{ij}	length of arc (i, j) [miles]
$avail_{ij}$	1 if arc (i, j) is available for use, 0 otherwise
q	maximum intended travel window for all
	origin-destination round trips [hours]

Calculated Data [units]

λ_{ij}	interval width on arc (i, j) for calculating piecewise linear congestion $\lambda_{ij} = 2u_{ij}/\bar{r}$
h_{ijr}	total travel time for all vehicles traversing segment r on arc (i, j) $h_{ijr} = \left(r\lambda_{ij}\right)\left(\frac{d_{ij}}{s_{ij}}\right)\left(1 + 0.15\left(\frac{r\lambda_{ij}}{u_{ij}}\right)^4\right)$
$slope_{ijr}$	slope of segment r for arc (i, j) $slope_{ijr} = \frac{h_{ijr} - h_{ijr-1}}{\lambda_{ij}}$
$intercept_{ijr}$	y intercept of line section r for arc (i, j) $intercept_{ijr} = -slope_{ijr}(r\lambda_{ij}) + h_{ijr-1}$

Decision Variables [units]

Y_{stij}	flow rate of supply originating at node s destined for node t transiting arc (i, j) [VPH]
Y_{ij}	total flow rate transiting arc (i, j) [VPH]
Z_{ij}	vehicles on arc (i, j) [vehicles]
$Dropped_{st}$	dropped quantity of supply originating at node s destined for node t [vehicles]
$Excess_{st}$	excess quantity of demand originating at node s destined for node t [vehicles]

Formulation

$$\min_{Y,Z,Dropped,Excess} \quad \sum_{(i,j)\in A} Z_{ij} + \sum_{(s,t)\in D, s\neq t} \frac{q}{2} \cdot Dropped_{st} \tag{3.1}$$

$$
\begin{aligned}
\text{s.t.} \quad & \sum_{(i,j)\in Out_i} Y_{stij} - \sum_{(j,i)\in In_i} Y_{stji} + Dropped_{st} = b_{st} && \forall i \in N, (s,t) \in D, i = s && (3.2)\\
& \sum_{(i,j)\in Out_i} Y_{stij} - \sum_{(j,i)\in In_i} Y_{stji} - Excess_{st} = -b_{st} && \forall i \in N, (s,t) \in D, i = t && (3.3)\\
& \sum_{(i,j)\in Out_i} Y_{stij} - \sum_{(j,i)\in In_i} Y_{stji} = 0 && \forall i \in N, (s,t) \in D, i \neq s, i \neq t && (3.4)\\
& Y_{stij} \leq b_{st} && \forall (s,t) \in D, (i,j) \in A && (3.5)\\
& Y_{ij} = \sum_{s,t\in D} Y_{stij} && \forall (i,j) \in A && (3.6)\\
& Y_{ij} \leq 2u_{ij} avail_{ij} && \forall (i,j) \in A && (3.7)\\
& Z_{ij} \geq intercept_{ijr} + slope_{ijr} \cdot Y_{ij} && \forall (i,j) \in A, \forall r \in R && (3.8)\\
& Excess_{st} = Excess_{ts} && \forall (s,t) \in D && (3.9)\\
& Dropped_{st} = Dropped_{ts} && \forall (s,t) \in D && (3.10)\\
& Y_{stij}, Y_{ij}, Z_{ij}, Dropped_{st}, Excess_{st} \geq 0 && \forall (i,j) \in A, (s,t) \in D && (3.11)
\end{aligned}
$$

Discussion

The objective function (3.1) combines the total cost (in vehicle-hours) of placing traffic along each arc (i, j) and the total penalty for any dropped flow. The penalty for dropped flow is a combination of the quantity of vehicles that do not travel due to congestion weighted by half of the maximum allowable round-trip travel time. Constraints (3.2), (3.3), and (3.4) enforce the balance-of-flow for supply nodes, demand nodes, and transshipment nodes, respectively. Constraints (3.5) enforce the capacity of flow for supply (s, t) on arc (i, j). Constraints (3.6) calculate the intermediate variable for total flow on each arc. Constraints (3.7) require the total flow on arc (i, j) to be less than its capacity. Constraints (3.8) require that the total travel time on each arc (i, j) be lower-bounded by the piece-wise sections $r \in R$. Constraints (3.9) and (3.10) enforce symmetry for elastic variables. Stipulations (3.11) specify nonnegativity on the other decision variables.

The optimization model involves traffic *rates*. In order to examine the capability of the road system to support traffic flows, we assume all available traffic departs from the origins within the first hour. This results in a (worst-case) supply rate at a given location equal to the supply of vehicles at that location. We assume an intended three-hour travel window for one-way trips from origin to destination. This serves to approximate a six-hour intended maximum travel window allowing for round trips from origin to destination and returning to origin ($q = 6$). We assume people decide to stay home if the travel time for a single one-way trip exceeds six hours in duration.

Due to the nonlinear congestion, the actual round trip travel time can exceed the intended maximum travel window. We expect this to happen only as we approach $Y_{ij} = 2u_{ij}$.

A Piece-wise Linear Approximation for the Travel-Time Function

Given total flow Y_{ij}, the average travel time along arc (i, j) is given by the Bureau of Public Roads (BPR) function (Peeta et al. 2015), which is defined as $f_{ij}(Y_{ij}) = \frac{d_{ij}}{s_{ij}}\left(1 + 0.15\left(\frac{Y_{ij}}{u_{ij}}\right)^4\right)$. Then, the total travel "cost" (in vehicle-hours) on arc (i, j) is the product of its total flow Y_{ij} and the travel time $f_{ij}(Y_{ij})$, which is nonlinear. To use mixed-integer linear programming, we bound the total travel time Z_{ij} from below by a sequence of linear approximations $r \in R$ as defined in Constraints (3.8). We follow the convention in Alderson et al. (2017b) and use $\bar{r} = 40$, which yields a suitable approximation given other definitions.

3.4 Computation and Post-processing

We implement and solve this model on a MacBook Pro with 16 gigabytes of memory and an Intel Core i7 processor. The full network model of St. Croix has a run time of approximately two hours and 21 minutes.

Removal of artificial flows (cycles)

The formulation in Section 3.3 is an equilibrium model, and as such it tends to seek flows that "balance" the objective function cost across all of the various routes. As a result, it is possible that small flows exist along routes that might not follow the shortest path as measured by time or distance. It also does not explicitly prevent cycles in flow.

We perform post-processing on the "raw" model output to remove artificial flows. Specifically, for each (s, t) commodity, we extract the flows as a standalone network and (1) make sure that traffic correctly makes its way from origin to destination, and (2) remove any artificial flows, such as cycles. The resulting network flows are then ready for visualization and reporting.

3.5 Demonstrating Last-Mile Supply Chain Analysis with a Simple Road Network

We present a simple network to demonstrate the data structure and model execution (Figure 3.6). Nodes, and their associated attributes, are adapted from nodes within the surface road network of St. Croix.

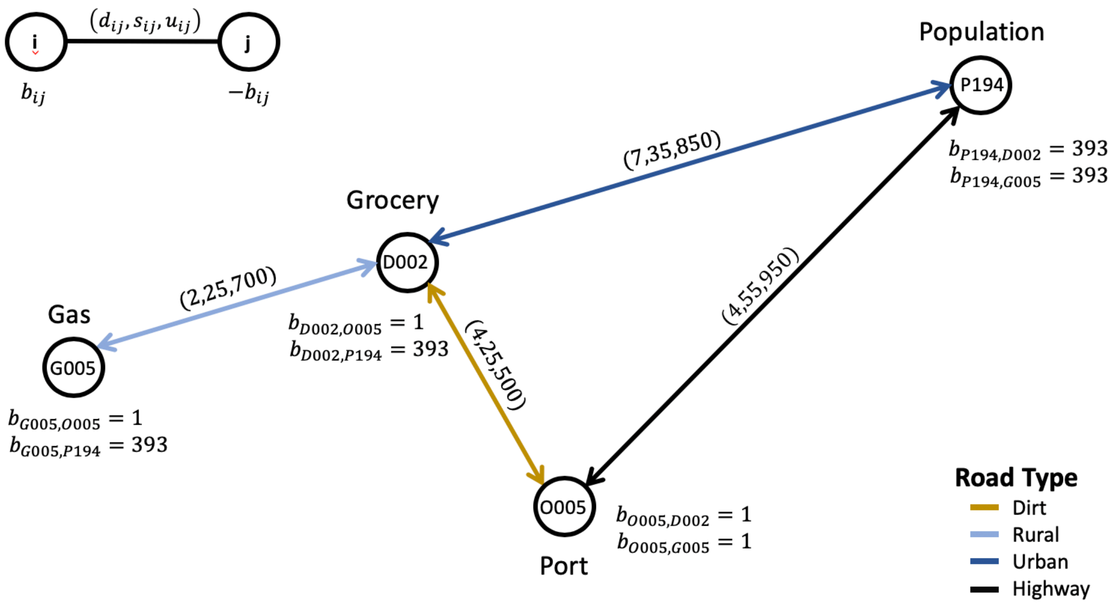

Figure 3.6. A simple road network to demonstrate the functionality of the model. The nodes are separated into origins (e.g., Population, Port) and destinations (e.g., Grocery, Gas). The arcs are subdivided into separate categories based on road type (e.g., Dirt, Rural, Urban, Highway). The arcs are labeled with (Distance, Speed, Capacity). The nodes are labeled with supply rates for each applicable commodity.

3.5.1 Model Inputs

To initiate the model build, we provide a set of supply rates for each commodity (s, t), as well as capacity, speed, distance, and availability data for each arc (i, j). The supply rate data (annotated on each origin node in Figure 3.6) assumes 40% of a population center's vehicles travel to grocery stores, 40% travel to gas stations, and the remaining 20% to hardware or miscellaneous stores. Furthermore, we assume the port provides a single vehicle to each supply access location.

Capacity flow rates (as annotated in Figure 3.6) are assigned to each arc (i, j) based on the road type classification. Roads in the network are classified into four broad categories; dirt, rural, urban, and highway. General roadway flow capacity limits are derived from Zegeer et al. (2008) and are assumed to be 1000 VPH per lane, 1600 VPH per lane, 1700 VPH per lane, and 1900 VPH per lane for dirt, rural, urban, and highway road classifications respectively. For the simple road network we scale the capacity flow values by half in order to create conditions that yield congestion.

Similar to the capacity flow rates, unrestricted speed limits are annotated on Figure 3.6 and are assigned based on general road classification within the territory. DPW utilizes 25 MPH, 35 MPH, and 55 MPH for roads designated dirt and urban, rural, and highway respectively (Gajewski 2019).

Distance values are assigned to each arc (i, j) using a straight-line distance between two adjacent nodes based on their location in terms of latitude and longitude. These values are also annotated on each undirected edge in Figure 3.6. We acknowledge that using straight line distances introduces minor inaccuracy into the model, but feel the model simplicity gained from having fewer arc sections justifies the minor decrease in total accuracy.

3.5.2 Model Outputs and Analysis

The simple road network solves for the optimum network flow (in a run time of approximately 0.73 seconds) to meet origin-destination pairing demand requirements at the minimum possible cost.

Analysis of Arcs

For each arc (i, j), we calculate the flow to capacity ratio, travel times based on congestion build-up, and the resulting arc travel speed based on the same congestion (Table 3.2).

We use the data in Table 3.2 to map the flow-to-capacity ratios on the simple road network (Figure 3.7). The darker colors represent undirected edges with higher flow-to-capacity ratios. These higher flow ratio edges represent areas of higher congestion within the network.

We use the BPR function from Peeta et al. (2015) to calculate actual travel times resulting

Table 3.2. We solve the model for the optimum flow (Y_{ij}) through the network to meet demand requirements while minimizing costs. We use the flow results to calculate flow-to-capacity ratios ($\frac{Y_{ij}}{u_{ij}}$), travel times restricted by congestion ($f_{ij}(Y_{ij})$), and the resulting reduction in arc transit speeds ($\frac{d_{ij}}{f_{ij}(Y_{ij})}$).

i	j	Y_{ij}	u_{ij}	$\frac{Y_{ij}}{u_{ij}}$	s_{ij}	$\frac{d_{ij}}{s_{ij}}$	$f_{ij}(Y_{ij})$	$\frac{d_{ij}}{f_{ij}(Y_{ij})}$
P194	D002	595	700	0.850	35	0.199	0.214	32
P194	O005	190	950	0.201	55	0.076	0.076	55
O005	P194	190	950	0.201	55	0.076	0.076	55
O005	D002	192	500	0.386	25	0.175	0.175	25
D002	O005	192	500	0.386	25	0.175	0.175	25
D002	P194	595	700	0.850	35	0.199	0.214	32
D002	G005	394	850	0.464	25	0.090	0.091	25
G005	D002	394	850	0.464	25	0.090	0.091	25

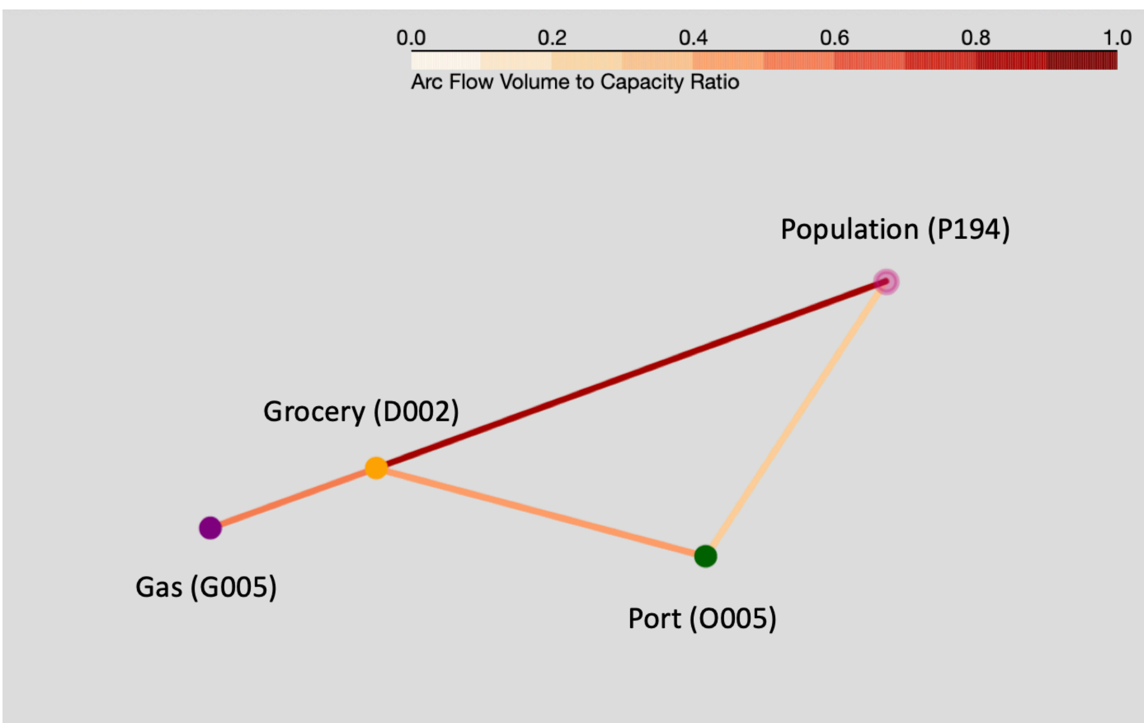

Figure 3.7. We calculate the ratio of flow-to-congestion for each directed arc (i, j). Darker colors represent arcs with higher flow-to-capacity ratios indicating increased congestion due to a greater volume of traffic flow.

from aggregated congestion within the simple road network (Table 3.2). Figure 3.8 shows the absolute difference between unrestricted travel times and travel times have been restricted based on congestion. We note that commodities within this simple network experience a one-minute increase in travel time, while only a single commodity experienced no increase in travel time.

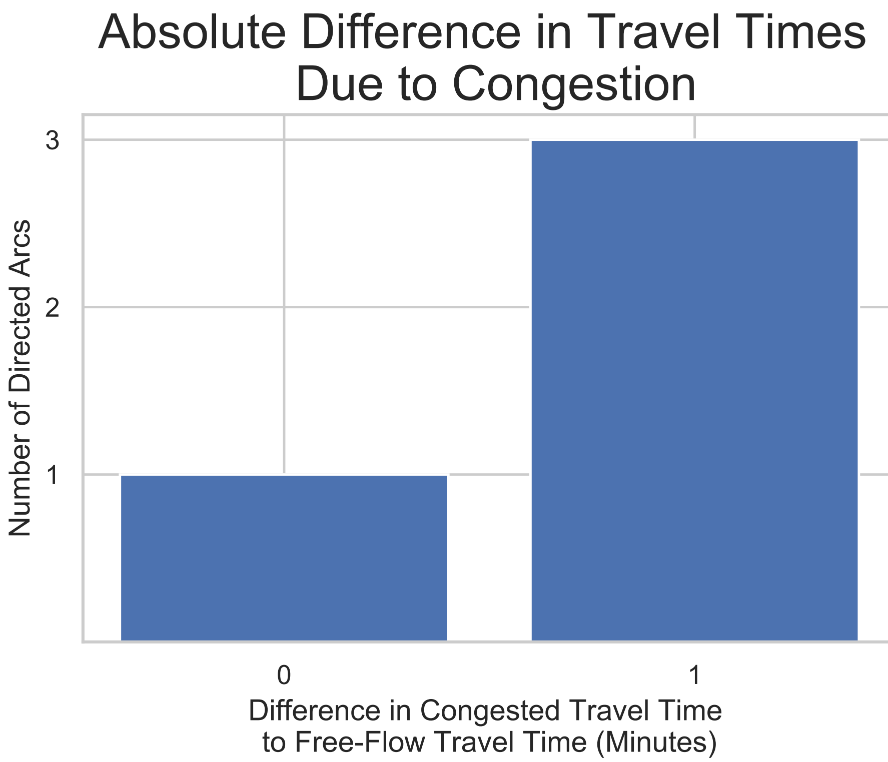

Figure 3.8. We calculate the absolute increase in restricted travel times due to congestion for each directed arc (i, j). We note that three arcs experienced a one-minute increase in travel time due to congestion, while only a single arc experienced no increase in travel time.

The restricted travel times are then used to calculate adjusted travel speeds for each directed arc (i, j) (Table 3.2). Figure (3.9) shows the absolute difference in travel speeds resulting from the aggregation of congestion within the system. We note that two directed arcs within the system experience a three-MPH decrease in travel speed across their length.

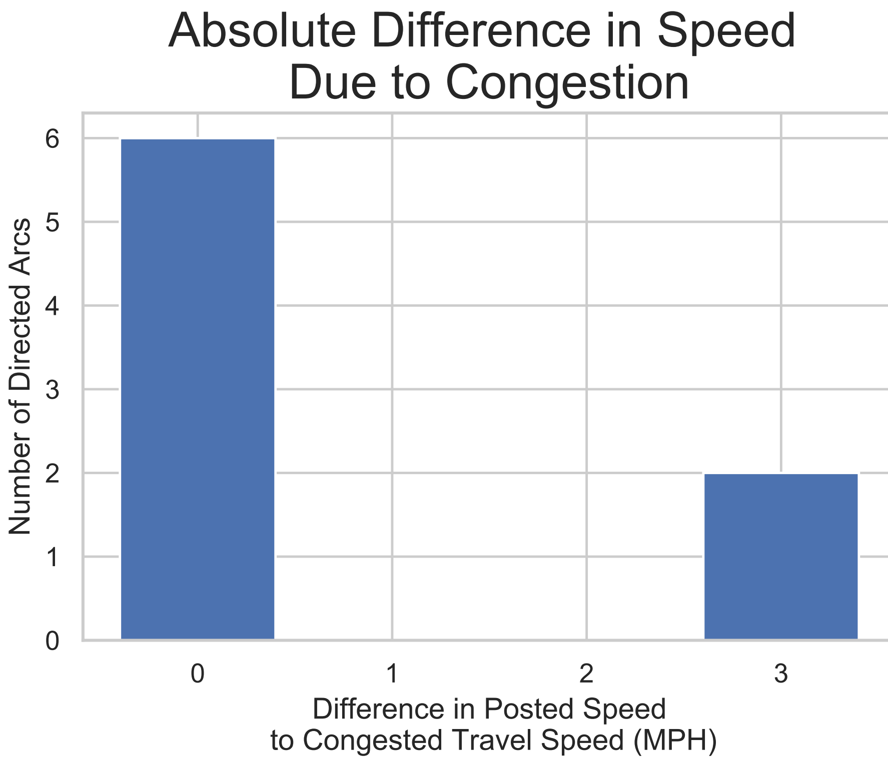

Figure 3.9. We calculate the absolute reduction in restricted travel speeds due to congestion for each directed arc (i, j). We note that two arcs experienced a 3-MPH reduction in travel speed due to congestion, while six arcs experienced no reduction in travel speed.

Analysis of Commodities

Aside from general traffic flow through the network, we are interested in the network's ability to meet the desired demands for each individual commodity in the system. Table 3.3 demonstrates our ability to define traffic flows, distances travelled, and travel times for the various commodities. From this, we can begin to evaluate which commodities must travel the furthest distances, or which commodities have the longest travel times due to accumulation of congestion along their routes.

Figure 3.10 shows the longest travel times for each origin by supply access destination. We note that the longest travel time is 18 minutes for the "P194-Population" origin going to the "G005-Gas" destination. Of interest is fact that the longest travel time for each of the origins is to the same destination location and that origin "P194-Population" has the longest travel times regardless of destination.

Finally, we geospatially represent the longest travel time for a commodity in Figure 3.11. In this representation we color the arcs associated with the longest travel time to match the destination coloring, in this case purple represents the gas stations within the network. The remaining arcs are rendered in green.

Table 3.3. We look at specific metrics for each commodity type (s,t) within the system. Specifically, we are interested in the type of stores filling the demand, the total flow of each commodity($\sum_{st} Y_{stij}$), the distance each commodity must travel (d_{ij}), and the various travel times associated with each commodity.

s	(s,t)	Destination Name	Store Type	$\sum_{st} Y_{stij}$	d_{ij}	$\frac{d_{ij}}{s_{ij}}$	$f_{ij}(Y_{ij})$
O005-Port	('O005', 'D002')	D002-Grocery	grocery	1	4	10	11
O005-Port	('O005', 'G005')	G005-Gas	gas	1	7	16	16
P194-Population	('P194', 'D999')	D002-Grocery	grocery	393	7	12	13
P194-Population	('P194', 'G999')	G005-Gas	gas	393	9	17	18

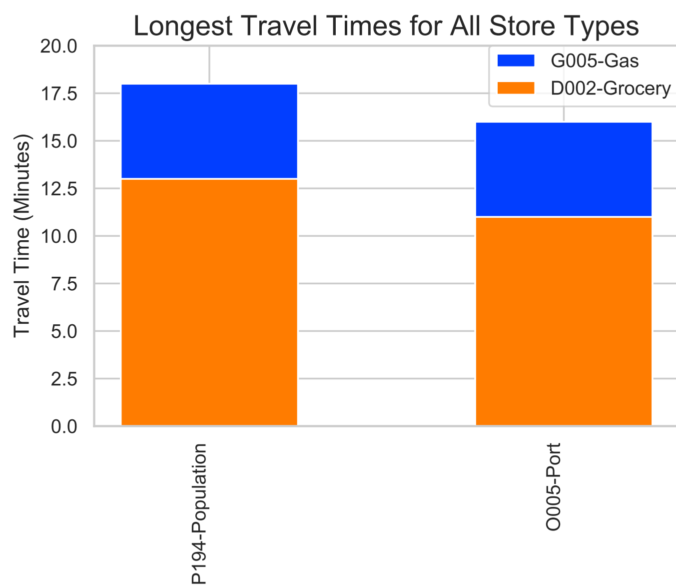

Figure 3.10. Longest travel times for the simple road network. The top of each bar indicates travel time in minutes to each supply access point from each origin. We note that the longest travel time is from the population node "P194-Population" to the supply access point "G005-Gas" at a time of 18 minutes.

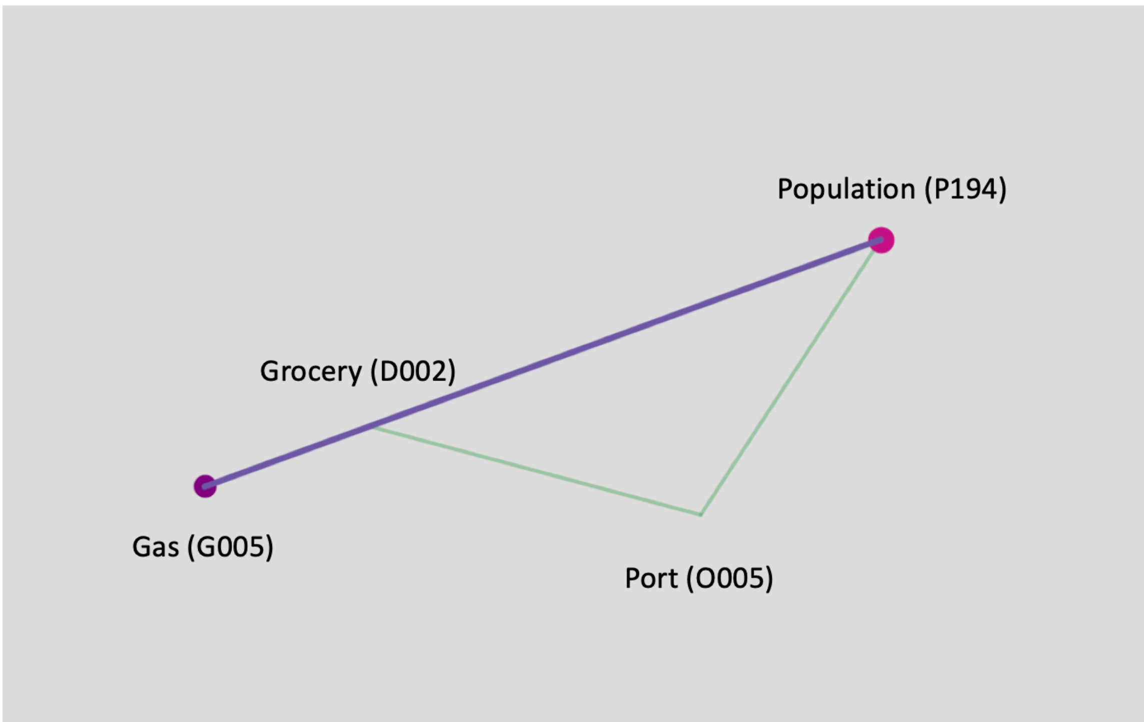

Figure 3.11. Geospatial representation of the simple network model. The arcs on the longest path are highlighted purple to match the destination designation, which in this case is "gas." The remaining arcs in the system are rendered in green. For emphasis, we only render the origin-destination nodes for the longest travel route.

CHAPTER 4:
Analysis and Results

We apply the model from Section 3.3 to the island of St. Croix. We consider a total of 234 origins (233 Estates and one Port) and 38 destinations (supply access points) that are connected over a network of 2353 road segments. As a point of reference, the island of St. Croix is only 19 miles long, and under ideal conditions, it takes 45 minutes to drive from one end to the other. We address several questions in turn:

1. For populations, what are the resulting round-trip times and congestion when travelers pick their destinations "selfishly"?
2. For populations, what are the resulting round-trip times and congestion when traveler destinations are "coordinated"?
3. For the port, what are the resulting travel times under "selfish" and "coordinated" traffic patterns?
4. Which road segments, if blocked, have the potential to create the most congestion and hardship on travelers?
5. What other analyses are possible with our model?

As with our analysis for the simple network in Section 3.5, we make several assumptions regarding traffic demand throughout this study. First, we assume that traffic from each population center is distributed with 40% of vehicles traveling to gas stations, 40% of vehicles to grocery stores, and the remaining 20% of vehicles to hardware or miscellaneous stores. Second, we assume only a single trip per vehicle originating from any given population center. Round trip times only include transit times from point of origin to destination. Service times at the destination are not included in the calculation of the travel times. Finally, in order to calculate the round-trip time from the port, we include only a single delivery to each supply access point.

4.1 Population Travel Times: "Selfish" Routing

The overall traffic demand for the island depends on the choice of destination for each traveler. We begin with the simple case where each traveler chooses to visit their nearest supply

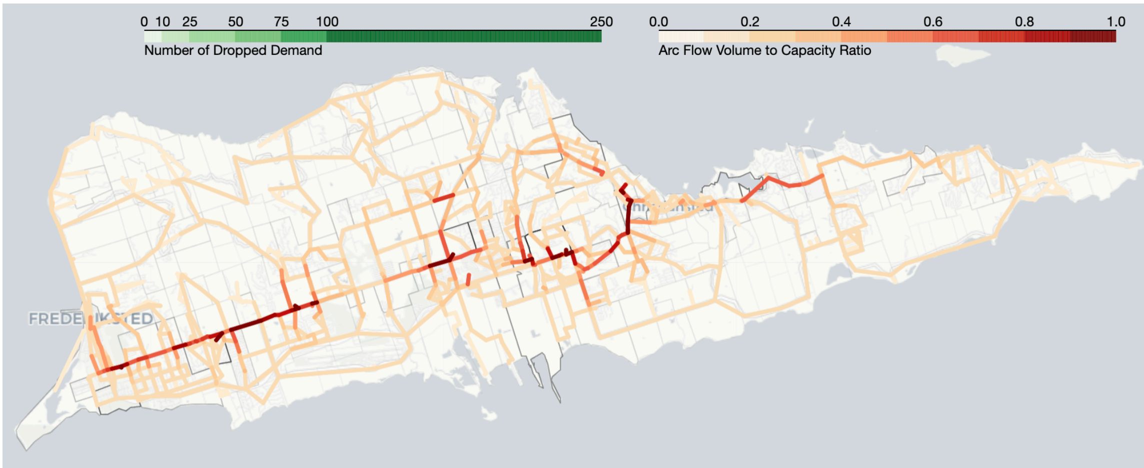

Figure 4.1. Map of flow ratios given "selfish" routing. Arcs are displayed according to their flow-to-capacity ratios. Higher ratios indicate higher congestion and are depicted by darker colors. If any estates have dropped demand, they are depicted in green with darker colors indicating higher levels of dropped demand (there are none in this scenario). Created using QGIS Development Team (2019) on 19 September 2019.

access point, a situation we term "selfish routing" because it reflects the uncoordinated effort of each traveler to minimize their travel time.

Figure 4.1 shows the resulting road congestion when each traveler attempts to visit their nearest supply point and return to their home, when we assume there are no road blockages or disruptions (i.e., a best-case scenario) and the intended maximum travel window for all origin-destination round trips is six hours ($q = 6$). Road segments are displayed according to their flow-to-capacity ratios. Higher ratios (indicating higher congestion) are depicted by darker colors. If any estates had dropped demand (because the round-trip time is expected to be greater than the travel window), they would be depicted in green with darker colors indicating higher levels of dropped demand (there are none in this case).

Figure 4.2 displays the distribution of round-trip travel times for grocery, gas, and hardware stores individually. We note that a majority of the round trips are less than 50 minutes in duration; however, we do see extended travel times for hardware stores on St. Croix. The longest travel time observed is in excess of 150 minutes in duration, which is still within the intended maximum travel window of six hours. The average travel time for all stores is 17.27 minutes with a standard deviation of 19.81 minutes. Grocery stores have a mean round trip travel time of 15.51 minutes with a standard deviation of 16.05 minutes. Gas stations average 11.77 minutes per round trip with a standard deviation of 14.28 minutes. Finally, hardware stores have a mean round trip travel time of 25.05 minutes and a 25.32 minute standard deviation.

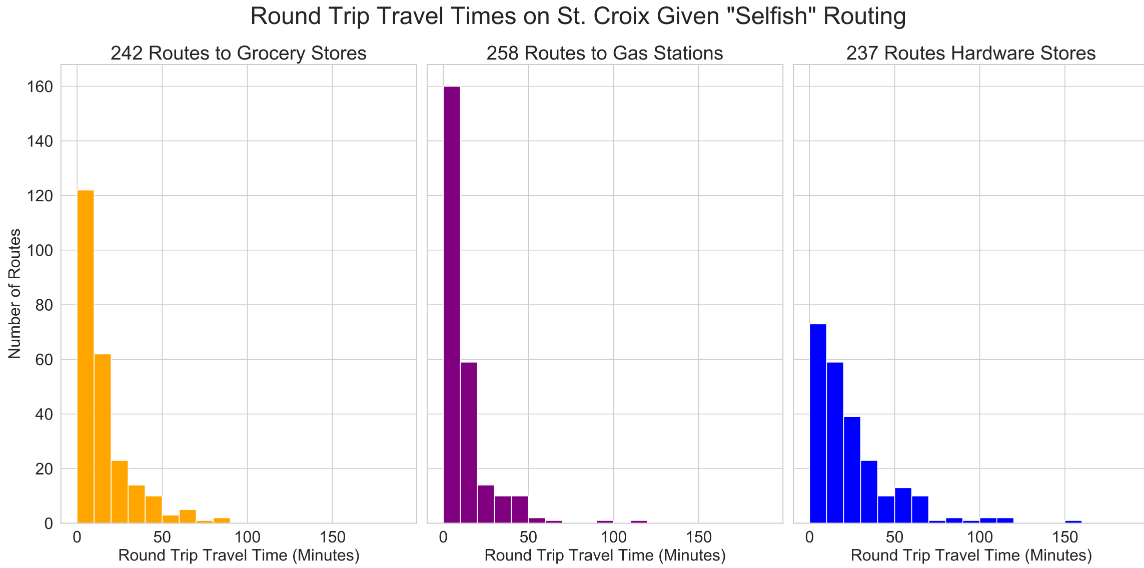

Figure 4.2. Distribution of round-trip travel times by store type given "selfish" routing. There are a total of 737 distinct routes (242 to grocery stores, 258 to gas stations, 237 to hardware stores) from the 233 estates in St. Croix. Although most of them are relatively short, we observe that some have round-trip times in excess of an hour.

In order to quantify the impact of congestion, we compare the round-trip travel times from a shortest path routing, as determined by Dijkstra's algorithm, with the round-trip travel times observed from our congestion based equilibrium model given "selfish" routing. Figure 4.3 shows the absolute difference between the shortest path and congestion based round-trip travel times for the given origin-destination pairs. A majority of travelers experience only a minor delay due to congestion, but many travelers experience delays in excess of 25 minutes. The longest travel delay is over 150 minutes in duration. The mean increase in travel time is 13.49 minutes with a standard deviation of 19.13 minutes.

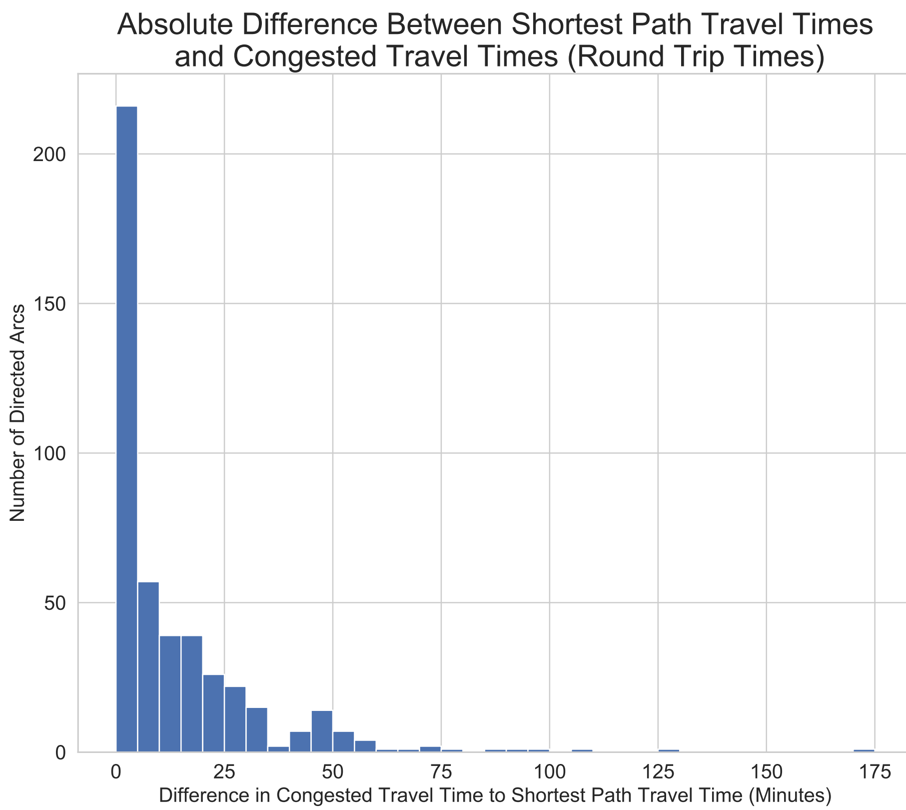

Figure 4.3. Absolute difference between the shortest path and congestion based round-trip travel times for the given origin-destination pairs given "selfish" routing.

We are particularly interested in identifying those populations that are most affected by long round-trip drive times on St. Croix if we assume a "selfish" traffic assignment. Figure 4.4 shows the longest drive times for all store types on the island. We note that the population "P081-River" has two of the top 20 longest drive times with round trips to "H001-Kmart" and "D002-Plaza Extra West Superstore" taking over 175 minutes and over 75 minutes respectively. It is interesting to note that 11 of the 20 longest drive times on St. Croix are to hardware or miscellaneous stores.

In a similar vein, Figure 4.5 displays the 20 longest drive times to grocery stores on the island given a "selfish" traffic assignment. We see population origin "P121-Clairmont" has the longest drive time to "D003-Pueblo Super Market at La Reine" and population origin "P081-River" has the second longest round trip time to "D002-Plaza Extra West Superstore." Each has a round trip lasting over 80 minutes in duration.

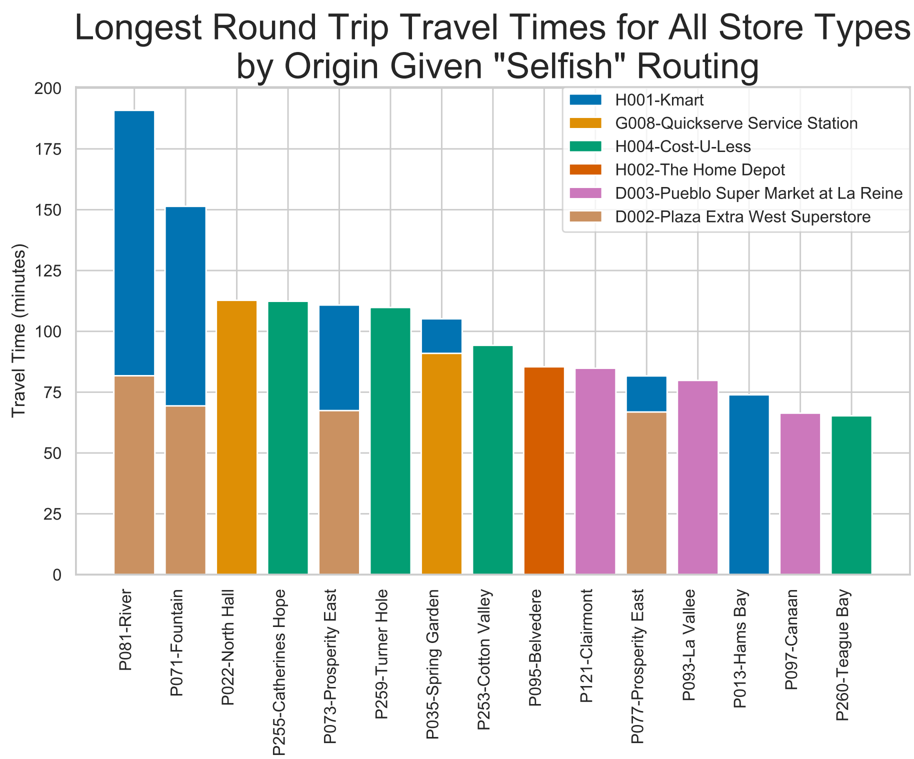

Figure 4.4. Longest round-trip travel times by origin for "selfish" routing. The height of the bar indicates the total travel time from a particular origin to a given store. Color of bar indicates the store. In cases where an origin has more than one longest round trip, the bars are superimposed with one color per store.

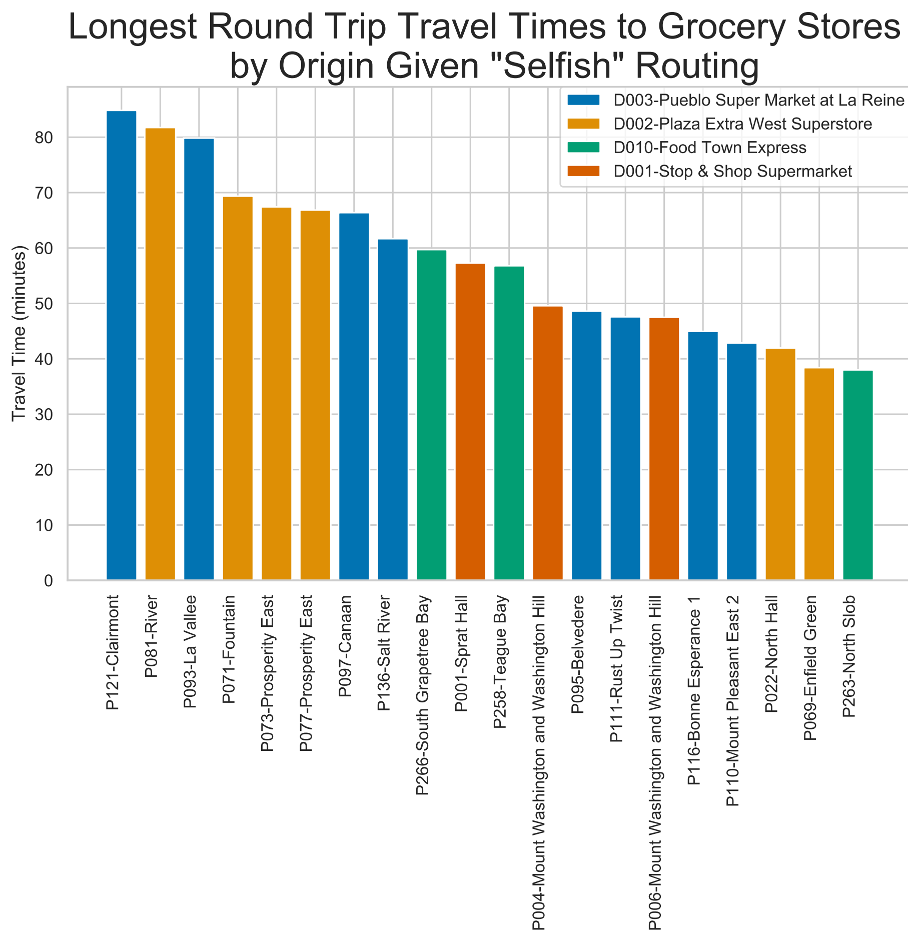

Figure 4.5. Longest round trip travel times for grocery stores by origin given “selfish” routing. The height of the bar indicates the total travel time from a particular origin to a given store. Color of bar indicates the store.

Figure 4.6 shows the longest travel times to gas stations on St. Croix. We see a significant decrease in round trip travel time between the second and third longest trips for gas due to the number of gas stations on the island. From Figure 3.2, we note that there are more gas stations located across the island than stores of any other type, giving people more options to purchase fuel for vehicles or generators. The longest round trip time is still in excess of 100 minutes despite the number of available gas stations.

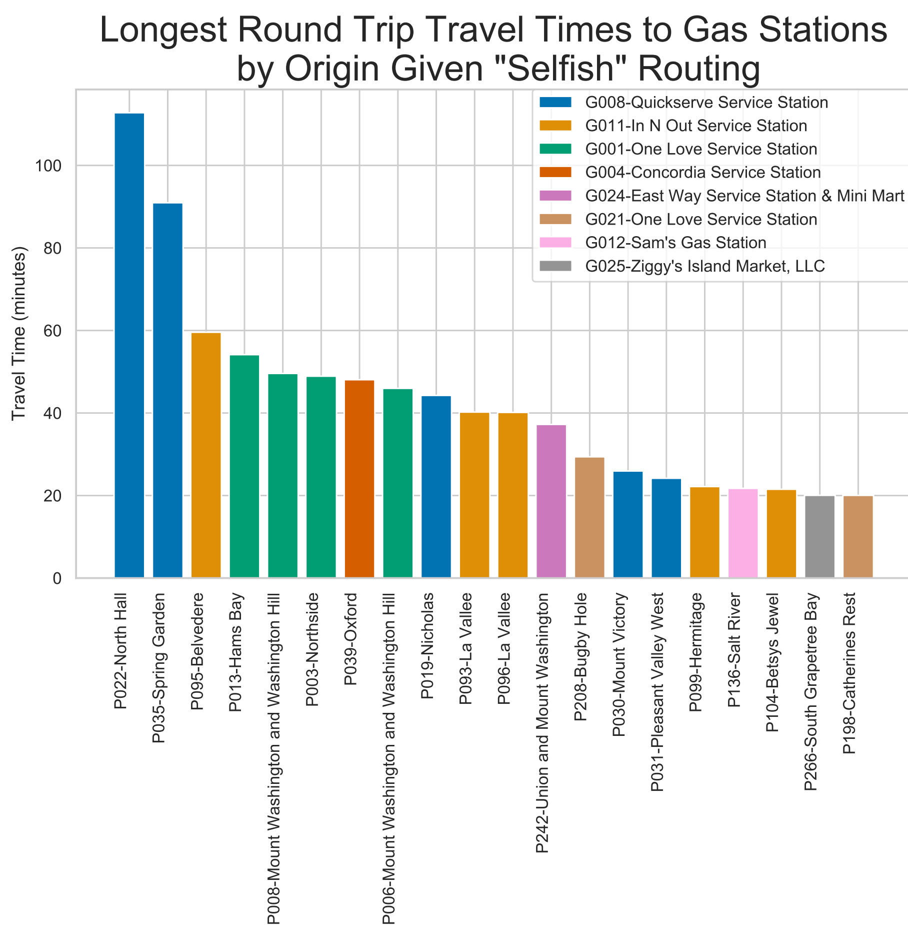

Figure 4.6. Longest round trip travel times for gas stations by origin given "selfish" routing. The height of the bar indicates the total travel time from a particular origin to a given store. Color of bar indicates the store.

The longest round trip travel times on the island are the hardware or miscellaneous stores, as seen in Figure 4.7. Travel from population "P081-River" experiences round trip times exceeding 175 minutes in duration, with population "P071-Fountain" experiencing times over 150 minutes in duration. Additionally all 20 longest round trip travel times exceed 50 minutes in duration with nine in excess of 75 minutes. From Figure 3.2, we note that there are only four hardware or miscellaneous stores located across the island, thus limiting the number of options for the population.

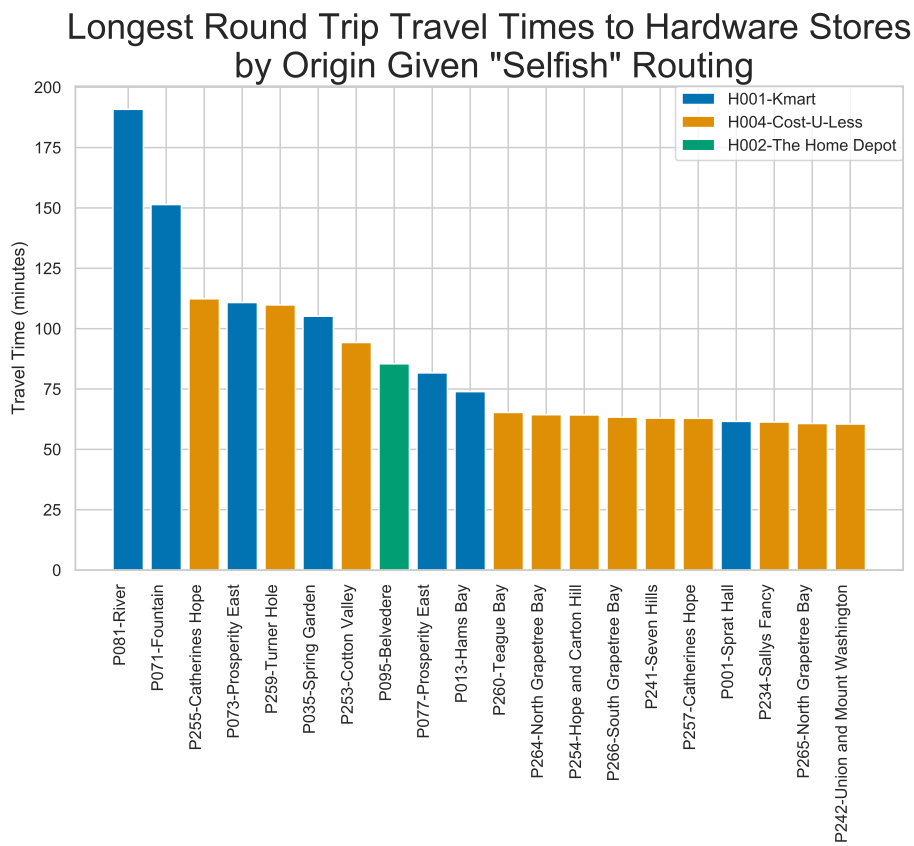

Figure 4.7. Longest round trip travel times for hardware stores by origin given "selfish" routing. The height of the bar indicates the total travel time from a particular origin to a given store. Color of bar indicates the store.

A natural extension of Figure 4.4 is to view the longest round trip times geospatially. Figure 4.8 displays the longest routes by round trip travel time for all store types given a "selfish" routing scheme. Route colors indicate the destination store type: blue for hardware stores, orange for grocery stores, and purple for gas stations. The remaining arcs are rendered in grey. We note the populations with the longest round trip travel times are located predominately in the northwest, an area with lower capacity dirt roads, and on the east end of the island where there are fewer supply access points of any type.

From Figure 4.8, we can begin to make initial decisions for placement of pre-storm emergency supply distribution points or post-storm relief locations. Furthermore, we can begin to make assumptions about which populations may be more prone to isolation from road blockages from debris accumulation or flooding events.

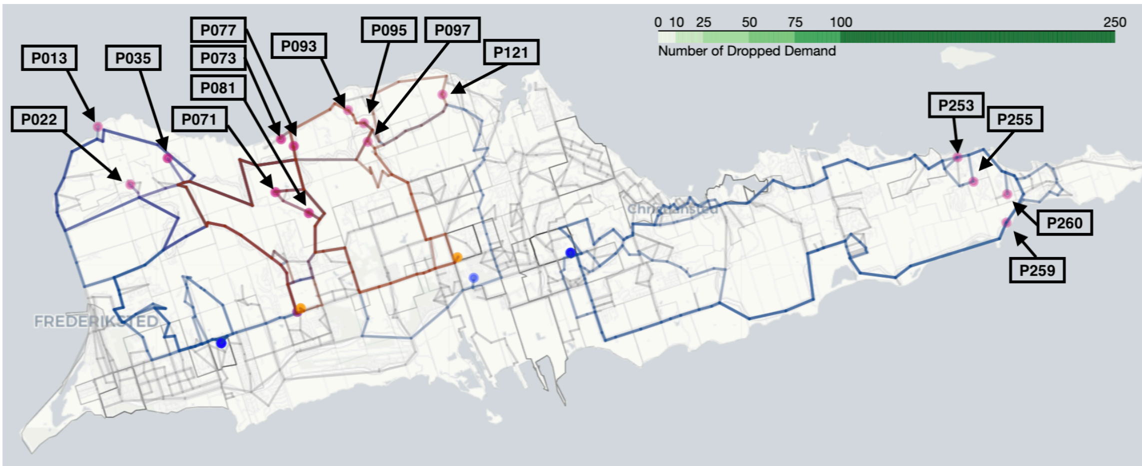

Figure 4.8. Map of longest routes by round trip travel time for all store types given "selfish" routing. Route colors indicate the destination store type: blue for hardware stores, orange for grocery stores, and purple for gas stations. The remaining arcs are rendered in grey. Any estates with dropped demand would be depicted in green with darker colors indicating higher levels of dropped demand. Created using QGIS Development Team (2019) on 19 September 2019.

4.2 Population Travel Times: "Coordinated" Routing

If travel destinations can be coordinated, perhaps by a central authority such as the Virgin Island Territory Emergency Management Agency (VITEMA) or FEMA, what might be the impacts on overall congestion? We repeat the analysis conducted in Section 4.1 when we consider a "coordinated" traffic assignment protocol for the island of St. Croix.

To implement this, we add additional "supersink" destination nodes to the original data corresponding to a grocery, gas, or hardware need, along with additional artificial arcs connecting each of the original access supply points to their corresponding supersink. Then, instead of specifying traffic demand, for example, for ("P073-Prosperity East", "D002-Plaza Extra West Superstore"), we simply specify demand for ("P073-Prosperity East","grocery") and let the model determine which grocery store should be visited. This allows the model to adjust travel to destination locations in a manner that is best for overall travel times, although in some cases individual estates could travel farther (but hopefully faster) to their destination.

Figure 4.9 shows the resulting road congestion when each traveler attempts to travel from their home to supply access points. We again assume a intended maximum travel window of six hours. Road segments are displayed according to their flow-to-capacity ratios. Higher ratios are depicted by darker colors. Any estates with dropped demand would be depicted in green with darker colors indicating higher levels of dropped demand. We note that there are no dropped demands with either the "selfish" or "coordinated" routing under normal (i.e., no road blockage) conditions.

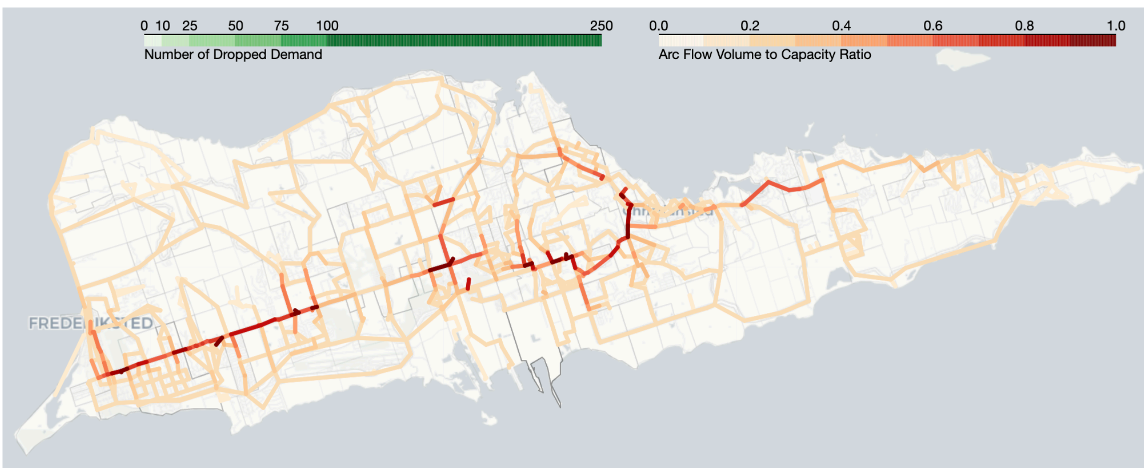

Figure 4.9. Map of flow ratios given "coordinated" routing. Arcs are displayed according to their flow-to-capacity ratios. Higher ratios are depicted by darker colors. Any estates with dropped demand would be depicted in green with darker colors indicating higher levels of dropped demand. Created using QGIS Development Team (2019) on 19 September 2019.

Furthermore, we note little difference in the flow-to-capacity ratios of the arcs when comparing the two traffic assignment protocols. This allows us to garner insight into the areas of high congestion on St. Croix, which has been corroborated by first hand accounts of traffic on the island (Gajewski 2019). From this we can also begin to identify potential high stress points within the surface road network.

Figure 4.10 shows the round trip travel time distributions by store type given a "coordinated" traffic routing protocol. We note fewer round trip travel times in excess of 50 minutes as compared to the "selfish" routing model. This behavior is expected due to the equilibrium properties of the "coordinated" model. The average travel time for all stores given "coordinated" routing is 16.86 minutes with a standard deviation of 20.23 minutes. Grocery stores have a mean round trip travel time of 18.99 minutes with a standard deviation of 25.98 minutes. Gas stations average 10.85 minutes per round trip with a standard deviation of 10.58 minutes. Finally, hardware stores have a mean round trip travel time of 21.49 minutes and a 19.86 minute standard deviation.

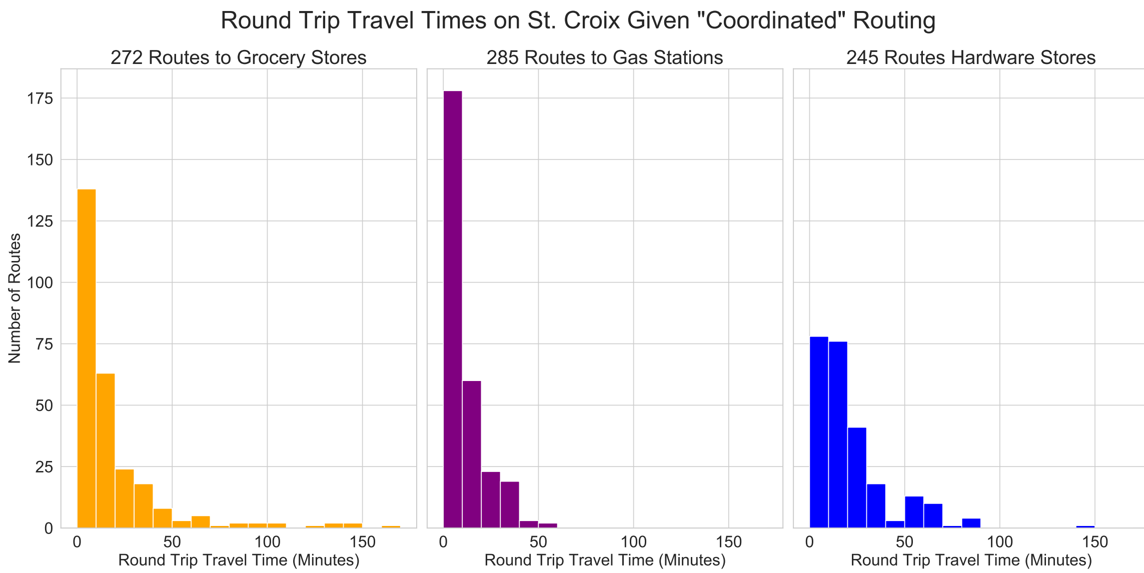

Figure 4.10. Distribution of round trip travel times by store type given "coordinated" routing. There are a total of 802 distinct routes (272 to grocery stores, 285 to gas stations, 245 to hardware stores) from the 233 estates in St. Croix. Although most of them are relatively short, we observe that some have round trip times in excess of an hour.

Figure 4.11 displays the absolute difference between the shortest path and congestion based round trip travel times for the given origin-destination pairs. Again, we see smaller differences in round trip travel times than experienced in the "selfish" routing (Figure 4.3) with a majority of the population experiencing delays of 20 minutes or less; however, we note a few larger round trip travel delays of approximately 120 minutes. The mean increase in travel time is 12.3 minutes with a standard deviation of 20.1 minutes.

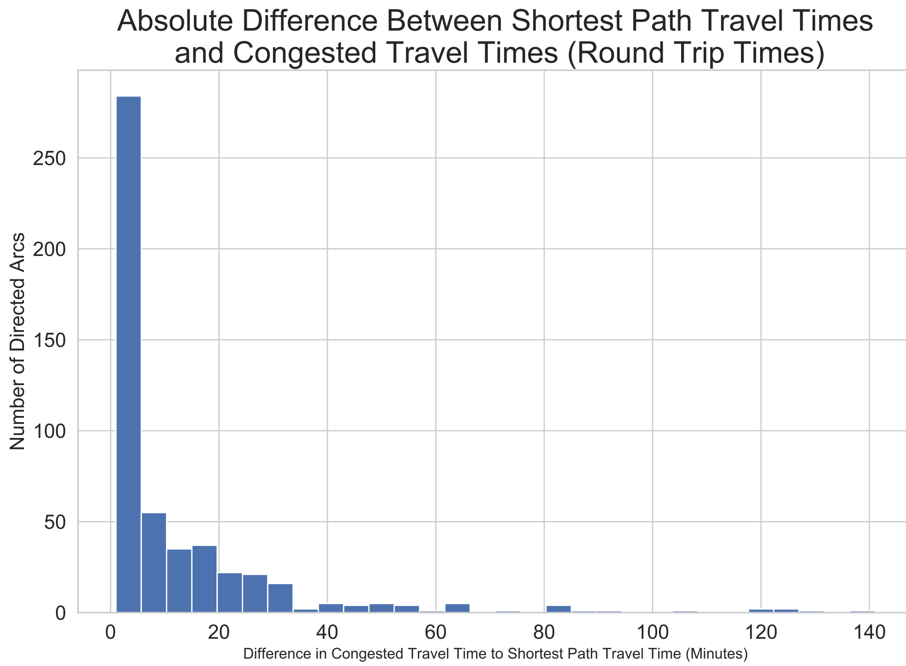

Figure 4.11. Absolute difference between the shortest path and congestion based round trip travel times for the given origin-destination pairs given "coordinated" routing.

Figure 4.12 displays the longest round-trip travel times to all stores given "coordinated" routing. Surprisingly, only six of the 20 longest round trip times are to hardware or miscellaneous stores. Population "P095-Belvedere" experiences the longest times to "D001-Stop & Shop Supermarket" and "D002-Plaza Extra West Superstore" with round trip travel times over 140 minutes. Interestingly, "P095-Belvedere" does not appear in the 20 longest times for the "selfish" model. The "coordinated" model appears to have a more "even" distribution of times with no significant drop-offs among the 20 longest.

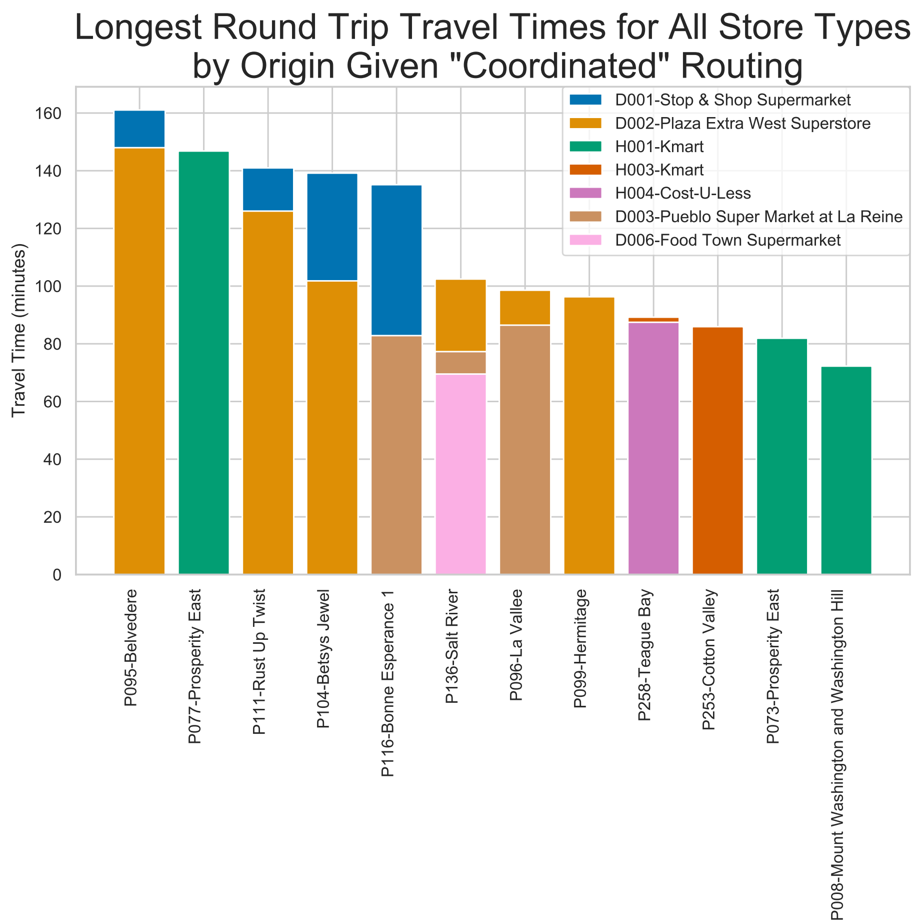

Figure 4.12. Longest round trip travel times for all store types by origin given "coordinated" routing. The height of the bar indicates the total travel time from a particular origin to a given store. Color of bar indicates the store. In cases where an origin has more than one longest round trip, the bars are superimposed with one color per store.

We look specifically at grocery store round trip travel times in Figure 4.13. Population "P095-Belvedere" experiences the first and second longest round trip times on the island. Both times exceed the longest times experienced in the "selfish" routing model with the longest time from the "coordinated" model nearly doubling that seen in the "selfish" model. Interestingly, populations "P121-Clairmont" and "P081-River" experience the two longest travel times in the "selfish" model, but only "P121-Clairmont" shows up near the bottom of the longest travel times in the "coordinated" model.

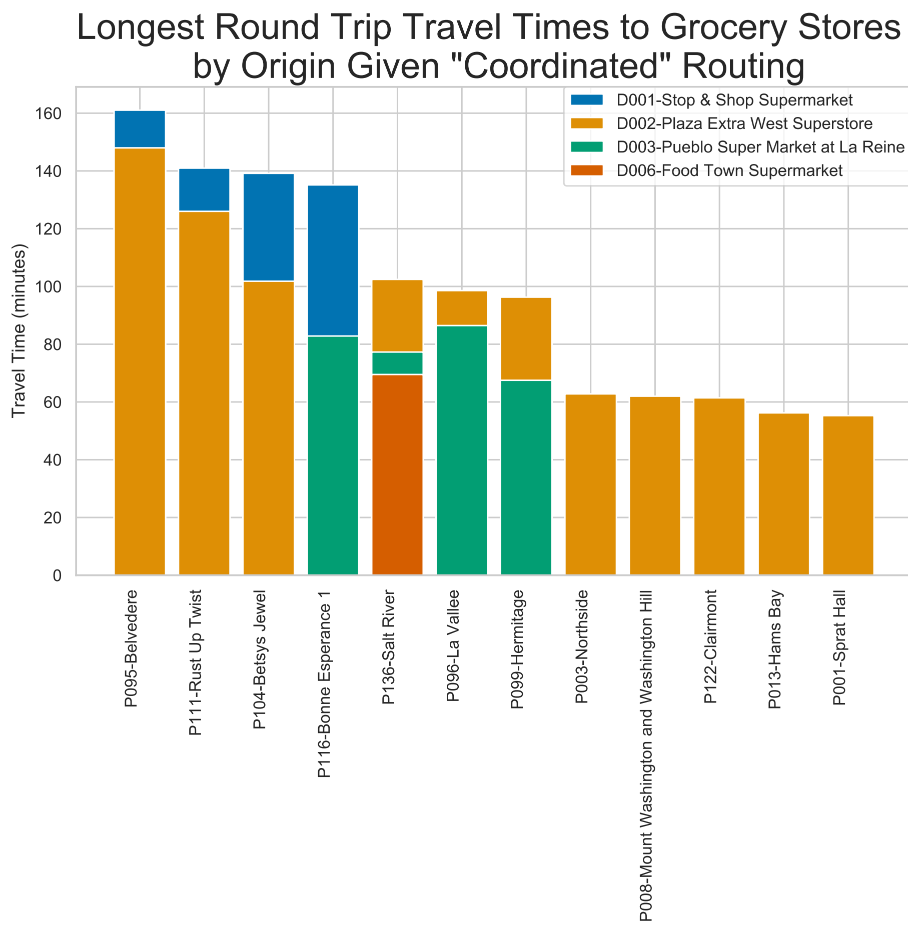

Figure 4.13. Longest round trip travel times for grocery stores given "coordinated" routing. The height of the bar indicates the total travel time from a particular origin to a given store. Color of bar indicates the store. In cases where an origin has more than one longest round trip, bars are superimposed with one color per store.

Routing to gas stations within the “coordinated” model (Figure 4.14) shows improvement over the “selfish” model routing. Specifically, we see only seven travel times in excess of 30 minutes in duration for the “coordinated” model contrasted with the 14 trips over 30 minutes in the “selfish” model. We also note a different composition of affected Estates and a more linear decrease in travel time across the 20 longest trips with the “coordinated” model. Finally, we note that the longest travel time given a “selfish” routing is more than twice the duration of the longest travel time given a “coordinated” routing.

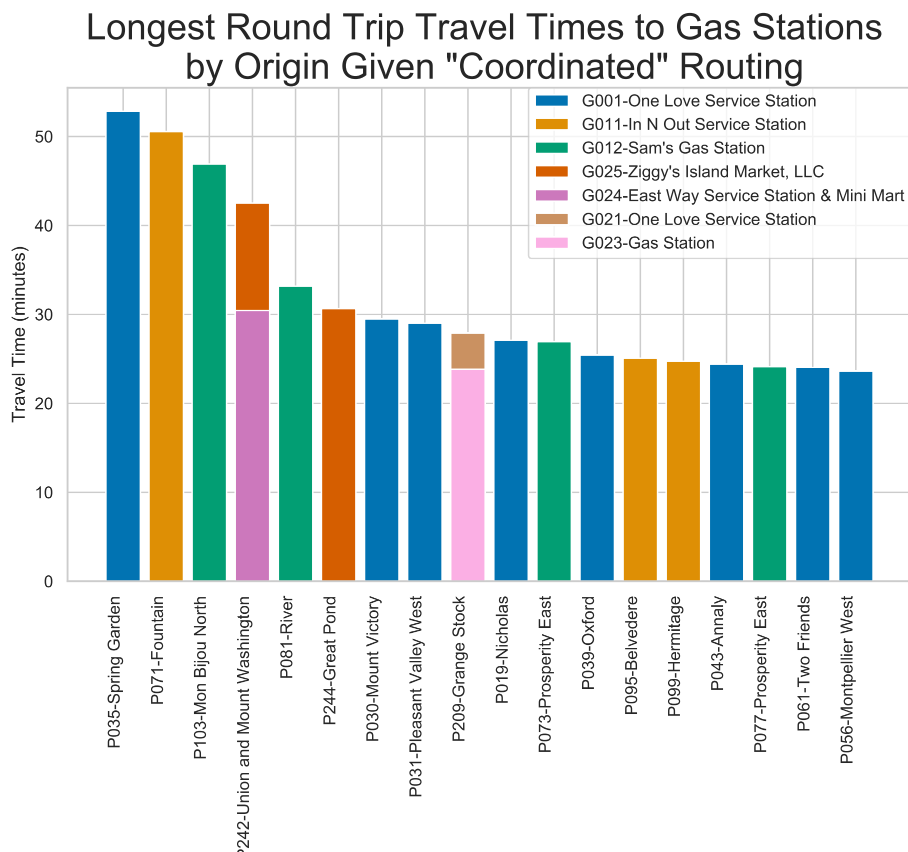

Figure 4.14. Longest round trip travel times for gas stations by origin given “selfish” routing. The height of the bar indicates the total travel time from a particular origin to a given store. Color of bar indicates the store. In cases where an origin has more than one longest round trip, bars are superimposed with one color per store.

Unlike the "selfish" routing model, the "coordinated" model experiences fewer of the longest round trip travel times on routes to hardware or miscellaneous stores (Figure 4.15). Population "P077-Prosperity East" experiences the longest round trip travel time in excess of 140 minutes. Similar to the longest grocery routes, we see a different composition of Estates with the longest hardware trip times in both the "selfish" and "coordinated" models.

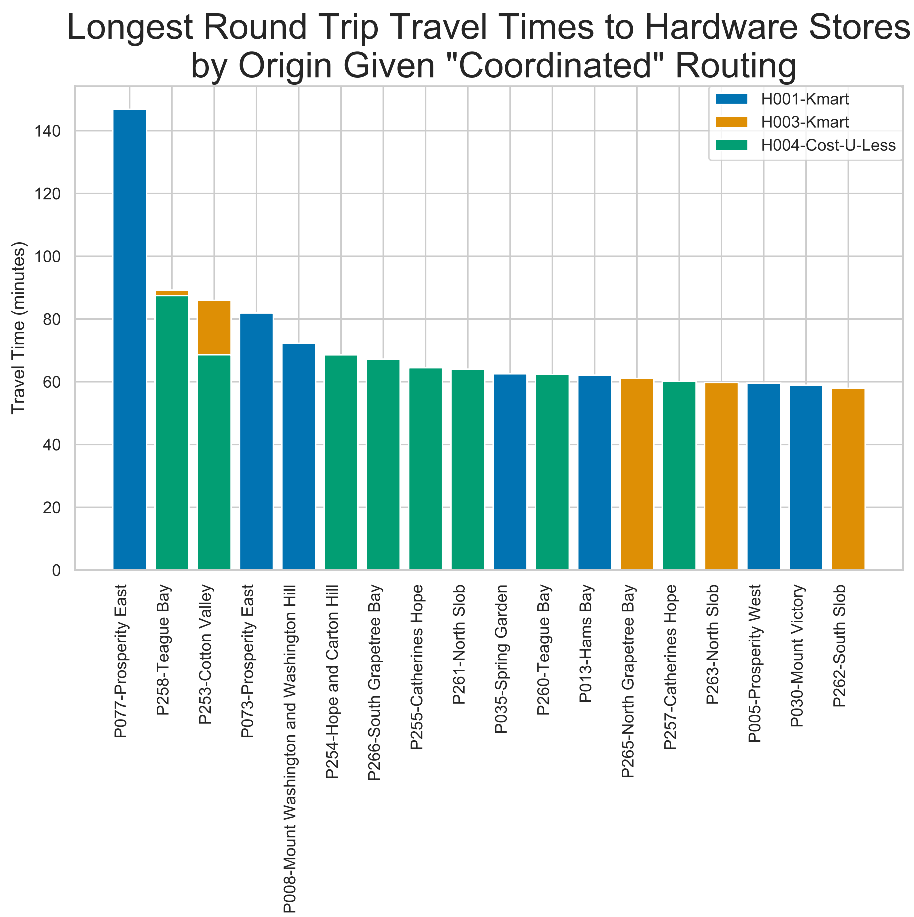

Figure 4.15. Longest round trip travel times for hardware stores by origin given "coordinated" routing. The height of the bar indicates the total travel time from a particular origin to a given store. Color of bar indicates the store. In cases where an origin has more than one longest round trip, bars are superimposed with one color per store.

We again view the longest round trip times geospatially. Figure 4.16 displays the longest routes by round trip travel time for all store types given a "coordinated" routing scheme. Route colors indicate the destination store type: blue for hardware stores, orange for grocery stores, and purple for gas stations. The remaining arcs are rendered in grey. Similar to Figure 4.8, we note the populations with the longest round trip travel times are located predominately in the northwest, an area with lower capacity dirt roads, and on the east end of the island where there are fewer supply access points of any type. However, we observe more gas stations with longer travel times, and different travel routes for similar population-store pairings observed in Figure 4.8.

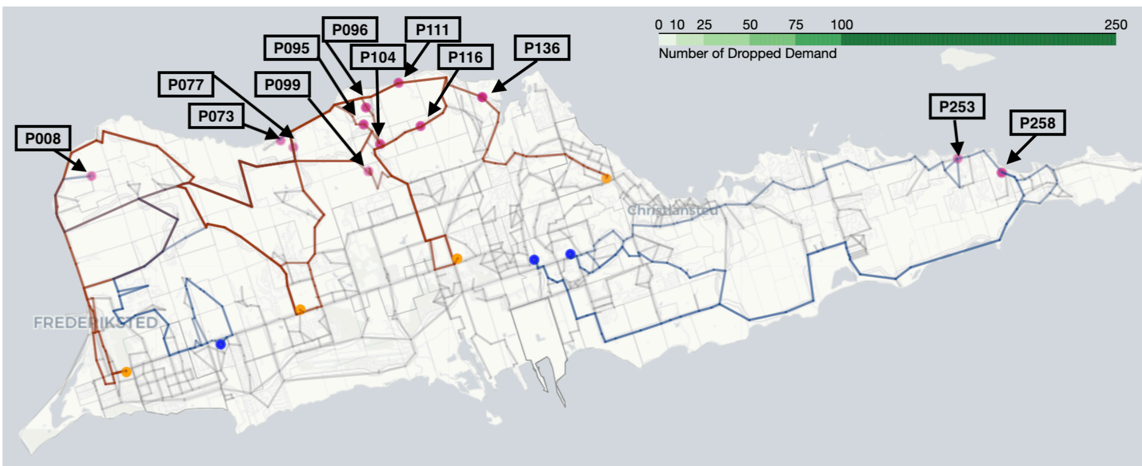

Figure 4.16. Map of longest routes by round trip travel time for all store types given "coordinated" routing. Route colors indicate the destination store type: blue for hardware stores, orange for grocery stores, and purple for gas stations. The remaining arcs are rendered in grey. Any estates with dropped demand would be depicted in green with darker colors indicating higher levels of dropped demand. Created using QGIS Development Team (2019) on 19 September 2019.

We can begin to make initial decisions for placement of pre-storm emergency supply distribution points or post-storm relief locations. Furthermore, we can begin to make assumptions about which populations may be more prone to isolation from road blockages from debris accumulation or flooding events. These locations are similar for both "selfish" and "coordinated" routing indicating the potential for disruption to these neighborhoods regardless of the chosen traffic assignment protocol.

It is important to remember that the "coordinated" traffic assignment protocol is an equilibrium model by nature, and as such it tends to seek flows that "balance" the objective function cost across all of the various routes. In other words, the model seeks to decrease overall congestion, which may result in some longer individual round trip travel times. Table 4.1 reinforces this notion by showing that the "coordinated" traffic assignment protocol has lower average round trip times for all stores combined, gas stores, and hardware stores.

Table 4.1. Average round trip travel time by store and traffic assignment type in minutes. We note faster average round trip travel times for all stores given "coordinated" traffic assignments. The only exception is a longer average "coordinated" travel time for grocery stores.

Average Round Trip Travel Time by Store Type (Minutes)				
Traffic Assignment Type	All Stores	Grocery	Gas	Hardware
"Selfish"	17.27	15.51	11.77	25.05
"Coordinated"	16.86	18.99	10.85	21.49

4.3 Travel Times from the Ports

Goods imported to St. Croix enter the island's surface road network at Wilfred "Bomba" Allick Port on the south side of the island and then proceed to specific destinations. The movement of goods from the port to stores is modeled as specific origin-destination pairs for both the "selfish" and "coordinated" traffic assignment protocols. There is no choice in location of delivery, and each store must receive a delivery. The following discussion focuses on how the choice of traffic assignment protocol for the population affects the ability to move goods from the port to their intended destinations.

Table 4.2. Average travel times from Wilfred "Bomba" Allick Port to all stores on St. Croix for each traffic assignment protocol.

Traffic Assignment Type	Average Round Trip Delivery Time (Minutes)	Standard Deviations
"Selfish"	29.18	12.30
"Coordinated"	29.30	10.70

Table 4.2 shows little difference in average round trip delivery times from the port given either traffic assignment protocol. Round trip delivery times do not include the time required to load cargo at the port or unload cargo at the destination. We observe that under "coordinated" routing the average delivery time actually increases slightly. However, of interest is the impact on delivery times (and routes) for deliveries to specific destinations.

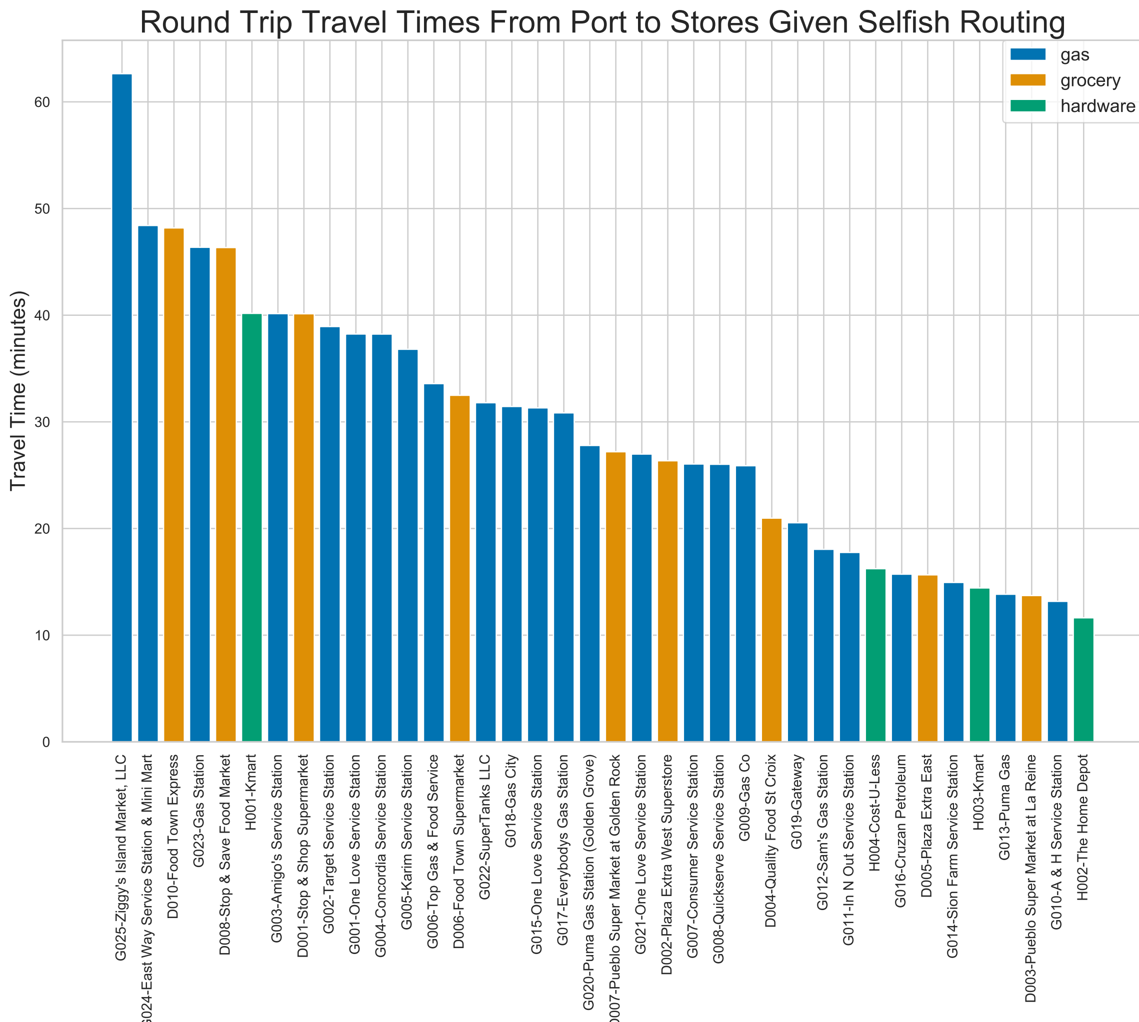

Figure 4.17. Round trip travel times in minutes from Wilfred "Bomba" Allick Port to all stores on St. Croix given a "selfish" traffic assignment protocol. Blue bars indicate gas stations, yellow are grocery stores, and green are hardware stores.

"Selfish" Routing

Figure 4.17 shows the round trip delivery times from the port to each supply access point (store) on St. Croix. All but one store, "G025-Ziggy's Island Market, LLC," have round trip delivery times less than 50 minutes. This implies, given sufficient drivers and available trucks, each store could receive up to six deliveries given an intended maximum travel window of six hours not accounting for loading and unloading times.

The delivery routes from the port when population traffic follows "selfish" routing are displayed in Figure 4.18. It is interesting to note that the traffic from the port remains south of the noted areas of congestion in Figure 4.1 until it becomes necessary to travel north for the final leg of the delivery. This is also the first deliberate use of the highway that we see in any of the models.

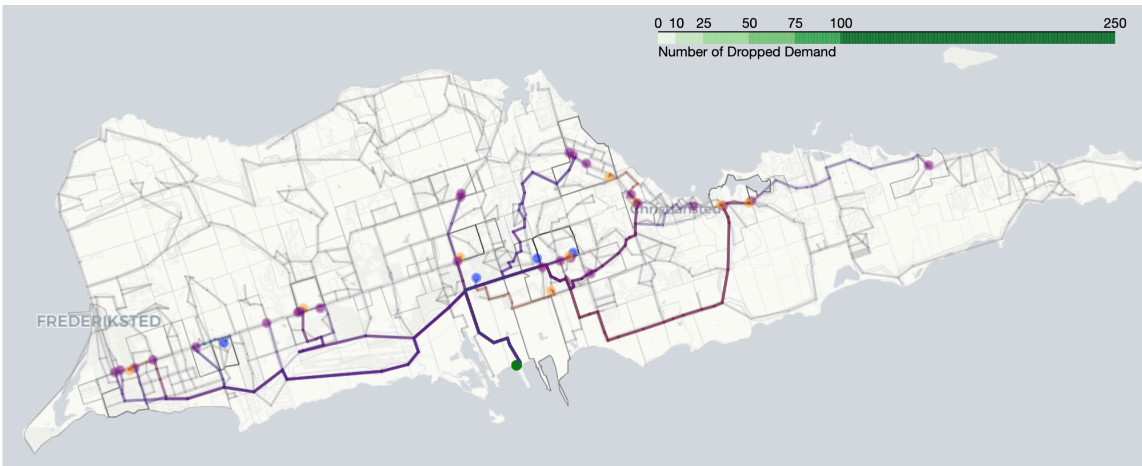

Figure 4.18. Geographic depiction of all routes from Wilfred "Bomba" Allick Port to all stores on St. Croix given a "selfish" traffic assignment protocol. The remaining arcs are rendered in grey. Any estates with dropped demand would be depicted in green with darker colors indicating higher levels of dropped demand. Created using QGIS Development Team (2019) on 21 September 2019.

"Coordinated" Routing

Figure 4.19 shows the round trip delivery times to all of the stores on St. Croix from Wilfred "Bomba" Allick Port when population traffic follows a "coordinated" traffic assignment protocol. All round trip delivery times for this model are under 50 minutes in duration with "G025-Ziggy's Island Market, LLC" once again having the longest time. It is interesting to note that the nine shortest trips are also the same for both traffic assignment protocols, but we notice a lot of variability within the length of trips to individual stores between the two models.

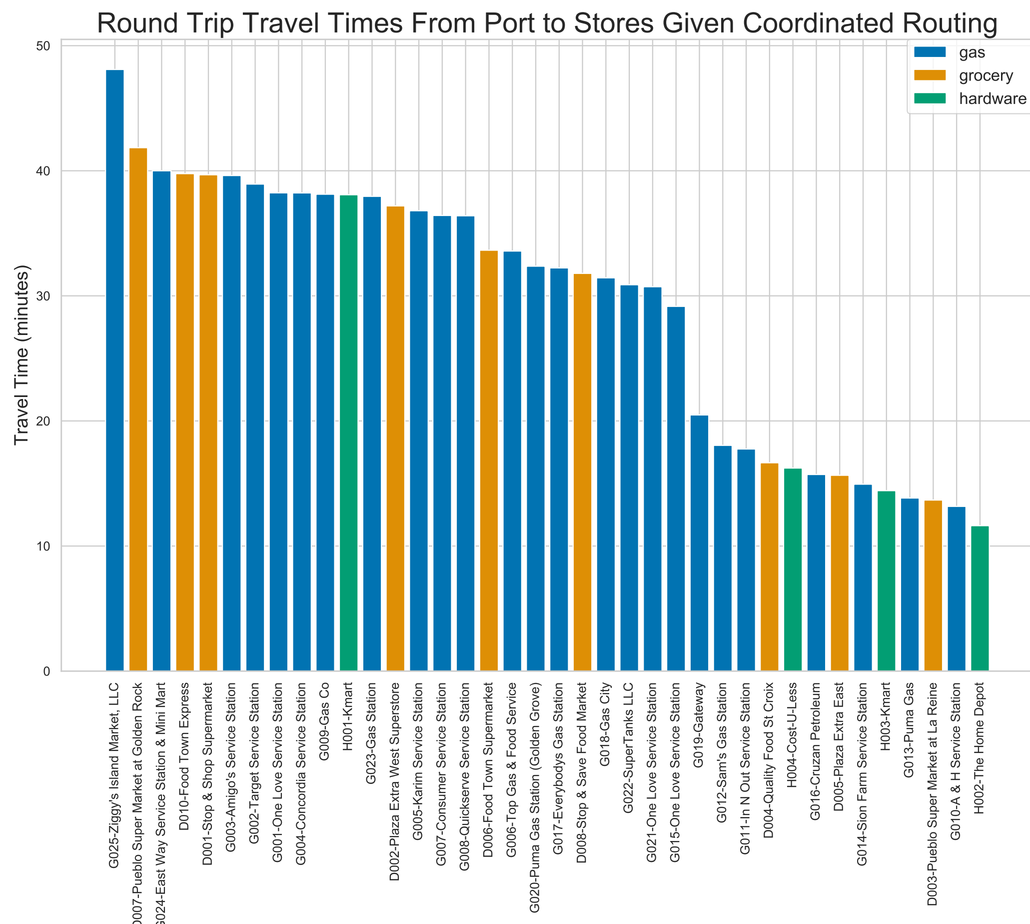

Figure 4.19. Round trip travel times in minutes from Wilfred "Bomba" Allick Port to all stores on St. Croix given a "coordinated" traffic assignment protocol. Blue bars indicate gas stations, yellow are grocery stores, and green are hardware stores.

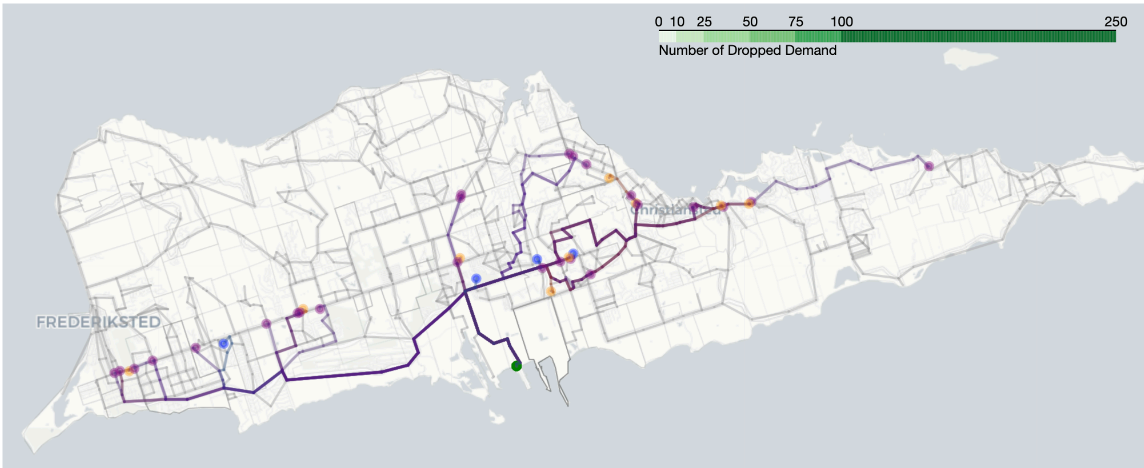

Figure 4.20. Geographic depiction of all routes from Wilfred "Bomba" Allick Port to all stores on St. Croix given a "coordinated" traffic assignment protocol. The remaining arcs are rendered in grey. Any estates with dropped demand would be depicted in green with darker colors indicating higher levels of dropped demand. Created using QGIS Development Team (2019) on 21 September 2019.

We also note different traffic routing with the "coordinated" traffic assignments (Figure 4.20) than what we observed given the "selfish" routing (Figure 4.18).

Impact on feasible deliveries

We are interested in estimating the number of deliveries a single truck could make to a given store assuming an intended maximum travel period of six hours. In order to calculate the round trip delivery times, we assume a 30-minute load time at the port based on first hand knowledge from Frazier (2019). We assume the same time to unload at the delivery location. Therefore, we calculate the round trip delivery times as 30-minute load time plus 30-minute unload time plus round trip travel times from the models. We then divide six hours by the estimated delivery time to calculate the approximate number of deliveries per intended maximum travel window. Table 4.3 gives the round trip travel times, total round trip delivery times, and estimated number of deliveries given a "selfish" or "coordinated" routing protocol. We note an increased expected number of deliveries for each store given a "coordinated" routing assignment. It is important to note the actual number of deliveries depends on the number of available trucks and drivers on the island.

Table 4.3. Estimated round trip delivery times from port when population traffic follows "selfish" or "coordinated" routing. We calculate the travel round trip time (RTT) and total RTT (including an assumed combined 60 minutes loading and unloading), and the implied number of deliveries in a six-hour travel window. We note that our model does not prioritize delivery traffic from ports, so although the "coordinated" traffic tends to result in lower RTTs and more deliveries, this is not always the case.

Delivery Location	"Selfish" Routing			"Coordinated" Routing		
	Travel RTT	Total RTT	Number of Deliveries	Travel RTT	Total RTT	Number of Deliveries
G025-Ziggy's Island Market, LLC	62.64	122.64	2.9	48.1	108.1	3.3
G024-East Way Service Station & Mini Mart	48.41	108.41	3.3	40.0	100.0	3.6
D010-Food Town Express	48.18	108.18	3.3	39.77	99.77	3.6
G023-Gas Station	46.37	106.37	3.4	37.95	97.95	3.7
D008-Stop & Save Food Market	46.34	106.34	3.4	31.8	91.8	3.9
H001-Kmart	40.17	100.17	3.6	38.08	98.08	3.7
G003-Amigo's Service Station	40.15	100.15	3.6	39.62	99.62	3.6
D001-Stop & Shop Supermarket	40.13	100.13	3.6	39.68	99.68	3.6
G002-Target Service Station	38.94	98.94	3.6	38.94	98.94	3.6
G001-One Love Service Station	38.23	98.23	3.7	38.23	98.23	3.7
G004-Concordia Service Station	38.23	98.23	3.7	38.23	98.23	3.7
G005-Karim Service Station	36.8	96.8	3.7	36.8	96.8	3.7
G006-Top Gas & Food Service	33.58	93.58	3.8	33.58	93.58	3.8
D006-Food Town Supermarket	32.49	92.49	3.9	33.65	93.65	3.8
G022-SuperTanks LLC	31.79	91.79	3.9	30.89	90.89	4.0
G018-Gas City	31.44	91.44	3.9	31.44	91.44	3.9
G015-One Love Service Station	31.31	91.31	3.9	29.16	89.16	4.0
G017-Everybodys Gas Station	30.84	90.84	4.0	32.23	92.23	3.9
G020-Puma Gas Station (Golden Grove)	27.79	87.79	4.1	32.37	92.37	3.9
D007-Pueblo Super Market at Golden Rock	27.2	87.2	4.1	41.85	101.85	3.5
G021-One Love Service Station	26.98	86.98	4.1	30.73	90.73	4.0
D002-Plaza Extra West Superstore	26.35	86.35	4.2	37.19	97.19	3.7
G007-Consumer Service Station	26.05	86.05	4.2	36.43	96.43	3.7
G008-Quickserve Service Station	26.02	86.02	4.2	36.4	96.4	3.7
G009-Gas Co	25.89	85.89	4.2	38.12	98.12	3.7
D004-Quality Food St Croix	20.97	80.97	4.4	16.66	76.66	4.7
G019-Gateway	20.54	80.54	4.5	20.48	80.48	4.5
G012-Sam's Gas Station	18.05	78.05	4.6	18.05	78.05	4.6
G011-In N Out Service Station	17.76	77.76	4.6	17.76	77.76	4.6
H004-Cost-U-Less	16.23	76.23	4.7	16.23	76.23	4.7
G016-Cruzan Petroleum	15.72	75.72	4.8	15.72	75.72	4.8
D005-Plaza Extra East	15.65	75.65	4.8	15.65	75.65	4.8
G014-Sion Farm Service Station	14.94	74.94	4.8	14.94	74.94	4.8
H003-Kmart	14.43	74.43	4.8	14.43	74.43	4.8
G013-Puma Gas	13.84	73.84	4.9	13.84	73.84	4.9
D003-Pueblo Super Market at La Reine	13.72	73.72	4.9	13.68	73.68	4.9
G010-A & H Service Station	13.17	73.17	4.9	13.17	73.17	4.9
H002-The Home Depot	11.63	71.63	5.0	11.63	71.63	5.0

4.4 Study of Road Interdictions

In addition to understanding how the surface road network operates under "normal" conditions, we are interested in assessing how it operates under stress. In this section, stress takes the form of roads that have become impassable due to some form of physical interruption (e.g., fallen utility pole, landslide, flood). The model from Section 3.3 allows us to block (or *interdict*) any road segment by setting $avail_{ij} = 0$ for any arc (i, j). By systematically blocking road segments individually or in combination, we can assess the impact on traffic congestion as well as "worst-case" disruption scenarios.

As a start, we consider the impact of individually interdicting each of the ten road segments with the largest quantity of flow under "selfish" and "coordinated" traffic assignment protocols. Table 4.4 shows the ten undirected edges with the highest flow values given either routing. We note nine of the ten highest flow roads are the same for each model, with the exceptions being Centerline Road near Airport Road in the "selfish" model and Centerline Road near Campo Rico Road in the "coordinated" model. Both are ranked as the fifth highest flow for their respective routing protocol. Figure 4.21 displays the corresponding geographic location of the road segments in Table 4.4.

Table 4.4. Undirected edges with the highest volume of traffic flow. "S" ranks indicate rank value under "selfish" routing, while "C" ranks indicate rank value under "coordinated" routing. Routing column indicates which routing protocol the road segment was ranked using.

Highest Flow Edges							
Rank		Routing	i	j	Flow	Road Name	Nearest Cross Street
S1	C1	"Both"	T387	T386	1760	Christiansted Bypass	VI 703
S2	C3	"Both"	T298	T290	1650	Queen Mary Highway	Pepper Tree Road
S3	C2	"Both"	T335	T330	1647	Queen Mary Highway	Constitution Hill Road
S4	C4	"Both"	T154	T150	1555	Centerline Road	Paradise Road
S5		"Selfish"	T119	T107	1357	Centerline Road	Airport Road
	C5	"Coordinated"	T044	T043	1327	Centerline Road	Campo Rico Road
S6	C6	"Both"	T388	T386	1343	Christiansted Bypass	VI 83
S7	C7	"Both"	T142	T139	1341	Centerline Road	VI 705
S8	C8	"Both"	T217	T234	1324	Centerline Road	Queen Street
S9	C9	"Both"	T317	T324	1308	Queen Mary Highway	Sion Valley Road
S10	C10	"Both"	T385	T383	1288	Northside Road	VI 703

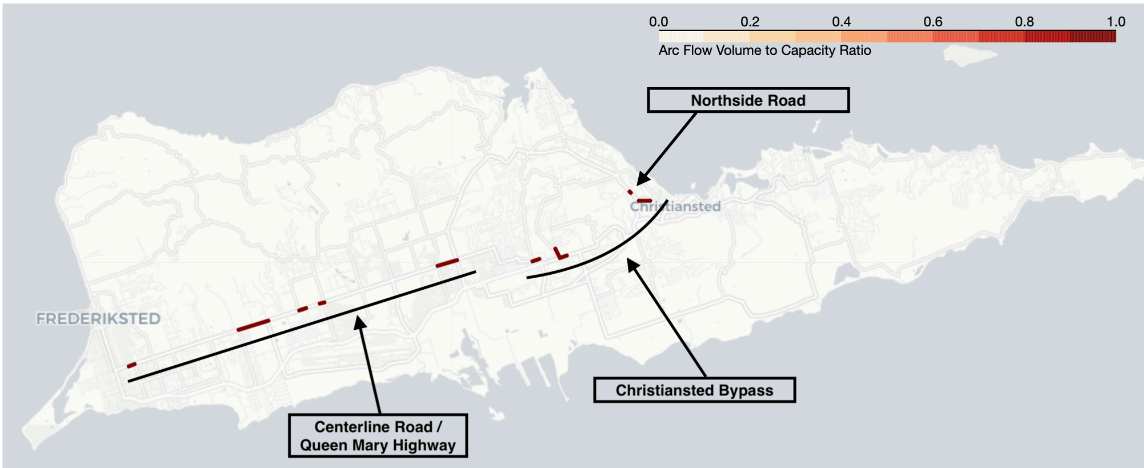

Figure 4.21. Geographic representation of highest flow edges for both "selfish" and "coordinated" routing. Created using QGIS Development Team (2019) on 21 September 2019.

In our analysis, we consider a disruption to each of these road segments in isolation. Not surprisingly, a blockage on the Christiansted Bypass has the largest impact on congestion. We focus our discussion on those results, and comment on other interdiction scenarios worthy of additional study.

4.4.1 Blockage on Christiansted Bypass

Blockages to undirected edge (T387, T386), known as the Christiansted Bypass near VI 703, creates the largest buildup of congestion within the "selfish" routing model for any single interdiction. Figure 4.22 shows the resulting flow-to-capacity ratios with the interdicted edge highlighted in black. Interestingly, the system has enough built-in "flexibility" to reroute traffic in order to avoid dropped demand.

Figure 4.23 shows the distribution of round trip travel times by store type for the "selfish" routing model with a single interdiction. We note an increased number of routes to grocery stores and hardware stores with travel times over 100 minutes. Interestingly, we note fewer gas station travel times over 50 minutes in the "stressed" model than we experienced in the "normal" model. Table 4.5 shows the average travel times for all stores, and each store type individually for the "selfish" routing model in the presence of road blockages and under "normal" operation. We note an increase in average travel time for the blockage model

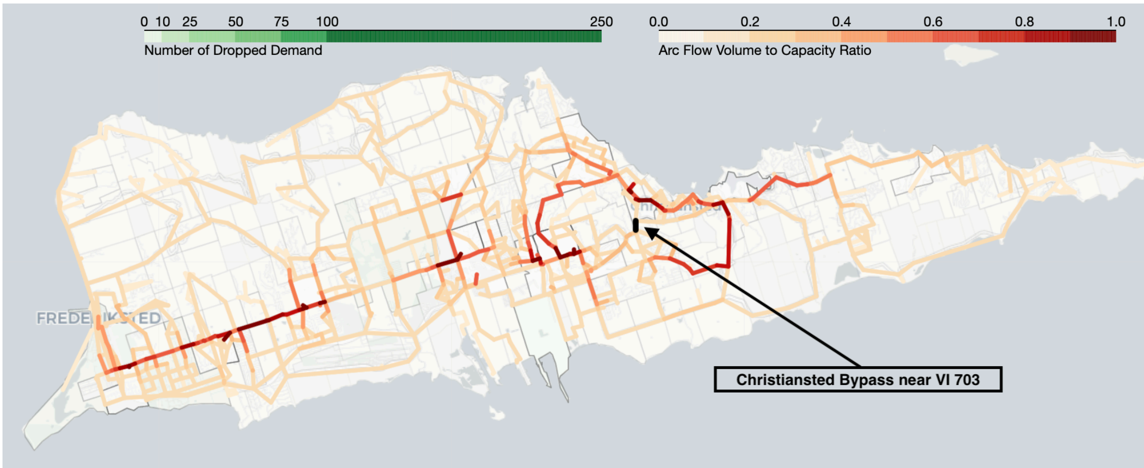

Figure 4.22. Map of flow ratios given "selfish" routing with a single interdiction. Arcs are displayed according to their flow-to-capacity ratios. Higher ratios are depicted by darker colors. The interdicted road segment is annotated with in black. Any estates with dropped demand would be depicted in green with darker colors indicating higher levels of dropped demand. Created using QGIS Development Team (2019) on 24 September 2019.

for all stores and grocery stores, but we note a slight decrease in average travel time for hardware stores. The average travel time for gas stations shows little change.

Figure 4.24 shows the absolute difference between the shortest path and congestion based round-trip travel times for the given origin-destination pairs. A majority of travelers experience only a minor delay due to congestion, but many travelers experience delays in excess of 25 minutes. The longest travel delay is over 150 minutes in duration. The mean increase in travel time is 13.92 minutes with a standard deviation of 19.24 minutes. We note little difference between the increases in travel times due to road blockages (Figure 4.24) and the increases in travel time experienced from normal congestion (Figure 4.3).

Similarly, we see little change in the composition of overall round trip travel times for all stores given a "selfish" routing with a single road blockage (Figure 4.25). "P081-River" still experiences the longest drive to "H001-Kmart", but now also experiences the longest drive to a grocery store, "D002-Plaza Extra West Superstore." We see some shuffling in the order of estates experiencing long drives between Figure 4.4 and Figure 4.25, but little difference in the actual drive times.

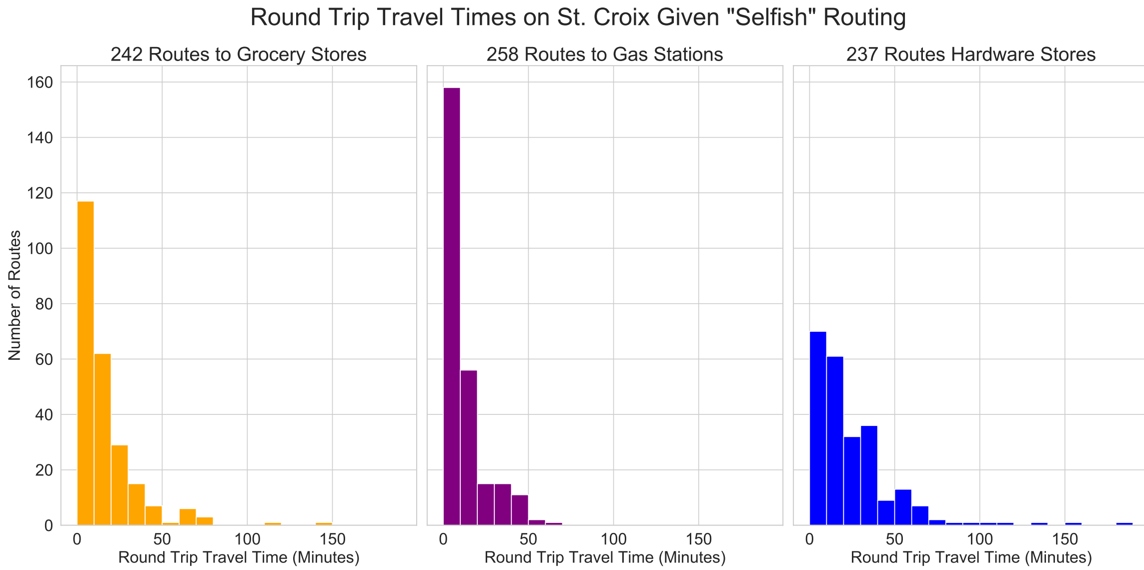

Figure 4.23. Distribution of round trip travel times by store type given "selfish" routing and a single interdiction. There are a total of 737 distinct routes (242 to grocery stores, 258 to gas stations, 237 to hardware stores) from the 233 estates in St. Croix. Although most of them are relatively short, we observe that some have round trip times in excess of two hours.

Figure 4.26 depicts the longest routes by round trip travel time for all store types given "selfish" routing with a single road interdiction. The road blockage is annotated in black on the map. The routing depicted in Figure 4.26 demonstrates the system's ability to "flex" and reroute flow in order to meet population demand.

The road segment blockage that caused the greatest buildup in congestion within the "selfish" model also causes the largest increase in congestion within the "coordinated" model. Figure 4.27 shows the resulting flow-to-capacity ratios with the interdicted edge highlighted in black. Again, we see the inherent flexibility in the system to reroute traffic without dropping any demand.

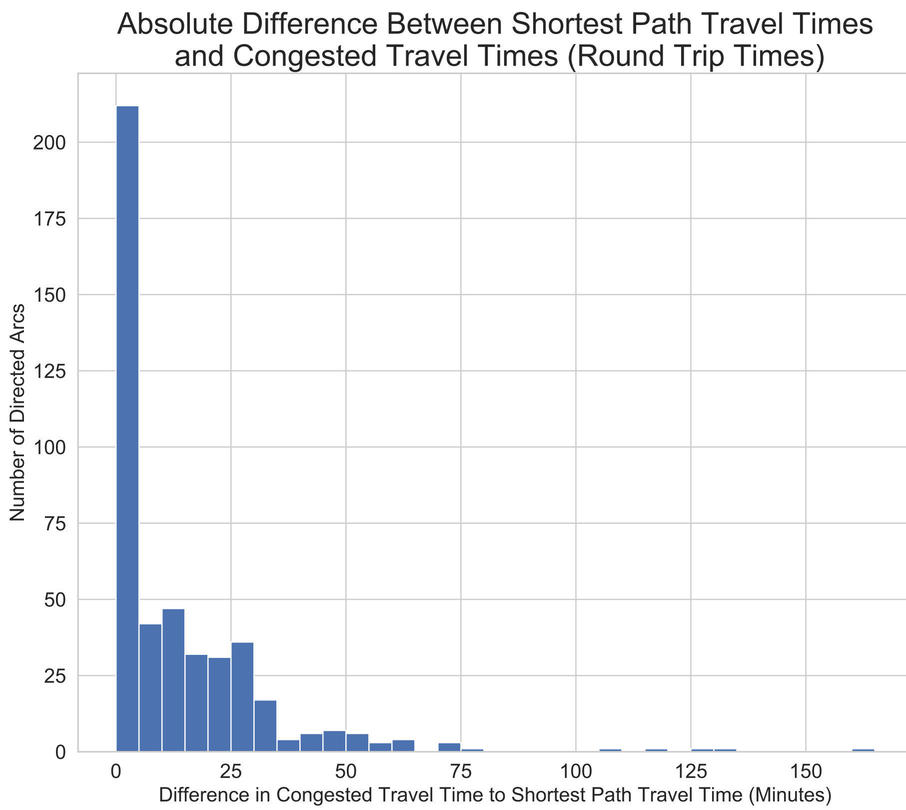

Figure 4.24. Absolute difference between the shortest path and congestion based round-trip travel times for the given origin-destination pairs given "selfish" routing and a single road segment blockage.

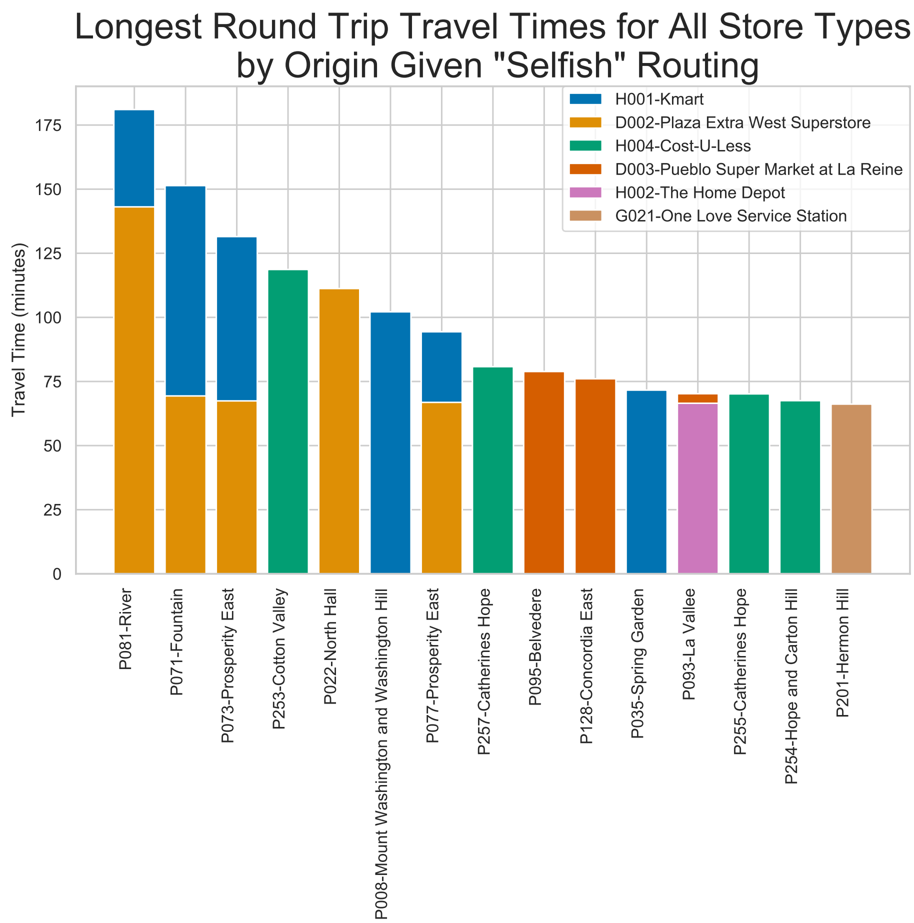

Figure 4.25. Longest round-trip travel times by origin for "selfish" routing given a single road interdiction. The top of the bar indicates the total travel time from a particular origin to a given store. Color of bar indicates the store. In cases where an origin has more than one longest round trip, there is one color per store.

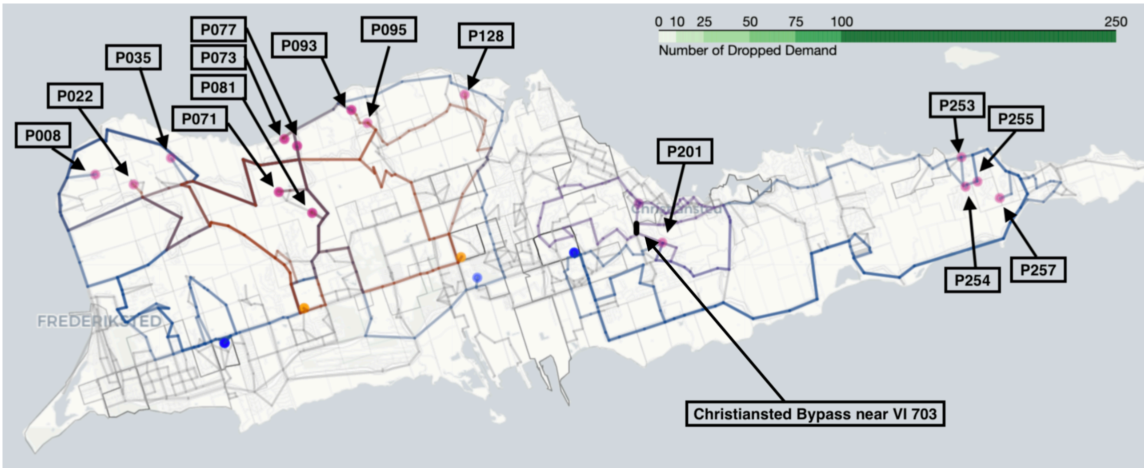

Figure 4.26. Map of longest routes by round trip travel time for all store types given "selfish" routing with a single road interdiction (annotated in black). Route colors indicate the destination store type: blue for hardware stores, orange for grocery stores, and purple for gas stations. The remaining arcs are rendered in grey. Any estates with dropped demand would be depicted in green with darker colors indicating higher levels of dropped demand. Created using QGIS Development Team (2019) on 24 September 2019.

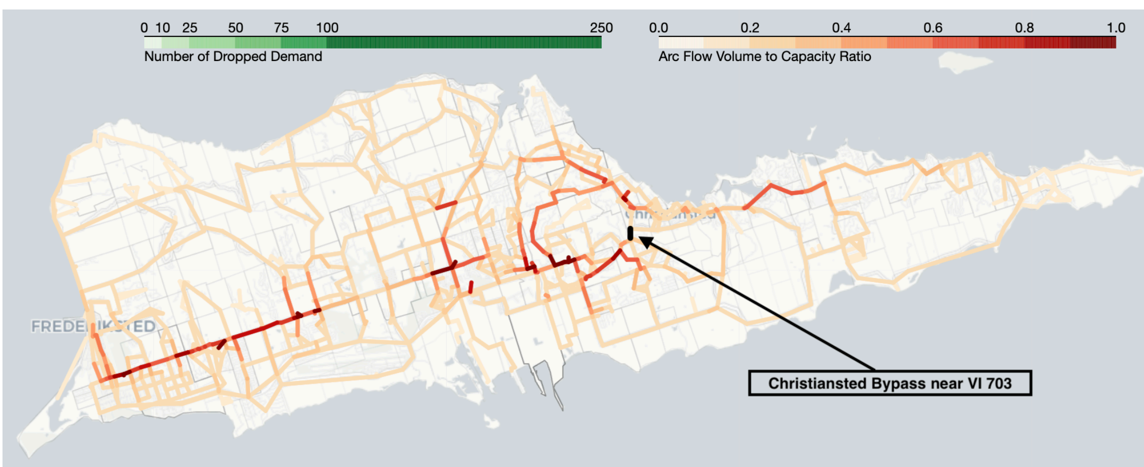

Figure 4.27. Map of flow ratios given "coordinated" routing with a single interdiction. Arcs are displayed according to their flow-to-capacity ratios. Higher ratios are depicted by darker colors. The interdicted road segment is annotated with in black. Any estates with dropped demand would be depicted in green with darker colors indicating higher levels of dropped demand. Created using QGIS Development Team (2019) on 24 September 2019.

When we investigate the travel time distribution for the "coordinated" system we note very few changes from the system when it is under normal operations (Figure 4.10). Table 4.5 shows the average travel times for all stores, and each store type individually for the "coordinated" routing model in the presence of road blockages and under "normal" operation. We note an increase in average travel time for the blockage model for all stores, gas stations, and hardware stores, but we note a slight decrease in average travel time for grocery stores. None of the changes are greater than one minute in duration.

Table 4.5. Average round trip travel time by store in minutes for both routing protocols with a single road blockage and without.

Average Round Trip Travel Time by Store Type (Minutes)					
	Road Blockage	All Stores	Grocery	Gas	Hardware
"Selfish"	No	17.27	15.51	11.77	25.05
	Yes	17.49	16.35	11.76	24.89
"Coordinated"	No	16.86	18.99	10.85	21.49
	Yes	17.09	18.36	11.32	22.34

The absolute difference between the shortest path and congestion based round-trip travel times for the "coordinated" routing protocol indicates that a majority of travelers experience only a minor delay due to congestion, but many travelers experience delays in excess of 40 minutes. The longest travel delay is approximately 130 minutes in duration. This is less than the longest increase in travel time experienced in the "selfish" routing model with a single road blockage (Figure 4.24). The mean increase in travel time is 13.19 minutes with a standard deviation of 19.70 minutes.

We note several changes in the composition of overall round trip travel times for all stores given a "coordinated" routing with a single road blockage (Figure 4.28). "P099-Hermitage" now experiences the longest drive to "D001-Stop & Shop Supermarket", and the third longest drive to "D002-Plaza Extra West Superstore." We see significant shuffling in the order of estates experiencing long drives from Figure 4.12 with 11 new stores appearing in Figure 4.28.

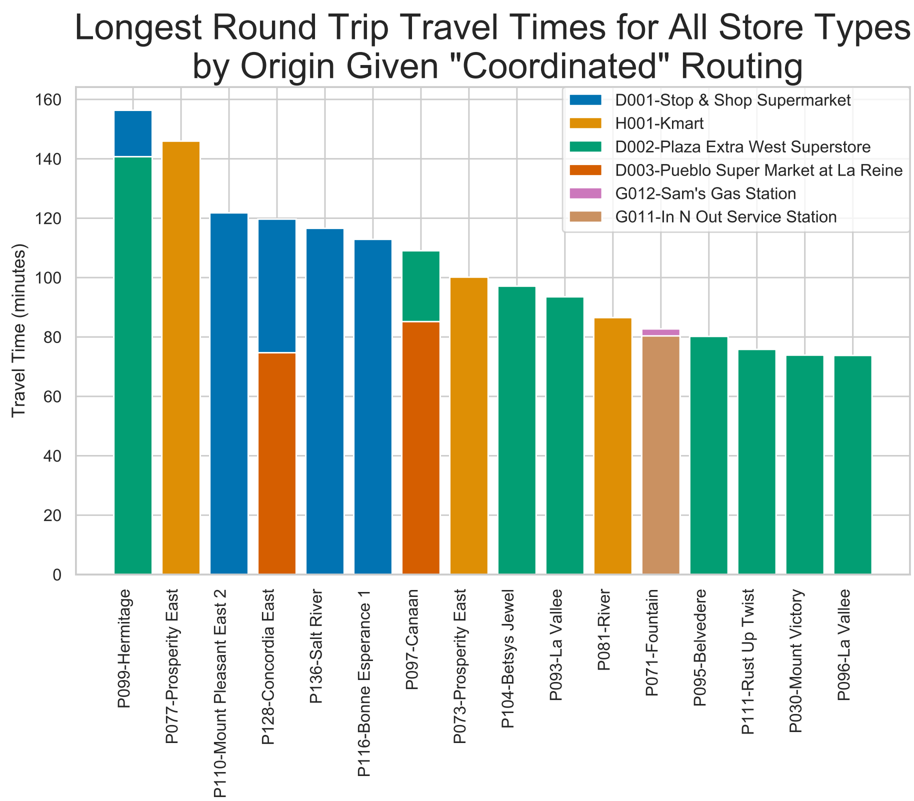

Figure 4.28. Longest round-trip travel times by origin for "coordinated" routing given a single road interdiction. The top of the bar indicates the total travel time from a particular origin to a given store. Color of bar indicates the store. In cases where an origin has more than one longest round trip, there is one color per store.

Figure 4.29 depicts the longest routes by round-trip travel time for all store types given "coordinated" routing with a single road interdiction. The road blockage is annotated in black on the map. The routing depicted in Figure 4.29 once again demonstrates the system's ability to "flex" and reroute flow in order to meet population demand. Of interest, we note that all of the longest round trip travel times are from estates on the northern side of St. Croix. We no longer observe the longest drive times coming from the eastern end of the island.

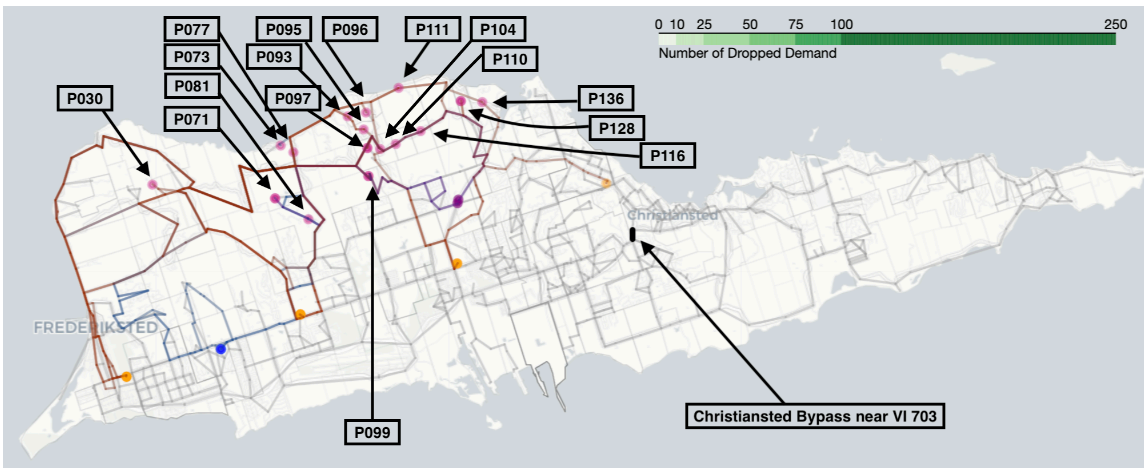

Figure 4.29. Map of longest routes by round trip travel time for all store types given "coordinated" routing with a single road interdiction (annotated in black). Route colors indicate the destination store type: blue for hardware stores, orange for grocery stores, and purple for gas stations. The remaining arcs are rendered in grey. Any estates with dropped demand would be depicted in green with darker colors indicating higher levels of dropped demand. Created using QGIS Development Team (2019) on 24 September 2019.

Round trip delivery times originating at Wilfred "Bomba" Allick Port shows little increase in mean travel time due to blockage on the Christiansted Bypass road segment. Table 4.6 shows the most significant increase in mean travel time is experienced in the "coordinated" model with an increase of nearly two minutes. Despite the small change in mean travel time, Figures 4.30 and 4.31 show significant changes in traffic flow near the road blockage than was seen with either traffic assignment protocol under "normal" operations (Figures 4.18 and 4.20).

Table 4.6. Average travel times from Wilfred "Bomba" Allick Port to all stores on St. Croix for each traffic assignment protocol with single road interdiction.

Traffic Assignment Type	Average Round Trip Delivery Time (Minutes)	Standard Deviations
"Selfish"	29.61	11.80
"Coordinated"	31.12	12.56

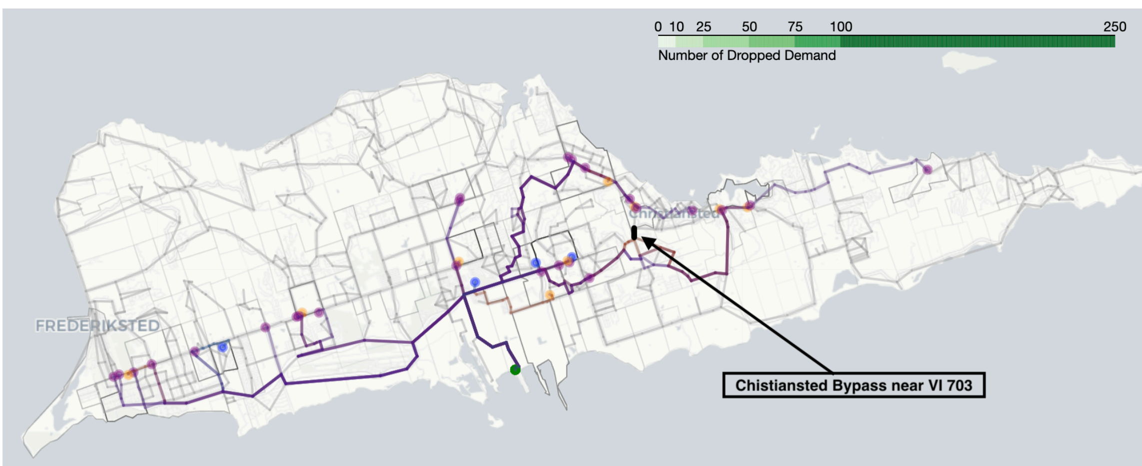

Figure 4.30. Geographic depiction of all routes from Wilfred "Bomba" Allick Port to all stores on St. Croix given a "selfish" traffic assignment protocol with a single road blockage (annotated in black). The remaining arcs are rendered in grey. Any estates with dropped demand would be depicted in green with darker colors indicating higher levels of dropped demand. Created using QGIS Development Team (2019) on 24 September 2019.

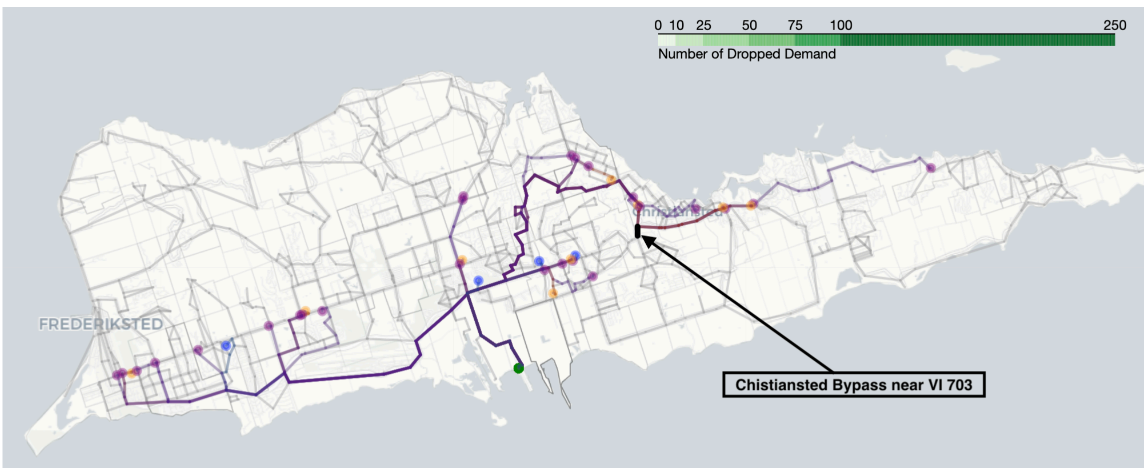

Figure 4.31. Geographic depiction of all routes from Wilfred "Bomba" Allick Port to all stores on St. Croix given a "coordinated" traffic assignment protocol with a single road blockage (annotated in black). The remaining arcs are rendered in grey. Any estates with dropped demand would be depicted in green with darker colors indicating higher levels of dropped demand. Created using QGIS Development Team (2019) on 24 September 2019.

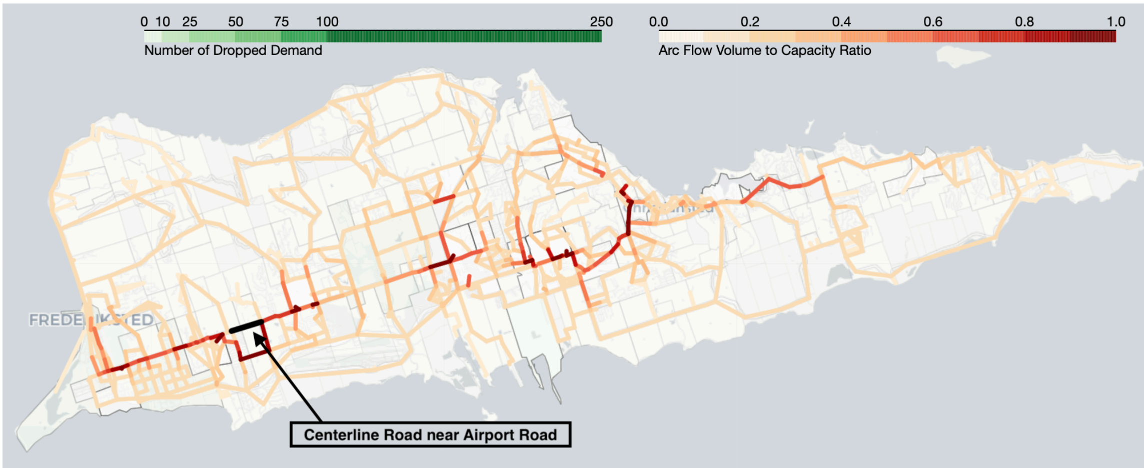

Figure 4.32. Map of flow ratios given single blockage to Centerline Road near Airport Road. Created using QGIS Development Team (2019) on 25 September 2019.

4.4.2 Blockage on Centerline Road

Throughout these analyses, Centerline Road stands out as a major thoroughfare for transit across St. Croix. Of particular interest is the impact of a blockage along this road. Figure 4.32 shows a single breakage to Centerline Road near Airport Road and the resulting flow-to-capacity ratios. This particular road segment has the fifth highest flow rate for the "selfish" routing protocol. We note that the surface road system on St. Croix possesses enough inherent "flexibility" to absorb the impact of a single break along Centerline Road by rerouting flows around it. However, we expect that multiple road blockages along Centerline Road would likely cause more significant (perhaps even catastrophic) disruptions and should be investigated in future work.

4.4.3 Blockage on Melvin H. Evans Highway

The Melvin H. Evans Highway is a multi-lane road on St. Croix with a speed limit of 55 MPH and a vehicle capacity much larger than any other roadway on the island. Interestingly, the highway does not carry significant traffic flow in any of the models under consideration. Any blockages to the highway would likely have very little impact on the overall performance of the surface road system.

4.5 Opportunities for Additional Analysis

The formulation presented in Section 3.3 is flexible enough to allow analytical excursions of many types.

Impact of Losing Supply Access Points

We could investigate the effect of systematically removing individual supply access points on the overall congestion within the system. For example, the loss of a grocery store or gas station will shift demand to (a fewer number of) other supply access points, creating more congestion on the surrounding roads as well as increasing the service load on each store. We expect that some locations will have a larger impact than the others, and it would be useful to characterize them in terms of this notion of priority.

Optimal Placement of Relief Locations

The existing model could be used to conduct analysis on the optimal placement of emergency relief distribution locations for pre- or post-storm support. This could be done in preparation for or loss of any set of roads or supply access points. Of particular interest would be the identification of supply locations that are robust to many different loss scenarios.

Emergency Response Times

Because an output of the model is the one-way (or round-trip) travel time between any two locations on the island, it can be used to estimate emergency response times (e.g., from a police station, fire station, or hospital) to any estate in the territory, both under normal traffic conditions and under stress.

Disruptions to Multiple Road Segments

We could use the model investigate the impact of multiple disruptions occurring simultaneously within the system. In the current analysis, we consider only a single interdiction, which is conservative and unrealistic in the aftermath of a major tropical storm or hurricane. In practice, one expects multiple roads to be affected at the same time. We have several options for considering such scenarios. For example, we could perform a probabilistic sweep over all roads (e.g., based on hurricane winds) and generate Monte Carlo realizations of blocked roads. Alternatively, we could consider specific correlated events, such as flooding or washouts. coordinate with information from watershed data, drainage “ghuts”, etc. (Alderson 2018).

Prioritized Road Clearing

If for each of the scenarios listed above we have estimate road clearing and/or repair times, we can conduct a different kind of worst-case analysis for road interdiction (e.g., Alderson et al. 2017a) that considers short-term versus long-term consequence. We can also consider prioritization of which roads to clear first. Similar studies have shown the importance and potential impact of knowing what to restore first (e.g., Wallace et al. 2001; Matisziw et al. 2010).

Evacuation Modeling

By changing the input data for different traffic demands, we could investigate the ability of the road system to support other traffic patterns, such as evacuation (e.g., from a tsunami). Because the existing road system has evolved to support “normal” traffic patterns, one should expect that it might not perform well under abnormal extreme demands.

Construction for Improved or New Road Segments

Perhaps most importantly, the model can be used to identify how specific road construction projects, either to improve or harden existing roads or to build new road altogether, can benefit the capacity of this system to support traffic demands for any of the scenarios or conditions presented above.

CHAPTER 5:
Summary and Conclusions

We conclude with a summary of contributions and results, along with a list of potential topics for additional study.

5.1 Summary

This thesis performs three modeling and analysis tasks; (1) we construct a dataset useful for the analysis of traffic congestion and shipping supplies on surface roads within the island of St. Croix, (2) we develop a four-stage traffic model that measures the round-trip travel times for supplies and civilians to reach locations of distribution during normal and degraded traffic conditions, and (3) using data and models to determine the capability of surface roads in St. Croix to enable access to disaster relief supplies, we identify which St. Croix communities may have the greatest difficulty accessing locations of distribution during normal and worst-case situations.

We identified the importance of relevant data when performing traffic flow analysis for a surface road network. We were able to construct and curate the dataset using open-source information and software packages. However, professionally collected and curated data, for the express purpose of traffic analysis, would increase the efficacy and accuracy of the model.

Furthermore, we identified the importance communication can play in reducing the overall level of congestion within the surface road system. The ability to communicate, especially when the system is degraded, enhances the system's ability to support a broader set of customers for the "greater" good.

Finally, we were able to determine that under "normal" circumstances, the road network for the island of St. Croix has sufficient capacity to support the entire population. However, this analysis does not take the length of service time at the corresponding supply points into consideration.

5.2 Future Work

The next phase in this research should expand the scope of analysis for the surface road networks to include the islands of St. Thomas and St. John, in order to provide a complete view of traffic within the territory. Priority should be placed on St. Thomas as the center of government and tourism within the USVI.

In a similar vein, the surface road network is but one part of a complex set of interdependent infrastructure systems within the territory. It will be important to take a comprehensive look at disruptions in the surface road network and their effects on other critical infrastructure systems, such as the effects of road blockages on water truck deliveries.

The road network model presented in Section 3.3 can be expanded to conduct many different types of analyses to benefit stakeholders in the USVI. As outlined in Section 4.5, recommended topics for analysis include identifying the most advantageous locations for additional relief distribution points, assessing the impact of congestion on emergency response times (e.g., medical, fire, police), the impact of constructing new roads within the existing network, or the impact of congestion when considering other, non-standard, traffic patterns (e.g., evacuation).

There are also opportunities to improve the computational workflow supporting these types of analyses. There is considerable overhead associated with each phase of data curation, modeling & analysis, and visualization described in Figure 3.1, and computational tools that streamline or automate these tasks have the potential to improve analyst productivity. In addition, each solve of the equilibrium traffic model takes considerable time, making analysis of many scenarios very time-consuming. Finding ways to improve the computational runtimes on individual machines or using supercomputing or other online (e.g., cloud-based) platforms has the potential to increase the scope of analysis. Finally, developing new ways for stakeholders to engage with the results of these analyses, either in the form of improved visualizations or interactive decision support tools, remains a priority.

We recommend the further development of our model to include these features and that organizations in the USVI, including VITEMA and DPW, build on these model results in their hazard mitigation and response planning efforts.

List of References

Alderson D (2018) Operational resilience analysis and capacity building in the US Virgin Islands. Proposed Statement of Work, Center for Infrastructure Defense, Operations Research Department, and Energy Academic Group, Naval Postgraduate School, Monterey, CA.

Alderson D, Brown G, Carlyle W, Wood R (2017a) Assessing and improving the operational resilience of a large highway infrastructure system to worst-case losses. *Transportation Science* (4):1012–1034.

Alderson D, Brown G, DiRenzo J, Engle R, Jackson J, Maule B, Onuska J (2012) Improving the resilience of coal transport in the Port of Pittsburgh—an example of defender-attacker-defender optimization-based decision support. Technical Report NPS-OR-12-004, Naval Postgraduate School.

Alderson DL, Brown GG, Carlyle WM (2014) Assessing and improving operational resilience of critical infrastructures and other systems. *Bridging Data and Decisions*, 180–215 (INFORMS), https://pubsonline.informs.org/doi/abs/10.1287/educ.2014.0131.

Alderson DL, Brown GG, Carlyle WM (2015) Operational models of infrastructure resilience. *Risk Analysis* 35(4):562–586.

Alderson DL, Brown GG, Carlyle WM, Cox Jr LA (2013) Sometimes there is no "most-vital" arc: Assessing and improving the operational resilience of systems. *Military Operations Research* 18(1):21–37.

Alderson DL, Brown GG, Carlyle WM, Wood RK (2017b) Assessing and improving the operational resilience of a large highway infrastructure system to worst-case losses. *Transportation Science* 52(4):1012–1034, available electronically from https://pubsonline.informs.org/doi/abs/10.1287/trsc.2017.0749.

Alderson DL, Bunn BB, Eisenberg DA, Howard AR, Nussbaum DA, II JT (2018) Interdependent infrastructure resilience in the U.S. Virgin Islands: Preliminary assessment. Technical report, NPS-OR-18-005, NPS, December 2018. Available electronically from https://faculty.nps.edu/dlalders/USVI/NPS-OR-18-005.pdf.

Apte A (2011) Strategic and operational prepositioning in case of seasonal natural disasters: a perspective. *Wiley Encyclopedia of Operations Research and Management Science* (Wiley Online Library) 1–13.

Brewer RS, Hatfield ER (2019) Personal communication. Interview with United States Coast Guard, St. Thomas. 25 March 2019.

Bunn B (2018) An operational model of interdependent water and power distribution infrastructure systems. Master's Thesis. Naval Postgraduate School, Monterey, CA. Available electronically from https://calhoun.nps.edu/handle/10945/60368, last accessed 10 May 2019.

Calderon A (2019) Personal communication. Tropical Shipping first person account of Hurricanes Irma and Maria, St. Croix. 28 March 2019.

Delacruz C (2011) Defending the maritime transport of cargo for the Hawaiian Islands. Master's Thesis. Naval Postgraduate School, Monterey, CA.

Derrible S (2017) Urban infrastructure is not a tree: Integrating and decentralizing urban infrastructure systems. *Environment and Planning B: Urban Analytics and City Science* 44(3):553–569.

Dickenson M (2014) Solving Operational Models of Interdependent Infrastructure Systems. Master's Thesis. Naval Postgraduate School, Monterey, CA. Available electronically from https://calhoun.nps.edu/handle/10945/44550, last accessed 10 May 2019.

Dixon C (2011) Assessing Vulnerabilities in Interdependent Infrastructures using Attacker-Defender Models. Master's Thesis. Naval Postgraduate School, Monterey, CA. Available electronically from https://calhoun.nps.edu/handle/10945/5606, last accessed 10 May 2019.

Farlow CR (2011) Prepositioning for flooding in the Sacramento region. Master's Thesis. Naval Postgraduate School, Monterey, CA. Available electronically from https://calhoun.nps.edu/handle/10945/5721, last accessed 10 May 2019.

Frazier M (2019) Personal communication. Crowley Shipping first person account of Hurricanes Irma and Maria, St. Thomas. 25 March 2019.

Gajewski P (2019) Personal communication. Interview with Virgin Islands Department of Public Works, St. Thomas. 25 March 2019.

GeoPandas Development Team (2019) GeoPandas. Open source project. http://www.geopandas.org.

Google, Inc (2019) Google Maps. Online software tool, http://maps.google.com.

Heidtke CL (2007) Reducing the "Gap of Pain" : a strategy for optimizing federal resource availability in response to major incidents. Master's Thesis. Naval Postgraduate School, Monterey, CA. Available electronically from https://calhoun.nps.edu/handle/10945/3597, last accessed 10 May 2019.

Hendrickson L (2019) Personal communication. Email correspondence with Lucia Henderson at Bunkers of St. Croix, Inc. concerning fuel delivery on the island of St. Croix. 8 May 2019.

Lahmar M, Assavapokee T, Ardekani A (2006) A dynamic transportation planning support system for hurricane evacuation. *2006 IEEE Intelligent Transportation Systems Conference*, 612–617 (IEEE).

Lee II EE, Mitchell JE, Wallace WA (2007) Restoration of services in interdependent infrastructure systems: A network flows approach. *IEEE Transactions on Systems, Man, and Cybernetics, Part C (Applications and Reviews)* 37(6):1303–1317.

Maerivoet S, De Moor B (2005) Transportation planning and traffic flow models. *arXiv preprint physics/0507127* .

Malveo A (2013) Assessing the Impact of Congestion During a Multi-County Evacuation. Master's Thesis. Naval Postgraduate School, Monterey, CA. Available electronically from https://calhoun.nps.edu/handle/10945/32861, last accessed 10 May 2019.

Matisziw TC, Murray AT, Grubesic TH (2010) Strategic network restoration. *Networks and Spatial Economics* 10(3):345–361.

McCall VM (2006) Designing and prepositioning humanitarian assistance pack-up kits (HA PUKs) to support Pacific fleet emergency relief operations. Master's Thesis. Naval Postgraduate School, Monterey, CA. Available electronically from https://calhoun.nps.edu/handle/10945/2480, last accessed 10 May 2019.

Mintzer D (2014) Optimizing the resilience of containerized cargo transportation infrastructure in the Port of Los Angeles. Master's Thesis. Naval Postgraduate School, Monterey, CA.

Moses R, Mtoi E (2012) Evaluation of free flow speeds on interrupted flow facilities in the state of Florida. *Funded by the Florida Department of Transportation, Systems Planning Office* Available electronically from https://rosap.ntl.bts.gov/view/dot/23430.

National Hurricane Center (2018) Costliest U.S. tropical cyclones tables updated. Technical report, National Oceanographic and Atmospheric Administration, Miami, FL, last Updated: January 26, 2018. Available electronically from https://www.nhc.noaa.gov/news/UpdatedCostliest.pdf, last accessed 20 July 2019.

OpenStreetMap contributors (2019) Planet dump retrieved from https://planet.osm.org . https://www.openstreetmap.org.

Peeta S, Liu H, He X (2015) *The Routledge Handbook of Transportation*. Available electronically from https://www.routledgehandbooks.com/doi/10.4324/9781315756684.ch3.

Plaskett S (2017) Emergency response and recovery: Central takeaways from the unprecedented 2017 hurricane season. Testimony before House Transportation and Infrastructure Committee, Washington, DC, 2 November 2017.

QGIS Development Team (2019) QGIS Geographic Information System. Open Source Geospatial Foundation Project. http://qgis.osgeo.org.

Raimondi A (2019) Personal communication. Interview with Virgin Islands Port Authority, St. Thomas. 26 March 2019.

Rinaldi SM, Peerenboom JP, Kelly TK (2001) Identifying, understanding, and analyzing critical infrastructure interdependencies. *IEEE Control Systems Magazine* 21(6):11–25.

Sabbaghtorkan M, Batta R, He Q (2019) Prepositioning of assets and supplies in disaster operations management: review and research gap identification. *European Journal of Operational Research* .

Schott T, Landsea C, Hafele G, Lorens J, Taylor A, Thurm H, Ward B, Willis M, Zaleski W (2012) The Saffir-Simpson hurricane wind scale. Accessed 17 September, 2019, https://www.nhc.noaa.gov/aboutsshws.php.

Sharma HK, Swami M, Swami BL (2012) Speed-flow analysis for interrupted oversaturated traffic flow with heterogeneous structure for urban roads. *International Journal for Traffic and Transport Engineering* 2(2):142–152.

Transportation Research Board (2000) *Highway Capacity Manual*. Washington, DC, http://www.trb.org/Main/Blurbs/175169.aspx.

US Census Bureau (2018) Current Estate State-based Shapefile. Available electronically from https://catalog.data.gov/dataset/tiger-line-shapefile-2018-state-united-states-virgin-islands-current-estate-state-based-shapefi, last accessed 20 February 2019.

US Virgin Islands Bureau of Economic Research (2014) The United States Virgin Islands 2015 Comprehensive Economic Development Strategy. Technical report, U.S. Virgin Islands Bureau of Economic Research, Charlotte Amalie, St. Thomas.

US Virgin Islands Department of Public Works (2018) About us. Accessed 10 August 2019, www.dpw.vi.gov/about-us.

US Virgin Islands Port Authority (2018) About us. Accessed 10 August 2019 http://www.viport.com/about/aboutus.html.

US Virgin Islands Water and Power Authority (2018) About us. Accessed 10 August 2019, http://www.viwapa.vi/about-us.

USVI Department of Public Works (2014) U.S. Virgin Islands 2040 Comprehensive Transportation Master Plan Report. Prepared by Parsons Brinkerhoff and Jaredian Design Group.

USVI Hurricane Recovery and Resilience Task Force (2018) Final Report. Technical report, Government of the U.S. Virgin Islands, St. Thomas, USVI, available electronically from https://www.usvihurricanetaskforce.org/, last accessed 8 July 2019.

Wallace WA, Mendonça D, Lee E, Mitchell J, Chow J (2001) Managing disruptions to critical interdependent infrastructures in the context of the 2001 World Trade Center attack. *Impacts of and Human Response to the September 11, 2001 Disasters: What Research Tells Us* .

Wenke W (2015) Assessing the operational resilience of the Port of Anchorage: Recommendations for investment and implications for policy. Master's Thesis. Naval Postgraduate School, Monterey, CA.

Yuhas T (2011) Escape from the Delta: preparation and evacuation for catastrophic flooding in California Emergency Management Agency Region IV.

Yusoff M, Ariffin J, Mohamed A (2008) Optimization approaches for macroscopic emergency evacuation planning: a survey. *2008 International symposium on information technology*, volume 3, 1–7 (IEEE).

Zegeer JD, Blogg M, Nguyen K, Vandehey M (2008) Default values for highway capacity and level-of-service analyses. *Transportation Research Record* 2071(1):35–43, available electronically from https://journals.sagepub.com/doi/abs/10.3141/2071-05.

THIS PAGE INTENTIONALLY LEFT BLANK

Initial Distribution List

1. Defense Technical Information Center
   Ft. Belvoir, Virginia

2. Dudley Knox Library
   Naval Postgraduate School
   Monterey, California